NASA-CR-193205

AN ASSESSMENT OF TWILIGHT AIRGLOW INVERSION PROCEDURES USING ATMOSPHERE EXPLORER OBSERVATIONS

GRANT
IN-46-CR
163209
P.81

NASA Grant NO. NAG 5-1502

Principal Investigators*

I. C. McDade# and W. E. Sharp

Space Physics Research Laboratory
Department of Atmospheric, Oceanic and Space Science
The University of Michigan

FINAL REPORT
April 1993

*PI transferred from McDade to Sharp in August 1991
#Present Address: Heraberg Institute of Astrophysics, National Research Council
100 Sussex Drive, Ottawa, Ontario K1A 0R6, CANADA
Tel. (613) 990-0710

TABLE OF CONTENTS

SUMMARY

The aim of this research project was to test and truth some recently developed methods for recovering thermospheric oxygen atom densities and thermospheric temperatures from ground-based observations of the 7320 Å $O^{+}(^{2}D-^{2}P)$ twilight airglow emission. The research plan was to use twilight observations made by the *Visible Airglow Experiment* (VAE) on the Atmosphere Explorer 'E' satellite as proxy ground-based twilight observations. These observations were to be processed using the twilight inversion procedures and the recovered oxygen atom densities and thermospheric temperatures were then to be examined to see how they compared with the densities and temperatures that were measured by the *Open Source Mass Spectrometer* and the *Neutral Atmosphere Temperature Experiment* on the satellite.

The activities performed under the one year performance period of the grant may be summarized as follows:

(1) A major survey of the Atmosphere Explorer 'E' data base was first performed in order to identify the orbits for which suitable *Visible Airglow Experiment, Open Source Mass Spectrometer* and *Neutral Atmosphere Temperature Experiment* observations existed.

(2) Satellite versions of the twilight airglow inversion program which allowed for the viewing geometry of the VAE observations were generated and tested using synthetic data. The inversion program was also modified to allow for the analysis of twilight observations which included contributions from regions of space with local solar zenith angles less than 90 degrees.

(3) The twilight observations made on selected orbits were inverted and the atomic oxygen densities and thermospheric temperatures recovered from these inversions were compared with the densities and temperatures measured at the satellite. The $O^{+}(^{2}P)$ ionization frequencies, which are also recovered as part of the inversion process, were compared with the frequencies deduced using other methods.

The results of the study show that at both low and high levels of solar activity, the atomic oxygen densities and thermospheric temperatures recovered from the inversions are in reasonably good agreement with the *in situ* satellite data. The $O^{+}(^{2}P)$ ionization

frequencies recovered for low levels of solar activity are in good agreement with previous evaluations, however, the ionization frequencies recovered from the twilight observations made closer to solar maximum exhibit a weaker than expected dependence on the solar $F_{10.7}$ flux.

A full journal article describing the results of this work is in preparation and an abstract is being submitted to the American Geophysical Union for presentation at the Fall 1992 AGU Meeting .

1. BACKGROUND TO THE RESEARCH ACTIVITIES

Atomic oxygen is undoubtedly the most important neutral constituent of the thermosphere and during the last two decades satellite-borne mass spectrometer measurements have provided a great deal of information about the solar cycle, seasonal and diurnal variations of the thermospheric atomic oxygen densities. Unfortunately, however, many aspects of both the long term and short term variations, such as those caused by geomagnetic storms, are still not fully understood. At present there are no satellites in orbit providing atomic oxygen data and there is, therefore, a well recognized need to establish alternative methods for monitoring the thermospheric oxygen atom densities. This need has stimulated a renaissance of interest in twilight airglow studies and recent research has demonstrated that ground-based twilight observations of selected airglow emission features may provide a great deal of information about the long term and short term variations in thermospheric temperatures and thermospheric oxygen atom densities.

One of the most promising ground-based thermospheric monitoring techniques proposed during the last few years is based upon twilight observations of the $O^+(^2D\text{-}^2P)$ airglow emission at 7320 Å (*Fennelly et al.*, 1991; *McDade et al.*, 1991). The method, originally pioneered by *Meriwether et al.* (1978) and *Noxon and Norton* (1979), would use twilight airglow emission rate measurements made at low elevation in the direction of the rising or setting sun to determine the oxygen atom densities and thermospheric temperatures. Unfortunately, as originally formulated, this method suffers from the limitation that detailed information about the solar EUV flux and the $O^+(^2P)$ ionization frequencies at the time of the observations is required in order to recover the densities and temperatures. However, *McDade et al.* (1991) have demonstrated that this limitation may be overcome, and valuable information about the $O^+(^2P)$ ionization frequencies can also be obtained, if the 7320 Å twilight observations are made in two different viewing directions - one at low elevation towards the sun and the other at higher elevation ideally towards the local zenith. Preliminary ground-based measurements using this approach are now underway, however, there are at present no satellite measurements of the oxygen atom densities being made and it will not be possible, therefore, to directly verify or truth the atomic oxygen densities and thermospheric temperatures recovered using this technique. Fortunately, during the Atmosphere Explorer 'E' mission simultaneous measurements of the 7320 Å twilight airglow emission (*Visible Airglow Experiment*) were made together with measurements of the thermospheric oxygen atom densities

(*Open Source Mass Spectrometer*) and the thermospheric temperatures (*Neutral Atmosphere Temperature Experiment*). Since some of the *Visible Airglow Experiment* (VAE) observations were made in a multi-directional spin-scan mode they should closely resemble ground-based observations and may, therefore, be used to truth and test the $O^+(^2D-^2P)$ 7320Å twilight inversion procedures. This report describes the results of a study carried out to assess the performance of the twilight inversion procedures using the Atmosphere Explorer 'E' data base.

2. THE TWILIGHT AIRGLOW INVERSION ALGORITHM

The twilight inversion procedures assessed in this work are discussed in detail by *McDade et al.* (1991) and are only briefly described here. The inversion algorithm is based upon the relatively complete understanding of the $O^+(^2P)$ photochemistry that has emerged from the AE-C and AE-D missions (*Rusch et al.* 1976, 1977).

The $O^+(^2P)$ ion, responsible for the airglow emission at 7620 and 7330 Å, is primarily produced under twilight conditions as a result of direct photoionization excitation of atomic oxygen by solar EUV photons with wavelengths less than ~ 666 Å,

$$O + h\nu\ (\lambda<666\ \text{Å}) \rightarrow O^+(^2P) + e \tag{1}$$

The ion may also be produced as a result of photoelectron impact ionization excitation of atomic oxygen, but this source is thought to make only a ~10% contribution under most twilight conditions (*Torr et al.* 1990). The $O^+(^2P)$ ions are lost through the radiative decay process

$$O^+(^2P) \rightarrow O^+(^2D, {}^4S) + h\nu\ (7320\text{-}30\text{Å}, 2470\text{Å}) \tag{2}$$

and are primarily quenched at thermospheric altitudes by atomic oxygen and molecular nitrogen,

$$O^+(^2P) + O \rightarrow O^+ + O \tag{3}$$

$$O^+(^2P) + N_2 \rightarrow O^+ + N_2 \ \text{ or } \ O + N_2^+ \tag{4}$$

Because of this relatively simply photochemistry, the twilight 7320-30 Å volume emission rate at any point in space defined by the altitude, z, and local solar zenith angle, β, may be expressed as

$$V(z,\beta) = \{\gamma \times A \times P(z,\beta)\} / \{A + k_O[O]_z + k_{N_2}[N_2]_z\} \tag{5}$$

where k_O and k_{N_2} are the rate coefficients for quenching of $O^+(^2P)$ by atomic oxygen and molecular nitrogen; A is the inverse radiative lifetime of the ^2P state; γ is the branching ratio for emission of the $(^2D_{5/2} \leftarrow {}^2P_{3/2,1/2})$ and $(^2D_{3/2} \leftarrow {}^2P_{3/2,1/2})$ pair of doublets at 7320 Å and 7330 Å ; and P(z,β) is the altitude and solar zenith angle dependent local $O^+(^2P)$ volume production rate.

The $O^+(^2P)$ volume production rate due to ionization excitation by EUV photons in a narrow wavelength interval centered on the wavelength λ_i is given by

$$Q_i(z,\beta) = [O]_z \times f_i \times I^* \times \exp[-\tau_i(z,\beta)] \quad (6)$$

where τ_i is the optical depth for the radiation at wavelength λ_i and f_i is the fractional contribution made by radiation in this interval to the total $O^+(^2P)$ ionization frequency, I^*, at zero optical depth. The total $O^+(^2P)$ volume production rate, $P(z,\beta)$, may be obtained by summing the $Q_i(z,\beta)$ over all wavelength intervals that contribute significantly to I^*. This is achieved by binning the solar EUV spectrum into the wavelength intervals described by *Torr et al.*, (1979). The contribution that photons in a given wavelength interval make to the total ionization frequency is calculated using only the spectral shape of a reference solar EUV spectrum.

As most of the twilight 7320-30 Å emission originates from altitudes above ~250 km (*Torr et al.*, 1990; *Fennelly et al.*, 1991) the atomic oxygen densities may be approximated by a single exponential profile. The oxygen atom density at any altitude can then be expressed in terms of two parameters - the atomic oxygen scale height H_O, which is determined by the thermospheric temperature, and the absolute oxygen atom number density, $[O]_{250}$, at an arbitrary reference altitude of 250 km. Similarly, the molecular nitrogen density at each altitude may be expressed in terms of the density at a reference altitude of 250 km and the nitrogen scale height $H_{N_2} = (16/28) \times H_O$.

In the thermosphere most of the attenuation of the EUV flux is due to absorption by atomic oxygen and molecular nitrogen and for exponential O and N_2 profiles, the optical depth at wavelength λ_i may be obtained from the expression

$$\tau_i(z,\beta) = \{[O]_a \times H_O \times \sigma_i^O \times Ch(\beta, H_O)\} + \{[N_2]_a \times H_{N_2} \times \sigma_i^{N_2} \times Ch(\beta, H_{N_2})\} \quad (7)$$

where σ_i^O and $\sigma_i^{N_2}$ are the total O and N_2 cross sections at λ_i; $Ch(\beta, H)$ is the grazing incidence Chapman function and $[O]_a$ and $[N_2]_a$ are the O and N_2 number densities at the minimum ray height of the grazing solar radiation.

By integrating the volume emission rates given by equation 5 along the line-of-sight corresponding to a particular ground-based or satellite-borne twilight observation, the measured 7320-30 Å column emission rate may be expressed in terms of the well known physical quantities appearing in (5), (6) and (7) and the four important, and variable, geophysical parameters I^*, H_O, $[O]_{250}$ and $[N_2]_{250}$. Consequently, it is possible in principle to deduce the later four quantities from a series of twilight observations by finding the set of four parameters that best reproduces the observations. In practice, however, the two parameters I^* and $[O]_{250}$ are strongly coupled and it is really only possible to separate these two quantities if the observational data consists of a series of measurements made over a range of solar depression angles at two different elevation angles, ideally one at low elevation towards the azimuth of the sun and the other towards the zenith (*McDade et al.*, 1991). It also turns out that the twilight emission rates are not particularly sensitive to the molecular nitrogen densities and the problem may be reduced to one of finding I^*, H_O,and $[O]_{250}$ if independently measured nitrogen densities or nitrogen densities from a standard atmospheric model are substituted for $[N_2]_{250}$.

The problem of finding the values for the parameters I^*, H_O, and $[O]_{250}$ that best reproduce a given set of twilight observations may be solved using a standard non-linear least squares fitting procedure such as the Marquardt gradient-expansion method described by *Bevington* (1969) and *Press et al.* (1986). This iterative procedure efficiently searches for the set of parameters that optimizes the agreement between a model and a set of observations through minimization of the χ^2 merit function.

3. THE VAE OBSERVATIONS AND THE TEST DATA REQUIREMENTS

3.1 *The Basic Data Requirements*

In order to make a meaningful assessment of the inversion procedures described in Section 2 it was important to use satellite observations that were obtained with viewing geometries that were as similar as possible to those that would be used to make the ground-based twilight measurements. Ideally, the ground-based observations would consist of a series of twilight brightness measurements made over a time interval during which the solar depression angle at the ground varied between 5 and 20 degrees (*McDade et al.*, 1991). Approximately one half of these observations would be made at an elevation angle of ~20° towards the azimuth of the setting, or rising, sun and the other half would be made towards the local zenith. The idealized ground-based observing geometry for which similar satellite observations were to be found is illustrated in Figure 1a.

3.2 *The Visible Airglow Experiment 7320-30 Å Observations*

The *Visible Airglow Experiment* (VAE) on the Atmosphere Explorer 'E' satellite (AE-E) was a filter wheel airglow photometer designed to measure various thermospheric emission features during both daytime and nighttime conditions. The photometer had two distinct optical channels, a high sensitivity channel with a large field of view (3° half cone angle) and a low sensitivity channel with a narrow field of view (3/4° half cone angle). The fields of view of the two channels were oriented at 90 degrees from each other. The counts from the narrow channel (channel 1) were integrated over a period of 32 msec and those from the wide channel (channel 2) were integrated over a 125 msec interval. The instrument operated in a number of different modes depending on the filter wheel position which could be held fixed to continuously monitor a particular airglow feature or stepped through a number of different interference filters at various stepping rates. Continuous observations of the airglow emission near 7320 Å were made in two of the eight possible VAE fixed wheel modes. In one of these modes, known as mode '73F6', the 7320 Å observations were made with the narrow channel of the instrument (channel 1); in another fixed wheel mode, mode '55F7', the wide channel (channel 2) was used to make the 7320 Å observations.

During normal satellite operation the VAE instrument was oriented so that the narrow channel pointed aft of the spacecraft and the wide channel pointed towards the earth.

However, for a significant part of the mission the spacecraft was operated in 'skid' or 'cartwheel' spin modes. In the 'skid' mode the satellite spin angular momentum vector was anti-parallel to the orbital angular momentum vector; this is referred to as the 'normal' spin mode. In the 'cartwheel' mode the satellite spin angular momentum vector was parallel to the orbital angular momentum vector and this is referred to as the 'inverted' spin mode. In either spin mode the two VAE channels scanned through all zenith angles within the orbital plane. Consequently, when the satellite passed through the terminator in the spinning mode with an active 7320 Å channel the instrument made the terminator in the spinning mode with an active 7320 Å channel the instrument made twilight observation of the $O^+(^2D-^2P)$ airglow in a manner similar to a ground-based twilight monitoring station as shown in Figure 1b.

3.3 *Primary Data Selection Criteria*

Given the nature of the basic data requirements and the operational characteristics of the AE-E VAE instrument the first task to be performed was to identify the satellite orbits which satisfied the following primary criteria:

(1) The satellite had to be operating in a spinning mode in a low altitude, near circular, orbit.

(2) The VAE instrument had to be operational as the satellite passed through the dusk or dawn terminator and the instrument had to be observing the 7320 Å airglow in either Channel 1 or Channel 2 .

(3) The *Open Source Mass Spectrometer* and the *Neutral Atmosphere Temperature Experiment* both had to be operating and providing good atmospheric density and temperature data.

4. IDENTIFICATION OF ORBITS SUITABLE FOR TESTING THE INVERSION ALGORITHM

The first step in the search for suitable orbits for testing the inversion algorithm was to find the AE-E orbits during which the VAE instrument was observing the 7320 Å airglow and the satellite was operating in the spin mode. These orbits are listed in the table of Appendix 1 along with some pertinent information identifying the VAE channel that was observing at 7320 Å - either 1 or 2; the spin mode of the satellite - either normal or inverted; the on/off times of the instrument and the satellite altitude and local times associated with the instrument on/off times. Having identified these orbits the next step was to check that the VAE instrument was operating when the satellite passed through the terminator and to confirm that density and temperature data from the *Open Source Mass Spectrometer* (OSS) and the *Neutral Atmosphere Temperature Experiment* (NATE) were available at that time. This was achieved using the AE database software available at the University of Michigan Space Physics Research Laboratory and the Atmosphere Explorer United Abstract Data files. The AE data base program 'NEWLIST' was used to examine the VAE, OSS and NATE data on the United Abstract (UA) files for all of the orbits listed in Table A1. The UA data files contain a summary of the data from all the AE instruments with a data point for every 15 second interval. The program NEWLIST allows the data satisfying specific selection criteria to be extracted to a file or plotted on a visual display unit. It should be noted that when the satellite was operating in a spin mode the UA files contain only the VAE observations made when the instrument channels were pointing towards the zenith. By running the NEWLIST program and selecting only the data acquired when the solar zenith angle at the satellite was between 85 and 145 degrees the AE-E orbits satisfying the criteria described above were identified. These orbits are listed in Table 1 which gives the date and orbit number as well as the number of the channel that was observing at 7320 Å. Table 1 also lists the Universal Time in seconds for the start and end of each twilight observing sequence and an indication of whether the satellite was passing from the dayside to the nightside (*i.e.*, sunset) or from the nightside to the dayside (sunrise).

Once the twilight passes listed in Table 1 were identified the actual VAE observations had to be examined in detail to make sure that the instrument was operating normally and to ascertain if the observations were of sufficient quality to satisfy our needs. Since the UA files only contained summary data of the VAE brightness measurements in the zenith, the full time resolution VAE data files had to be inspected.

This was performed using the Fortran program 'VAEREAD' which unpacks the VAE data files and extracts the VAE brightness measurements and the ancillary instrument and orbital data. A listing of the version of VAEREAD used in this project, TWIVAEREAD, is attached as Appendix 2. The program reads the channel 1 or channel 2 photometer counts, converts the observed counts into Rayleighs and makes zodiacal and galactic background corrections where possible. The program creates two output text (ASCII) files. One of the files lists sequentially the following quantities:

(1) The universal time in milliseconds

(2) The observed 7320 Å brightness in captured Rayleigh units

(3) The estimated error in the observed brightness based on the photometer count rate

(4) The satellite altitude in kilometers

(5) The zenith angle of the photometer line of sight in degrees

(6) The solar zenith angle at the satellite in degrees

The second output file contains the following quantities:

(1) The universal time in milliseconds

(2) The x, y and z coordinates of the satellite position in the Geocentric Equatorial Inertial (GEI) system (see *Russell*, 1971)

(3) The x, y and z coordinates of the sun in the GEI system

(4) The x, y and z coordinates of the photometer line-of-sight in the GEI system

Detailed examination of the high resolution VAE data for the orbits listed in Table 1 revealed that in many instances, particularly in the case of the channel 1 data, the observations were seriously and irrevocably contaminated by stars or that the zodiacal and galactic background corrections could not be performed. Furthermore, although the VAE instrument was equipped with a sophisticated baffle system, close examination of the data revealed that the twilight observations made at low elevations towards the sun were often contaminated by scattered sunlight. Because of these various undesirable effects most of the twilight passes listed in Table 1 had to be rejected. Having identified the passes which contained potentially useful data a final selection criterion then had to applied.

As described in Section 3 the ground-based thermospheric monitoring technique, and the twilight inversion procedure, require twilight 7320 Å measurements made in the zenith and at lower elevation towards the azimuth of the sun, i.e. the observations are made in a plane that is perpendicular or nearly perpendicular to the plane of the terminator. However, because of seasonal effects and the 20 degree inclination of the AE-E orbit, the angle between the orbital plane of the satellite and the plane of the terminator varied considerably and on many of the twilight passes the plane of the spin scan observations was not perpendicular to, or nearly perpendicular to, the plane of the terminator. Consequently, only a small number of the twilight passes listed in Table 1 actually provided observations of sufficient quality made under the appropriate geometry for testing the inversion algorithm. Of these the potentially most useful observations were the channel 2 sunset observations made on orbit 6855 and the channel 1 sunset observations made on orbit 7012.

Table 1.

AE-E spin twilight passes with OSS, NATE and VAE 7320 Å observations

Date yyddd	Orbit #	Channel #	Spin mode	Start time	End time	Condition
77003	5811	2	normal	25725	27165	sunrise
77007	5874	1	normal	19005	19830	sunrise
77007	5878	2	normal	40500	41295	sunrise
77007	5884	1	normal	72585	73485	sunrise
77009	5912	2	normal	50085	50910	sunrise
77009	5913	2	normal	53430	54540	sunset
77009	5913	2	normal	55155	55455	sunrise
77016	6019	2	normal	18495	18915	sunset
77016	6025	1	normal	50565	51165	sunset
77016	6029	2	normal	71955	72660	sunset
77040	6415	2	normal	68505	69495	sunrise
77047	6525	2	normal	52785	53865	sunset
77047	6525	2	normal	54540	54975	sunrise
77052	6597	1	normal	8910	9345	sunrise
77052	6612	2	normal	83970	84315	sunrise
77063	6776	1	inverted	19590	20505	sunset
77063	6777	1	normal	21495	22410	sunrise
77068	6855	2	inverted	12660	13560	sunset
77077	7012	1	normal	73320	74235	sunset
77077	7012	1	normal	75225	76140	sunrise
77081	7075	2	normal	65850	66810	sunset
77081	7075	2	normal	67725	68685	sunrise
77087	7168	1	normal	47970	48870	sunset
77087	7169	1	normal	51405	52320	sunrise
77100	7372	2	inverted	21795	22455	sunset
77100	7373	2	inverted	26790	27165	sunset
77108	7497	1	inverted	3045	4065	sunset
77108	7497	1	inverted	4875	5895	sunrise
77132	7895	1	inverted	60435	61005	sunset
77132	7895	1	inverted	61935	62895	sunrise
77132	7896	1	inverted	65445	65820	sunset
77138	7980	2	inverted	945	1305	sunset
77138	7980	2	inverted	1995	3075	sunrise
77142	8055	1	inverted	59115	60545	sunset
77142	8055	1	inverted	60545	61980	sunrise
77146	8122	2	inverted	76115	77550	sunrise
77155	8257	1	inverted	24075	24990	sunset
77176	8600	1	inverted	50265	50565	sunset
77176	8600	1	inverted	51435	52440	sunrise
77176	8601	1	inverted	54975	55645	sunset
77181	8672	2	inverted	6960	8375	sunset
77181	8672	2	inverted	45045	45525	sunrise
77364	11617	2	normal	55620	56820	sunrise
77364	11618	2	normal	59355	60450	sunset

5. INVERSION CODE MODIFICATIONS FOR INVERTING THE SATELLITE DATA

As already mentioned, the ground-based twilight inversion algorithm is designed to deal with observations made in the zenith and at low elevation in the azimuth of the sun. Since the spin plane of the twilight VAE observations was rarely oriented perpendicular to the plane of the terminator, the inversion algorithm had to be modified to allow for the finite angle between the azimuth of the sun and the photometer line-of-sight.

In order to allow for this effect the program which was used to read the VAE data files, TWIVAEREAD, was modified to extract the Geocentric Equatorial Inertial coordinates of (i) the satellite position vector, (ii) the sun vector, and (iii) the vector of the VAE photometer line-of-sight, as well as the observed 7320 Å column emission rates and photometer zenith angles. These vectors were then used within the inversion algorithm to calculate the local solar zenith angle at various intervals along the photometer line-of-sight. The section of code dealing with this problem is incorporated in the line integral calculation performed by the procedure 'BRIGHT' which appears on pages 5 and 6 of the listing given in Appendix 3.

Other modifications had to be made to the inversion code to allow for the fact that many of the VAE observations were made at smaller solar depression angles than would be accessible from the ground. In the case of ground-based observations tropospheric scattering of sunlight makes it very difficult to obtain good $O^+(^2D-^2P)$ 7320-30 Å measurements until the solar depression angle at the observing site is greater than about 7 degrees for zenith observations and about 12 degrees for low elevation angle sunward observations (*Meriwether et al.* ,1978; *Noxon and Norton,* 1979; *Fennelly et al.*, 1991; *McDade et al.*, 1991). However, tropospheric scattering does not interfere with the satellite measurements and good twilight data were obtained for satellite solar depression angles down to zero degrees. It was considered valuable to include these 'early' twilight observations but the early observations made at low photometer elevation angles inevitably included contributions from regions of space lying on the dayside of the terminator where the local solar zenith angle, β, was less than 90 degrees. The line integral calculation section of the original inversion code, procedure BRIGHT, was therefore modified to deal with this situation by including brightness contributions from both sides of the terminator. For contributing elements with local solar zenith angles greater than 90 degrees the grazing incidence Chapman function was used to calculate the optical depth as explained in Section 2 (equation 7). For elements with local solar zenith angles less than 90 degrees the normal Chapman function was used and the optical depth at each wavelength, λ_i , was calculated from the expression

$$\tau_i(z,\beta) = \{[O]_z \times H_O \times \sigma_i^O \times Ch(\beta, H_O)\} + \{[N_2]_z \times H_{N_2} \times \sigma_i^{N_2} \times Ch(\beta, H_{N_2})\} \quad (8)$$

where z is the altitude of the contributing element and $[O]_z$ and $[N_2]_z$ are the inferred atomic oxygen and molecular nitrogen densities at that height. The relevant section of the inversion code appears on pages 5 and 6 of Appendix 3.

6. RESULTS FROM THE INVERSIONS OF SELECTED SATELLITE ORBITS

In an ideal world it would be more desirable to test the inversion algorithm using the observations made with the narrow channel of the VAE instrument (channel 1). However, the narrow channel was about 50 times less sensitive than the wide channel and the advantages of using the channel with the smaller field of view (and shorter integration period) were strongly outweighed by the much higher signal to noise ratio in the channel 2 observations. Nevertheless, it was considered instructive to test the algorithm using both the wide channel and the narrow channel observations.

6.1 *Wide Channel Results - Orbit 6855*

For the purposes of this study the best VAE channel 2 twilight observations were the sunset observations made on orbit 6855 on day 68 of 1977. When the measurements were made the satellite was in a near circular orbit at a latitude of 12 °N, a longitude of 215 °E and an altitude of 257 km. The solar $F_{10.7}$ flux value for the day was 80.3 and the Ap index was 38. The angle between the orbital plane and the terminator was approximately 80 degrees as the satellite crossed the terminator and the angle between the azimuth of the photometer scan and the azimuth of the sun was 10.2 degrees. Although it was important to have the latter angle as small as possible (see Section 4), it did mean that the observations made at the lowest elevations in the sunward direction were prone to contamination by scattered sunlight. To avoid the danger of using observations with solar contamination we only considered the observations which were made when the angle between the sun and photometer line-of-sight was greater than 40 degrees. As a result, the analysis was restricted to zenith observations and sunward observations made at elevation angles greater than ~35 degrees. In Figure 2 we show part of the sequence of $O^+(^2D-^2P)$ 7320 Å column emission rates measured during the sunset pass of orbit 6855. The solid symbols show the 7320 Å emission rates measured when the photometer elevation angle at the midpoint of the sample integration period was within ± 5 degrees of the zenith direction; the open symbols show the emission rates measured in the sunward direction when the photometer elevation angle was between 35 and 45 degrees. Both sets of observations are plotted against the solar zenith angle at the satellite which was increasing with time. The satellite was spinning at approximately 4 revolutions per minute and the measurements shown in Figure 2 span a total observing period of about 5 minutes.

A comparison of the data shown in Figures 2 and 3 reveals the similarity between the VAE twilight measurements and the simulated ground-based observations discussed by *McDade et al.*, (1991). It should be noted, however, that relative to the zenith observations the sunward observations of Figure 2 are weaker than those of Figure 3. This is primarily due to the fact that the sunward VAE observations were made at an elevation angle of 40±5 degrees and the sunward simulations were calculated for an elevation of only 20 degrees. It is also evident that the uncertainties in the VAE measurements are considerably larger than those of the ground-based simulations in spite of the fact that the satellite observations were made in the absence of any tropospheric background scattering. However, it has to be recognized that each of the satellite observations was obtained with a sample integration period of only 0.125 seconds whereas the ground-based simulations were calculated for a one minute integration period using an instrument with a larger throughput. It should also be pointed out that not all of the scatter evident in the VAE observations is to be associated with noise because much of it is due to variations in the photometer elevation angle within the plotted ±5 degree elevation angle bands. This occurs because the satellite was spinning at approximately 24 degrees per second and the photometer counts were sampled every 0.125 seconds, therefore, there were usually three observations made on each spin between the elevation angles of 35 and 45 degrees and three observations made within ±5 degrees of the zenith. Since the observed twilight brightness depends on both the photometer elevation angle and the solar depression angle, the ±5 degree spread in elevation angles contributes to the scatter which should be greater in the case of the sunward viewing observations.

When the 7320 Å emission rates of Figure 2 were corrected for the $O^+(^2D\text{-}^2P)$ 7320 Å and 7330 Å doublet filter capture functions and processed using the twilight inversion program (see Appendix 3) the algorithm returned the following set of fitting parameters :

(i) an atomic oxygen scale height of $H_O = 62 \pm 3.4$ km

(ii) an oxygen atom density at 250 km of $[O]_{250} = 1.4 \pm 0.3 \times 10^9$ cm^{-3}

and (iii) an unattenuated $O^+(^2P)$ ionization frequency of $I^* = 6.2 \pm 0.6 \times 10^{-8}$ sec^{-1}

The fitting parameters were not found to depend significantly upon the first guess values used to initiate the inversion procedure although the number of iterations required to reach convergence did of course depend upon the initial guess. The fits to the zenith and sunward observations obtained using these best fit parameters are shown in Figures 4 and 5. In the case of the sunward observations, Figure 5, the fit is 'saw toothed' rather than smooth because of the ±5 degree spread in the elevation angles discussed above. Since the twilight brightness should not vary so strongly between +5 and -5 degrees of the zenith this effect does not show up in the fit to the zenith observations.

Clearly, the parameters recovered from the fit to the orbit 6855 observations do reproduce fairly well the input data. More significantly, however, they also reproduce the orbit 6855 observations that were not used in the inversion, *i.e.* the recovered fitting parameters also reproduce the VAE observations that were not used to obtain the parameters. This is illustrated in Figures 6, 7, 8 and 9 which show the fits to the sunward observations that were made at elevation angles in the ranges 45 to 55 degrees, 55 to 65 degrees, 65 to 75 degrees and 75 to 85 degrees.

The neutral atmospheric temperatures measured at 257 km by the *Neutral Atmosphere Temperature Experiment* (*NATE*) as the satellite passed through the sunset terminator on orbit 6855 varied between about 870 K and 950 K. Since the recovered atomic oxygen scale height of 62 ± 3.4 km is equivalent to an exospheric temperature of 970 ± 50 K we see that the thermospheric temperature inferred from the twilight observations is in very good agreement with the *NATE* temperature measurements. Similarly, the average atomic oxygen density measured by the *Open Source Mass Spectrometer* (*OSS*) during the twilight pass was 9 x 10^8 cm^{-3} at 257 km which compares very favorable with the inferred density of 1.2 ± 0.3 x 10^9 cm^{-3} based on the recovered density at 250 km and a scale height of 62 km. In Figure 10 we show how the atomic oxygen density profile constructed from the recovered fitting parameters H_O and $[O]_{250}$ compares with the profile based on the *NATE* temperature and the *OSS* density measurements. Figure 10 also shows the atomic oxygen density profile given by the MSIS-86 model (*Hedin*, 1987) for the sunset conditions on orbit 6855.

The value for the unattenuated $O^+(^2P)$ ionization frequency obtained from the inversion of the orbit 6855 channel 2 observations will be discussed in Section 7.

6.2 *Narrow Channel Results - Orbit 7012*

The best channel 1 twilight 7320 Å observations were those obtained on the sunset pass of orbit 7012 on day number 77 of 1977. When these observations were made the satellite was in a circular orbit at a latitude of 16 ^{o}N, a longitude of 322 ^{o}E and an altitude of 251 km. The solar $F_{10.7}$ flux value for the day was 75, the Ap index was 11 and the angle between the azimuth of the photometer scan plane and the azimuth of the sun was 14.5 degrees. As already mentioned the signal to noise ratios of the channel 1 observations were very much lower than those of the channel 2 observations. This is clearly illustrated in Figure 11 which shows the orbit 7012 channel 1 observations made within ±5 degrees of the zenith direction. Because of the low signal to noise ratios in the data it was not possible to simply invert the channel 1 observations made within ±5 degrees of the zenith and between 35 and 45 degrees elevation towards the sun, *i.e.* the very large uncertainties associated with the recovered fitting parameters rendered the inversion meaningless. However, somewhat more meaningful results were obtained when all of the observations acquired between elevations of 35 degrees and the zenith were considered. The entire set of observations obtained between satellite solar zenith angles of 90 and 105 degrees in the zenith and sunward in the elevation angle bands 35-45 , 45-55 , 55-65 , 65-75 and 75-85 degrees are shown in Figure 12.

When this entire set of observations was inverted the inversion algorithm returned the following set of best fit parameters:

(i) an atomic oxygen scale height of $H_O = 76 \pm 14$ km

(ii) an oxygen atom density at 250 km of $[O]_{250} = 7.0 \pm 0.4 \times 10^8$ cm^{-3}

and (iii) an unattenuated $O^+(^2P)$ ionization frequency of $I^* = 9.6 \pm 3.5 \times 10^{-8}$ sec^{-1}

The fit to the entire set of orbit 7012 observations obtained using these parameters is shown by the solid line through the smoothed data points in Figure 12.

The average neutral atmospheric temperature measured at 251 km by the *Neutral Atmosphere Temperature Experiment* (*NATE*) as the satellite passed through the sunset terminator on orbit 7012 was 880 K and the average atomic oxygen density measured by the *Open Source Mass Spectrometer* (*OSS*) during the same period was 1.0×10^9 cm^{-3}. Clearly, the recovered oxygen density of $7.0 \pm 0.4 \times 10^8$ cm^{-3} at 250 km agrees with the *OSS* measured density within the uncertainty limits. The recovered atomic oxygen scale height of 76 ± 14 km is equivalent to an exospheric temperature of 1180 ± 220 K which is somewhat hotter than the *NATE* measured temperature of 880 K.

6.3 *Results at Higher Levels of Solar Activity - Orbit 24564*

In order to rigorously assess the twilight inversion procedures it was considered highly desirable to test the inversion algorithm using VAE observations made at both low and high levels of solar activity. Unfortunately, most of the twilight passes which satisfied the primary selection criteria outlined in Section 3, and which contained data of a sufficiently high quality, were made at low levels of activity. However, there were a small number of passes made in 1980 close to solar maximum for which oxygen atom data were not available but which did involve channel 2 observations made when the satellite was spinning. One of these high activity orbits which contained apparently good data was orbit number 24564 on day 100 of 1980. The twilight observations made on the sunset pass of orbit 24564 towards the zenith and towards the sun at an elevation of 40±5 degrees are shown in Figure 13. When these observations were made the AE-E satellite was in a circular orbit at a latitude of 6.6 °N, a longitude of 80.4 °E and an altitude of 419 km. The solar $F_{10.7}$ flux value for the day was 244, the Ap index was 20, the angle between the azimuth of the photometer scan plane and the azimuth of the sun was 3.5 degrees and the satellite was operating in the inverted spin mode.

When the orbit 24564 column emission rates shown in Figure 13 were inverted the inversion procedure returned the following set of best fit parameters:

(i) an atomic oxygen scale height of $H_O = 94 \pm 8$ km

(ii) an oxygen atom density at 250 km of $[O]_{250} = 2.5 \pm 0.3 \times 10^9$ cm^{-3}

and (iii) an unattenuated $O^+(^2P)$ ionization frequency of $I^* = 9.3 \pm 1.0 \times 10^{-8}$ sec^{-1}

For the inversion of this data the shape of the EUV flux spectrum used in the algorithm (see Appendix page 14) was based on the 79050 spectrum reported by *Torr et al.* (1979), however, the results obtained from inversions using the shape of the standard F74113 spectrum of *Hinteregger* (1977) were not significantly different. The fits to the zenith and sunward observations obtained using the best fit parameters listed above are shown in Figures 14 and 15.

The average neutral atmospheric temperature measured by the *Neutral Atmosphere Temperature Experiment* (*NATE*) as the satellite passed through the sunset terminator on orbit 24564 was 1630 K and this compares quite favorable with the temperature of 1470 ± 120 K inferred from the recovered atomic oxygen scale height of 94 ± 8 km. Unfortunately, *OSS* oxygen atom data was not available for this orbit but the recovered density of 2.5 ± 0.3 x 10^9 cm^{-3} at 250 km compares very well with the density of 2.2 x 10^9 cm^{-3} given for the conditions by the MSIS-86 model (*Hedin*, 1987). However, as we will discuss in the next section, the recovered $O^+(^2P)$ ionization frequency of I* = 9.3 ± 1.0 x 10^{-8} sec^{-1} is substantially lower than might be expected for conditions close to solar maximum.

7. DISCUSSION AND CONCLUSIONS

The results described in the previous section clearly demonstrate that the inversion procedures for recovering thermospheric temperatures and atomic oxygen densities from bi-directional ground-based measurements of the $O^+(^2D-^2P)$ 7320 Å twilight airglow emission performed well when tested with the proxy satellite data. The atomic oxygen densities recovered from the inversions are in reasonable good agreement with the densities measured by the *Open Source Mass Spectrometer* on the AE-E satellite. The thermospheric temperatures inferred from the recovered atomic oxygen scale heights are also in reasonably good agreement with the measurements made on the satellite by the *Neutral Atmosphere Temperature Experiment*. Furthermore, the temperatures are also in good agreement with the temperatures that have been deduced using other techniques. This is illustrated in Figure 16 which shows how the temperatures recovered for orbits 6855, 7012 and 24564 compare with the temperatures deduced by *Yee and Abreu* (1982) from an analysis of the late twilight 7320 Å zenith intensities measured on these and other AE-E orbits.

The unattenuated $O^+(^2P)$ ionization frequencies recovered for orbits 6855 and 7012 are in good agreement with previous evaluations but the ionization frequency recovered for orbit 24564 is somewhat smaller than might be expected for conditions close to solar maximum. The solar cycle dependence of the $O^+(^2P)$ ionization frequencies has been studied by *Torr et al.* (1979) who used the solar EUV flux measurements on the Atmosphere Explorer satellites (*Hinteregger.*, 1977) to calculate the ionization frequencies on five selected days during the 1974 to 1979 period. *Abreu et al.* (1980) have also investigated the solar cycle dependence of the $O^+(^2P)$ ionization frequencies and used dayglow 7320 Å measurements made with the VAE instrument to determine the frequencies during the increasing phase of solar cycle 21. The ionization frequencies obtained from the work of *Torr et al.* (1979) and *Abreu et al.* (1980) are shown in Figures 17 and 18 where they are compared with the frequencies recovered here from the VAE twilight observations on orbits 6855, 7012 and 24564. Clearly, the frequencies recovered from orbits 6855 and 7012 are consistent with what should be expected at low levels of activity but the orbit 24564 frequency is not in keeping with the trends in the previous evaluations. Because of the lack of appropriately conditioned high activity twilight observations it is difficult to determine whether or not the seemingly low ionization frequency for orbit 24564 is indicative of a problem with the inversion algorithm. It is important to note, however, that the atomic oxygen scale height and densities recovered from the inversion of the orbit 24564 data are in good agreement with the temperatures measured on the satellite and the densities predicted by the MSIS-86 model. We should also point out that if the orbit 24565 observations are inverted with the $O^+(^2P)$ ionization frequency constrained to a value that is in keeping with the trends shown in Figure 18, then the recovered atomic oxygen scale height and densities are no longer in good agreement with the measured and modelled densities and temperatures. For example, if the ionization frequency is constrained to 1.3 x 10^{-7} sec^{-1} then the inversion algorithm returns an oxygen atom density at 250 km of 2.5 x 10^9 cm^{-3} and a thermospheric temperature of only 1320 K. It is possible, however, that the seemingly low value for the orbit 24564 ionization frequency is simply a reflection of (a) the natural variability of this quantity and (b) an incomplete correlation between the $O^+(^2P)$ ionization frequencies and the $F_{10.7}$ radio flux. We do note, for example, that the relative displacement of the orbit 24564 frequency from the trend line in Figure 18 is not inconsistent with the scatter in the measured frequencies at low $F_{10.7}$ flux values.

8. ACKNOWLEDGEMENTS

Support for this work under NASA Grant No. NAG 5-1502 to the University of Michigan's Space Physics Research Laboratory is gratefully acknowledged. We would also like to thank the Principal Investigators and Co-Investigators associated with the *Visible Airglow Experiment* (PIs - P. B. Hays and V. J. Abreu), the *Neutral Atmosphere Temperature Experiment* (PI - N. W. Spencer) and the *Open Source Mass Spectrometer* (PI - A. O. Neir) for providing an excellent aeronomical data base and for making the results of their experiments freely available for this work. We would also like to acknowledge the valuable contributions made to the study by Kris Kontz who participated in the project during the summer of 1991 as part of the National Science Foundation's *Research Experience for Undergraduates Program* at the University of Michigan. We are also greatly indebted to Edward Hume and Gerry Schmitt of the Space Physics Research Laboratory for their help with the AE and VAE data base software. Finally, very special thanks are due to Sam Yee for the excellence of his advice, his encouragement and his interest in the project at all times.

9. REFERENCES

Abreu, V. J., W. R. Skinner, and P. B. Hays, Airglow measurements of the variation of the $O^+(^2P)$ ionization frequency during solar cycle 21, *Geophys. Res. Lett.*, **7**, 109, 1980.

Bevington, P. R., *Data Reduction and Analysis for the Physical Sciences*, McGraw-Hill Book Company , New York, 1969.

Fennelly, J. A., D. G. Torr, P. G. Richards, M. R. Torr, and W. E. Sharp, A method for the retrieval of atomic oxygen density and temperature profiles from ground based measurements of the $O^+(^2D$-$^2P)$ 7320-Å twilight airglow, *J. Geophys. Res.*, **96**, 1263, 1991.

Hedin, A. E., MSIS-86 thermospheric model, *J. Geophys. Res.*, **92**, 4649, 1987.

Hinteregger, H. E., EUV flux variation during end of solar cycle 20 and beginning of cycle 21, observed from AE-C satellite, *Geophys. Res. Lett.*, **4**, 231, 1977.

Meriwether, J. W., Jr., D. G. Torr, and J. C. G. Walker, The $O^+(^2P)$ emission at 7320 Å in twilight, *J. Geophys. Res.*, **83**, 3311, 1978.

Noxon, J. F., and R. B. Norton, Changes in thermospheric composition inferred from twilight $O^+(^2P)$ emission, *Planet. Space Sci.*, **27**, 653, 1979.

McDade, I.C., W. E. Sharp, P. G. Richards, and D. G. Torr, On the inversion of $O^+(^2D$-$^2P)$ 7320 Å twilight airglow observations: A method for recovering both the ionization frequency and the thermospheric oxygen atom densities. *J. Geophys. Res.*, **96**, 259, 1991.

Press, W. H.,B. P. Flannery, S. A. Teukolsky, and W. T. Vetterling, *Numerical Recipes: The Art of Scientific Computing*, Cambridge University Press, New York, 1986.

Richards, P. G., and D. G. Torr, Ratios of photoelectron to EUV ionization rates for aeronomic studies, *J. Geophys. Res.*, **93**, 4060, 1988.

Rusch, D. W., D. G. Torr, P. B. Hays, M. R. Torr and A. O. Neir, Determination of the $O^+(^2P)$ ionization frequency using satellite airglow and particle data and its implications on the EUV solar flux,*Geophys. Res. Lett.*, **3**, 537, 1976.

Rusch, D. W., D. G. Torr, and P. B. Hays, The O II (7319-7330 Å) dayglow, *J. Geophys. Res.*, **82**, 719, 1977.

Russell, C. T., Geophysical coordinate transformations, *Cosmic Electrodynamics* **2**, 184, 1971

Torr, D. G., The photochemistry of the upper atmosphere, in *The Photochemistry of Atmospheres*, edited by J. S. Levine, Academic Press, New York, pp. 165-278, 1985.

Torr, M. R., D. G. Torr, R. A. Ong, and H. E. Hinteregger, Ionization frequency for major thermospheric constituents as a function of solar cycle 21, *Geophys. Res. Lett.*, **6**, 771, 1979.

Torr, M. R., D. G. Torr, P. G. Richards, and S. P. Yung, Mid and Low Latitude Model of Thermospheric Emissions: 1. $O^+(^2P)$ 7320 Å and N_2 2P 3371 Å, *J. Geophys. Res.*, In press 1990.

Yee, J. H. and V. J. Abreu, Exospheric temperatures deduced from 7320- to 7330-Å ($O^+(^2D)$-$O^+(^2P)$) twilight observations, *J. Geophys. Res.*, **87**, 913, 1982.

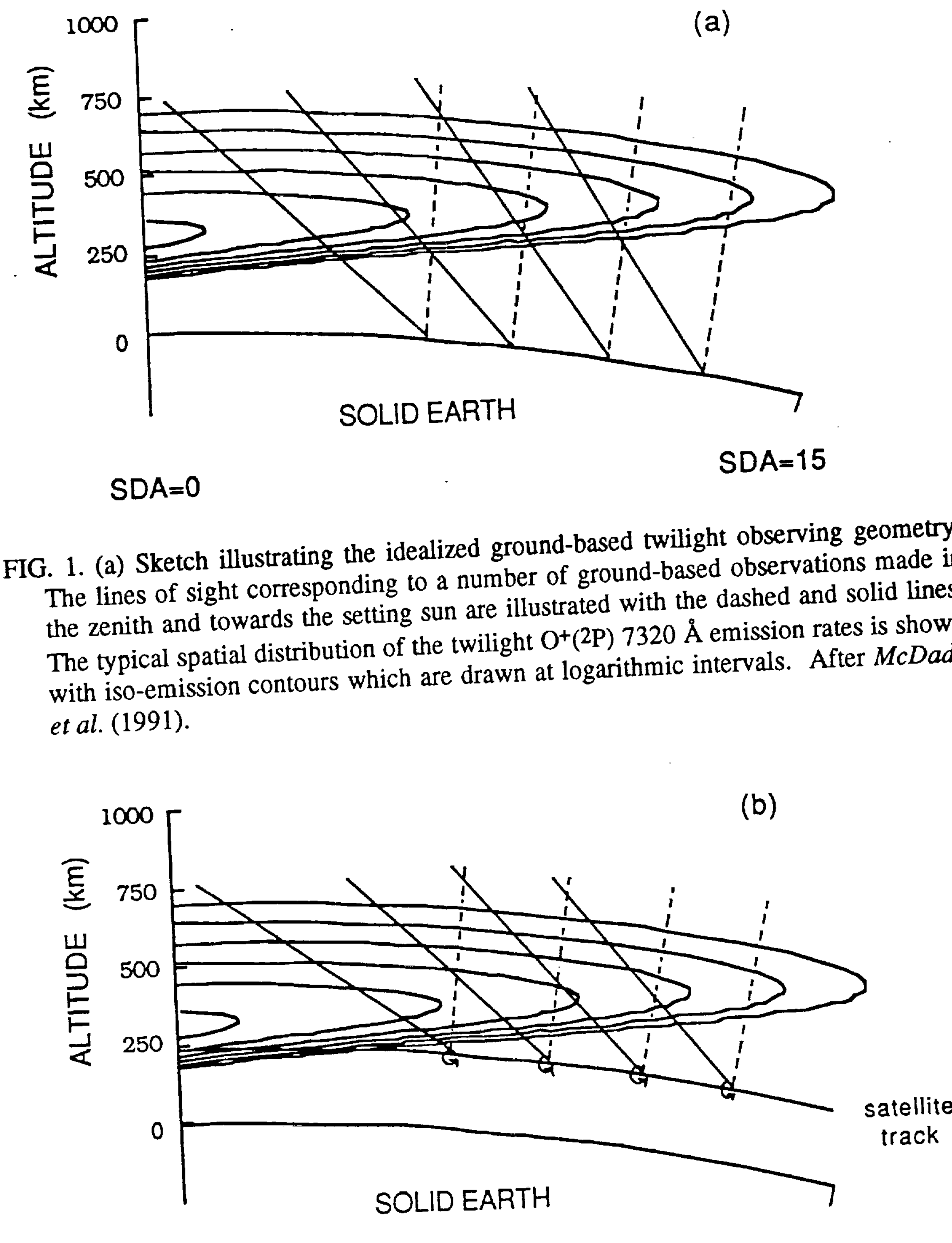

FIG. 1. (a) Sketch illustrating the idealized ground-based twilight observing geometry. The lines of sight corresponding to a number of ground-based observations made in the zenith and towards the setting sun are illustrated with the dashed and solid lines. The typical spatial distribution of the twilight $O^+(^2P)$ 7320 Å emission rates is shown with iso-emission contours which are drawn at logarithmic intervals. After *McDade et al.* (1991).

FIG. 1. (b) Same as Fig. 1a but illustrating how the twilight observations were made with the Visible Airglow Experiment on the AE-E satellite.

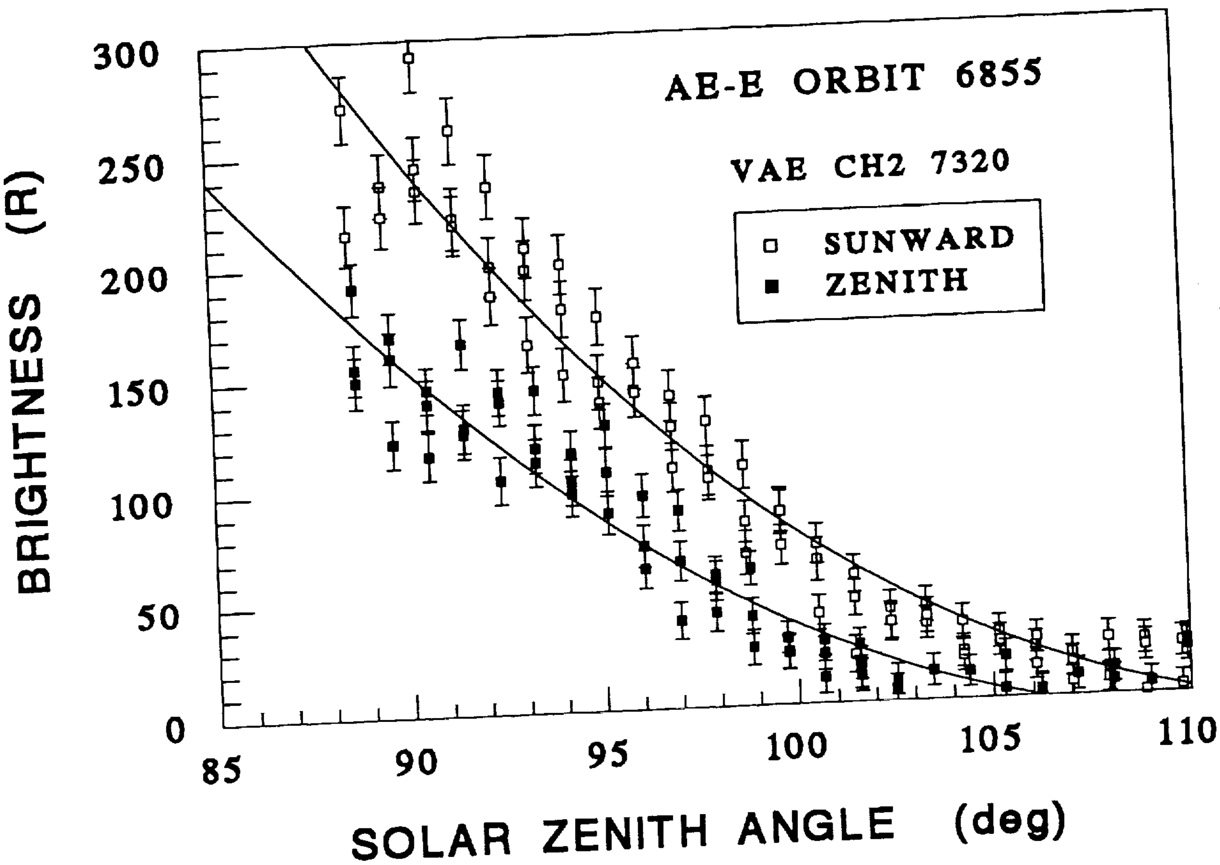

FIG. 2. The zenith and sunward twilight 7320 Å column emission rates measured by the VAE channel 2 on the AE-E sunset pass of orbit 6855. The zenith emission rates (solid squares) were measured within ±5 degrees of the zenith; the sunward emission rates (open squares) were measured at elevation angles ranging from 35 to 45 degrees.

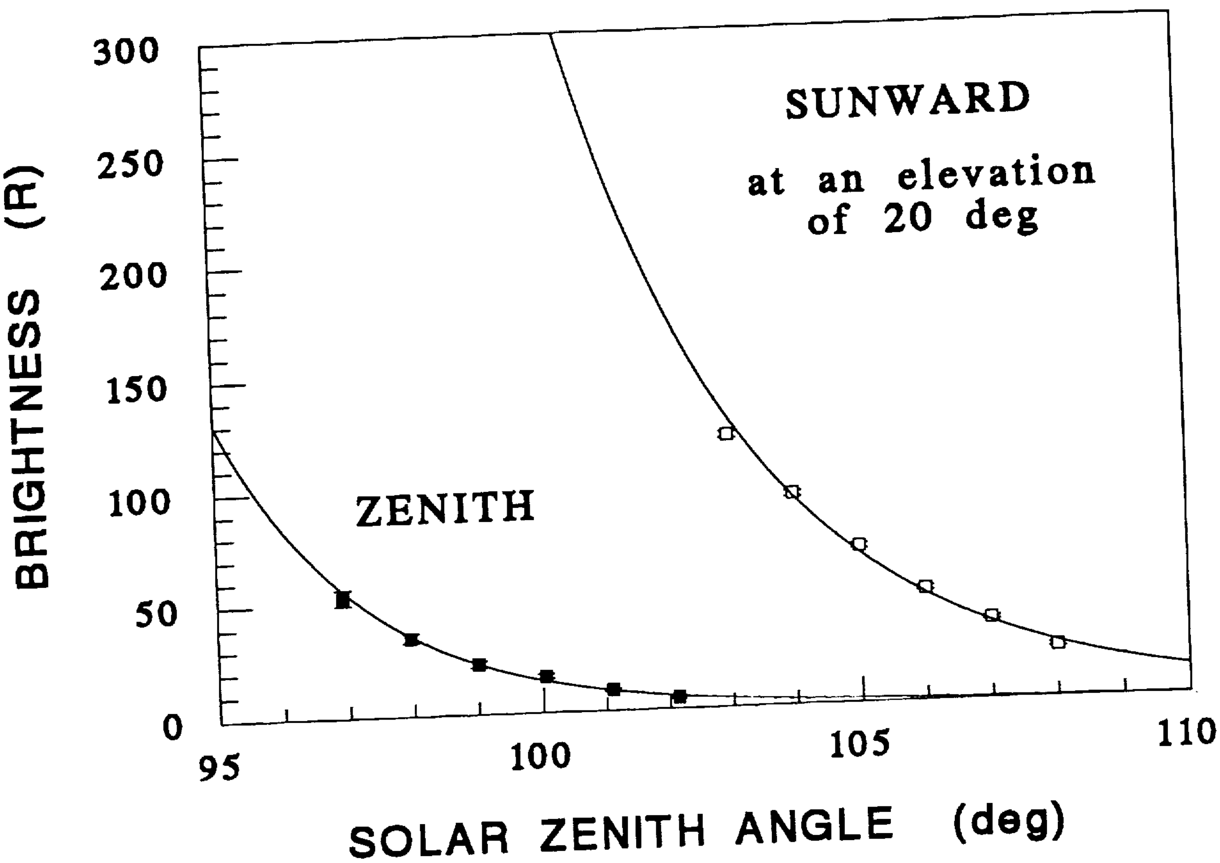

FIG. 3. The simulated ground-based twilight $O^+(^2P)$ 7320 Å observations discussed by *McDade et al.* (1991). The sunward column emission rates were calculated for an elevation of 20 degrees towards the azimuth of the setting sun.

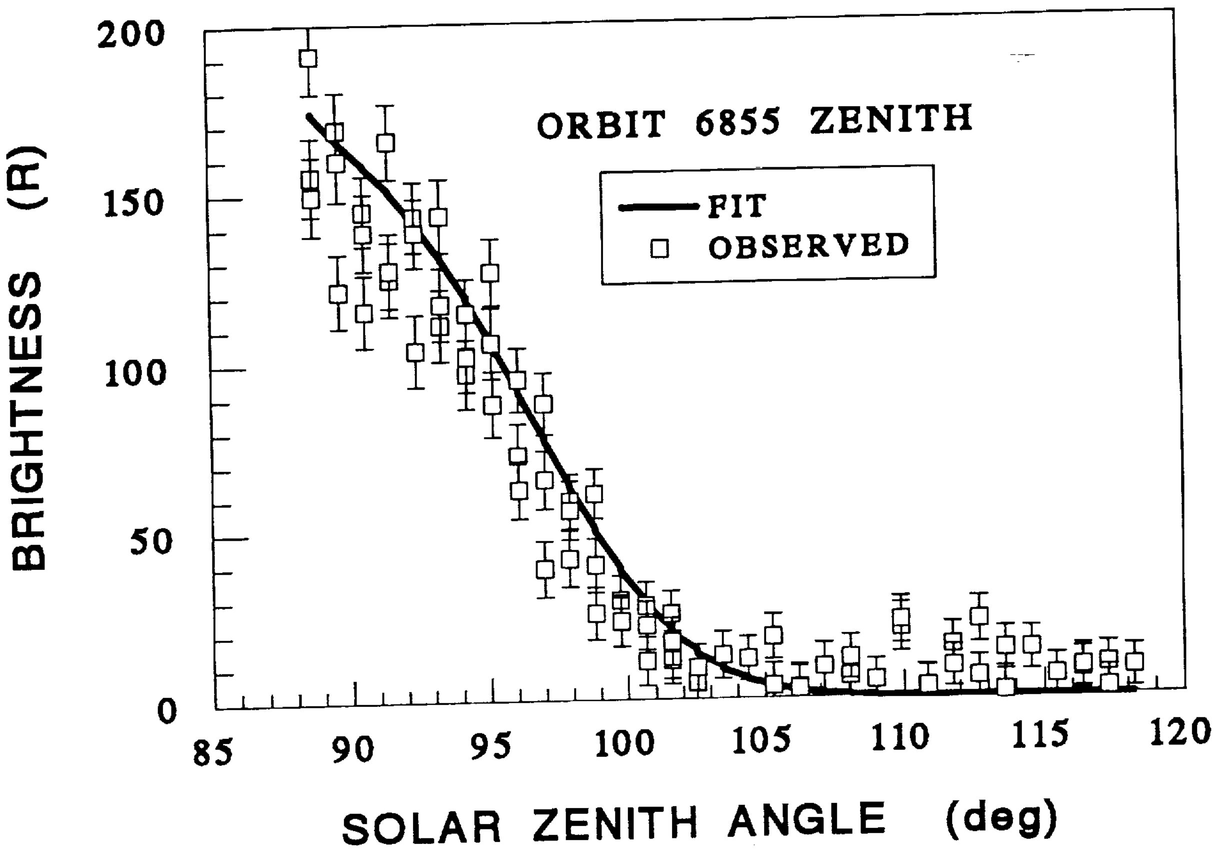

FIG. 4. The channel 2 VAE 7320 Å column emission rates measured within ±5 degrees of the zenith on AE-E orbit 6855 (data points) and the fit obtained using the parameters discussed in the text (solid line).

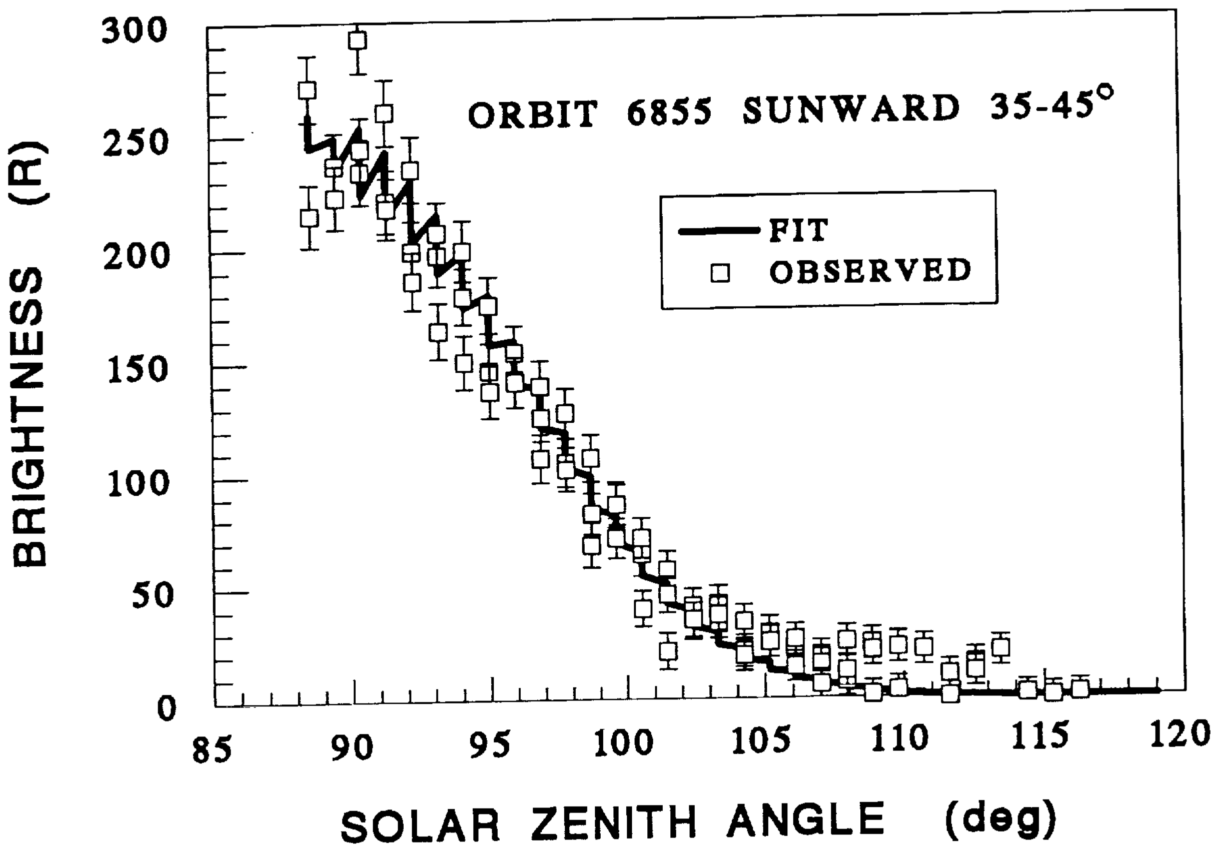

FIG. 5. The channel 2 VAE 7320 Å column emission rates measured in the sunward direction at elevation angles between 35 and 45 degrees on orbit 6855 (data points) and the fit obtained using the parameters discussed in the text (solid line).

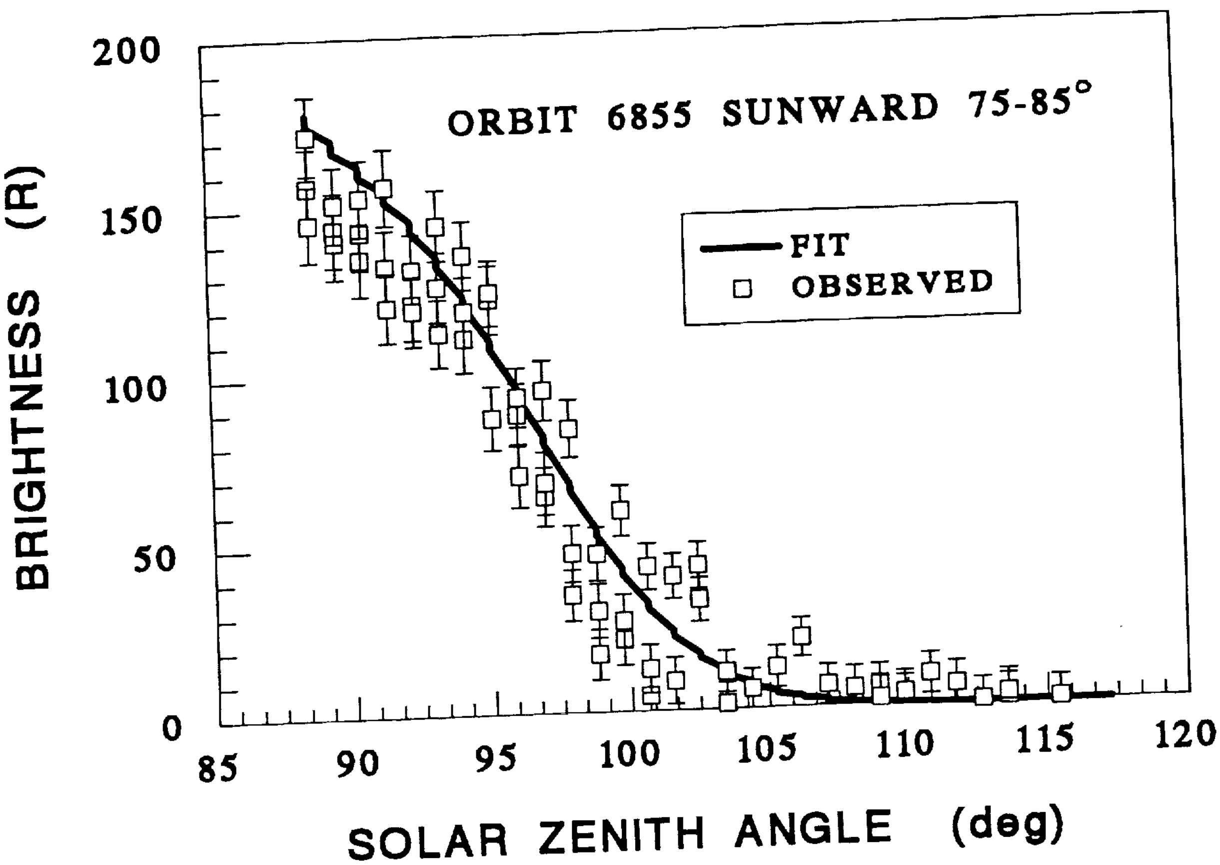

FIG. 6. The channel 2 VAE 7320 Å column emission rates measured in the sunward direction at elevation angles between 75 and 85 degrees on orbit 6855 (data points) and the fit obtained using the parameters discussed in the text (solid line). N.B. these observations were not used to find the fitting parameters.

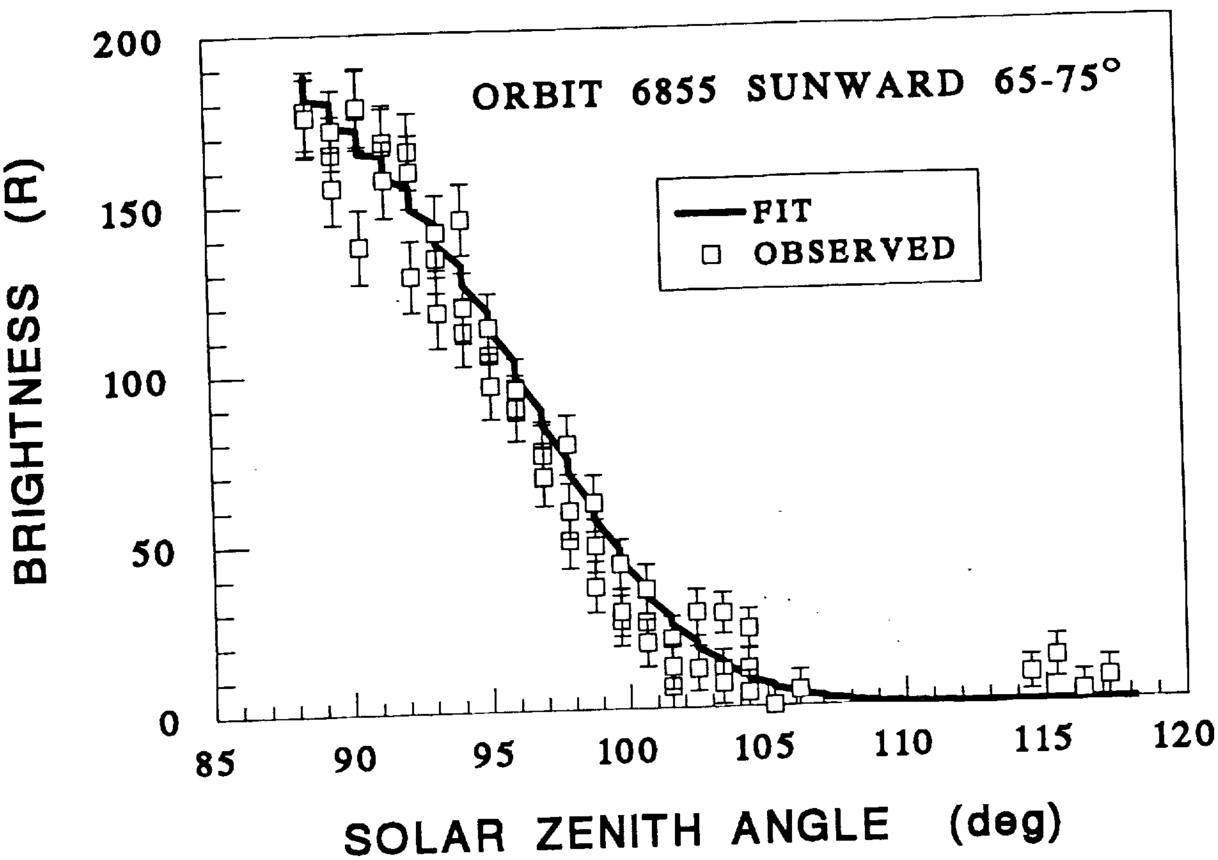

FIG. 7. The channel 2 VAE 7320 Å column emission rates measured in the sunward direction at elevation angles between 65 and 75 degrees on orbit 6855 (data points) and the fit obtained using the parameters discussed in the text (solid line). N.B. these observations were not used to find the fitting parameters.

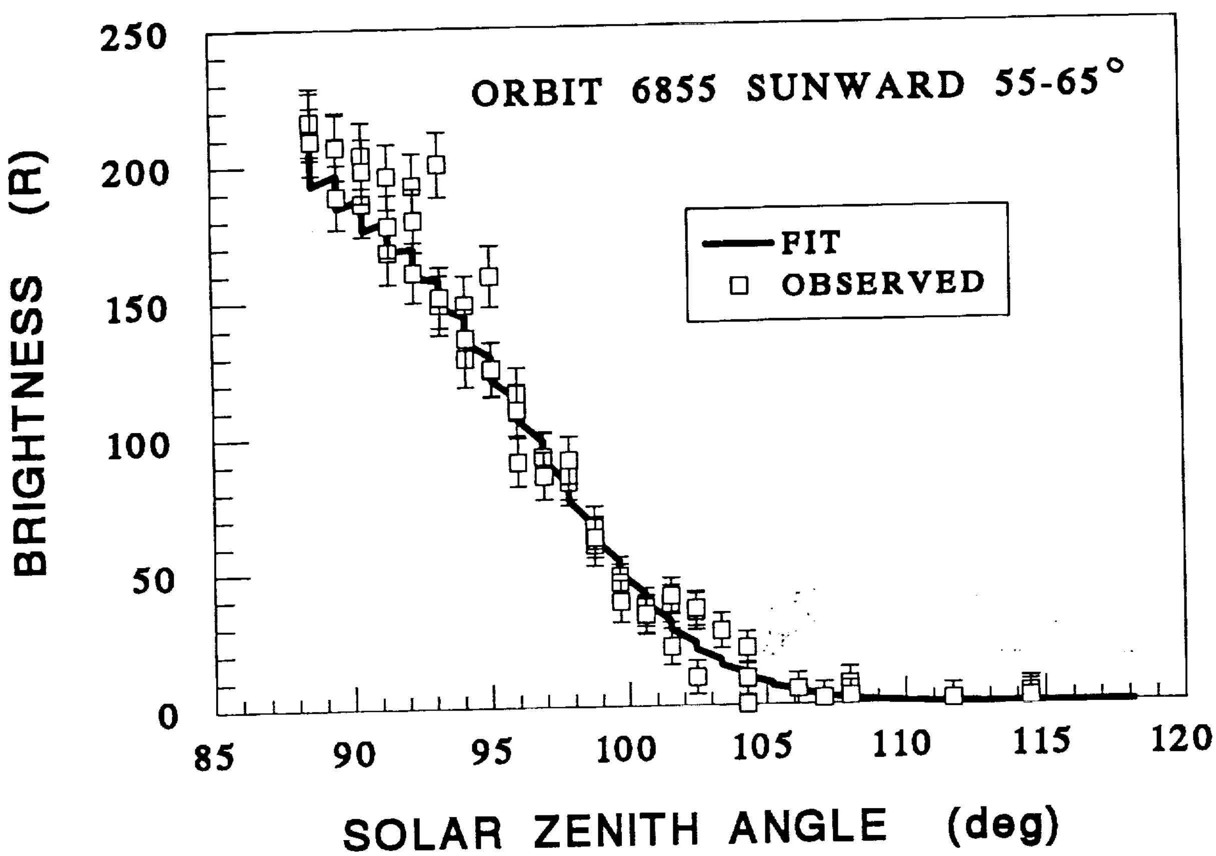

FIG. 8. The channel 2 VAE 7320 Å column emission rates measured in the sunward direction at elevation angles between 55 and 65 degrees on orbit 6855 (data points) and the fit obtained using the parameters discussed in the text (solid line). N.B. these observations were not used to find the fitting parameters.

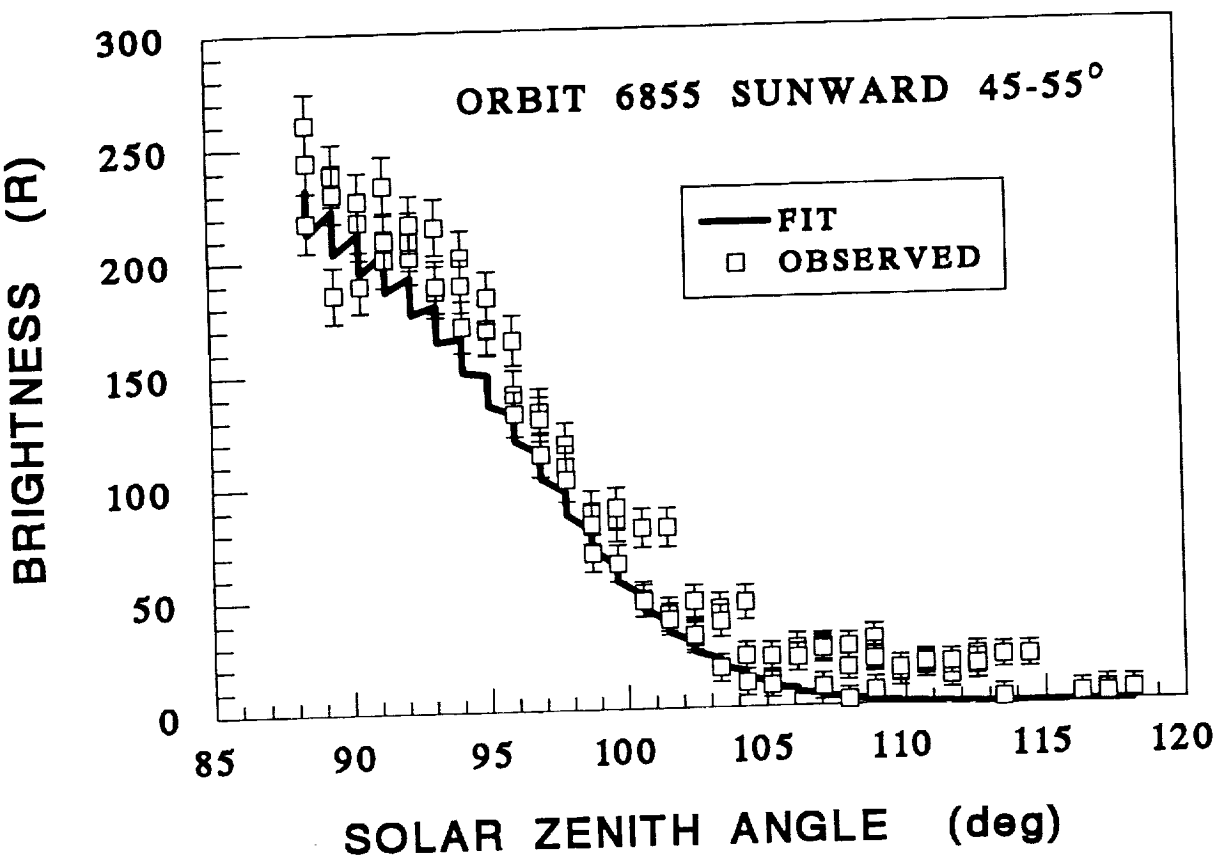

FIG. 9. The channel 2 VAE 7320 Å column emission rates measured in the sunward direction at elevation angles between 45 and 55 degrees on orbit 6855 (data points) and the fit obtained using the parameters discussed in the text (solid line). N.B. these observations were not used to find the fitting parameters.

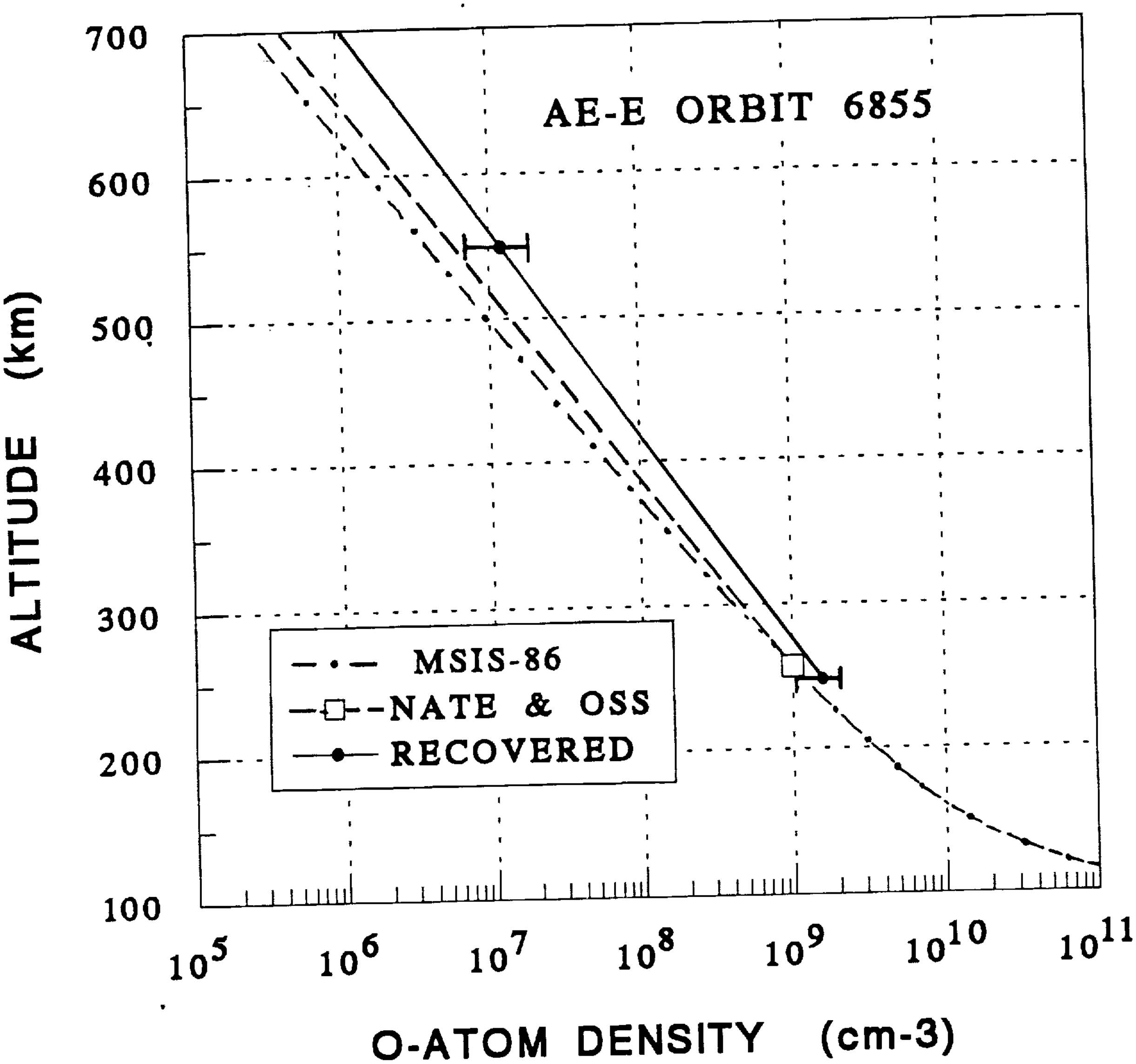

FIG. 10. The atomic oxygen density profile (solid line with error bars) reconstructed using the H_O and $[O]_{250}$ parameters obtained from the fit to the orbit 6855 twilight observations. The profile derived from the temperature and atomic oxygen densities measured by the *NATE* and *OSS* instruments is shown by the open square and dashed line. The atomic oxygen densities from the MSIS-86 model are represented by the dot-dashed curve.

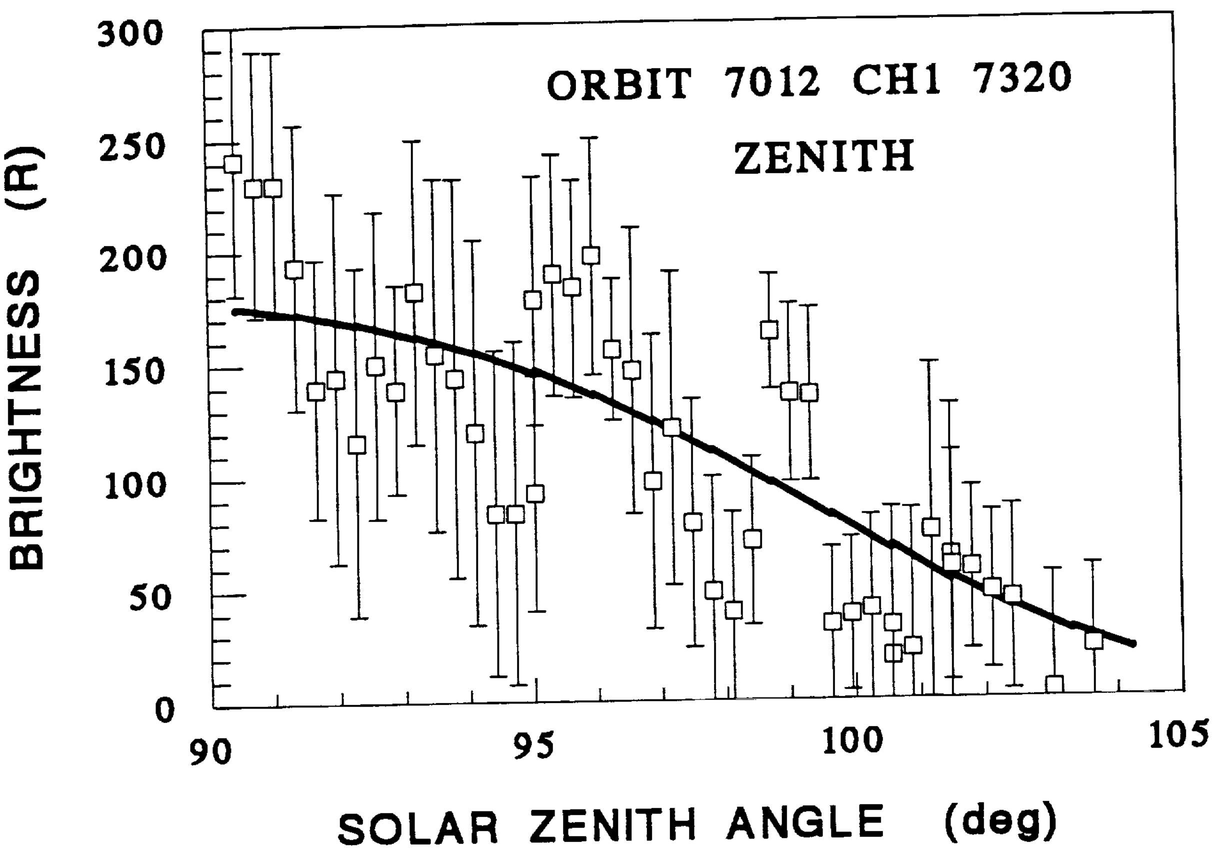

FIG. 11. The channel 1 VAE 7320 Å column emission rates measured within ±5 degrees of the zenith on AE-E orbit 7012 (data points). The emission rates were obtained by averaging the channel 1 counts over four 32 msec integration periods. The plotted data have been smoothed (in both the ordinate and abscissa) using a three point running average to illustrate the underlying trend.

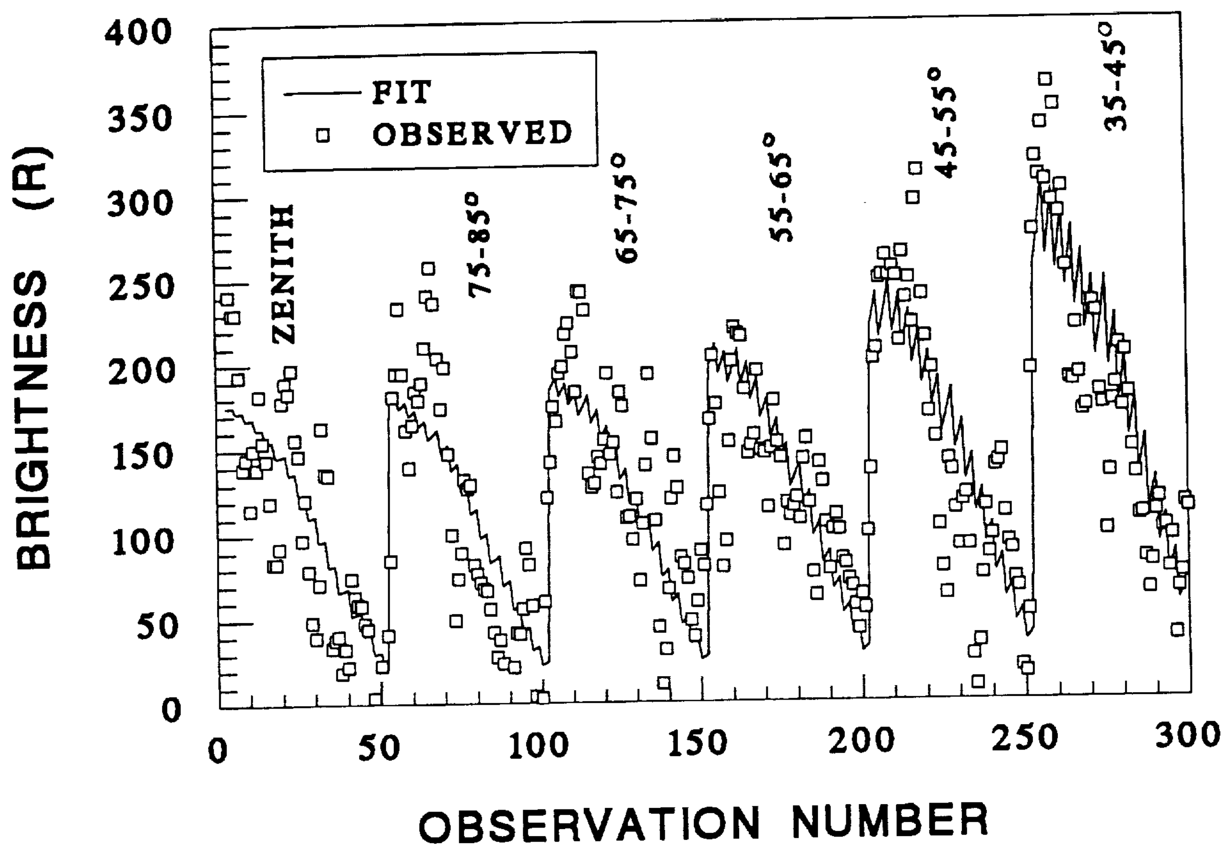

FIG. 12. The orbit 7012 channel 1 VAE 7320 Å column emission rates measured within ±5 degrees of the zenith and sunward in the elevation angle bands 35-45 , 45-55 , 55-65 , 65-75 and 75-85 degrees. Each sequence of 50 points shows how the emission rates varied between the solar zenith angles 90 and 105 degrees. The plotted data have been smoothed as in Fig. 11 to illustrate the underlying trend. The solid line shows the unsmoothed fit obtained using the parameters discussed in the text. N.B. for the inversion described in the text raw unsmoothed data were used.

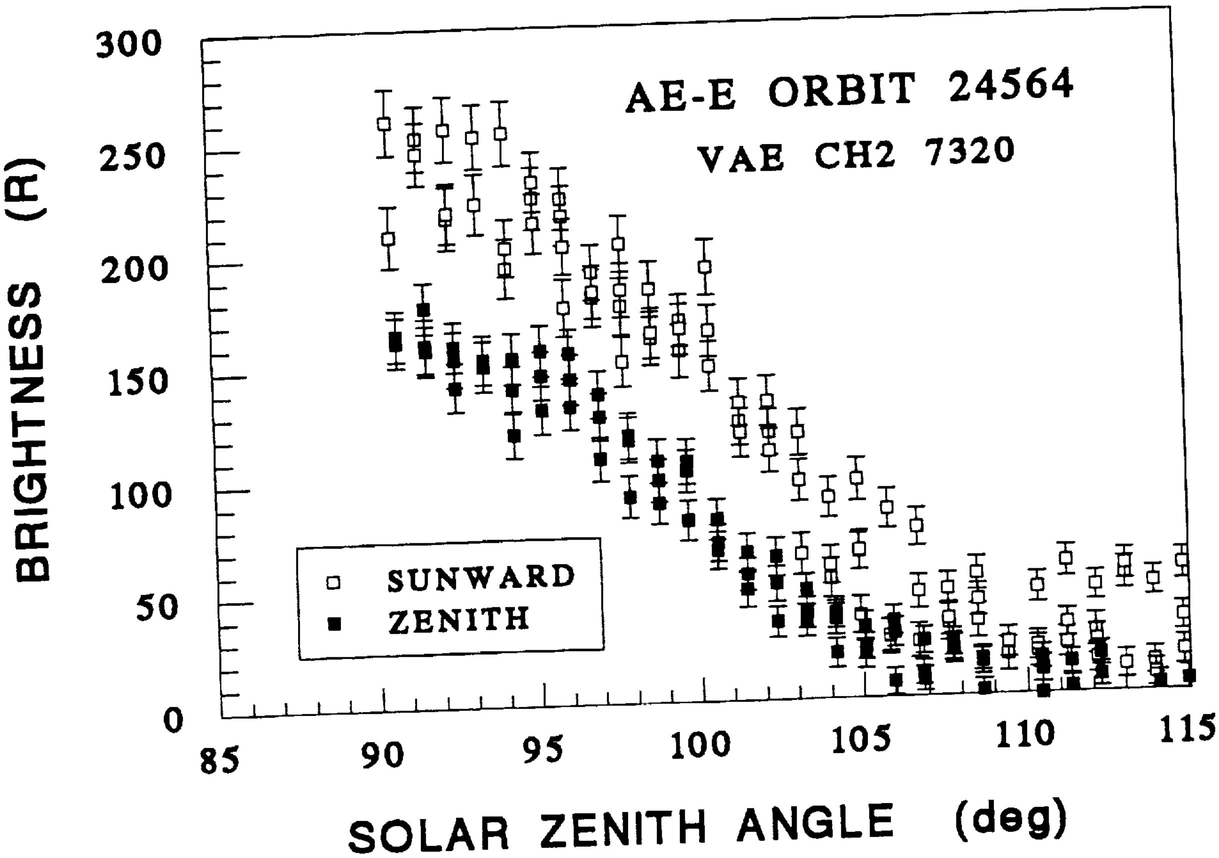

FIG. 13. The zenith and sunward twilight 7320 Å column emission rates measured by the VAE channel 2 on the AE-E sunset pass of orbit 24564. The zenith emission rates (solid squares) were measured within ±5 degrees of the zenith; the sunward emission rates (open squares) were measured at elevation angles between 35 and 45 degrees.

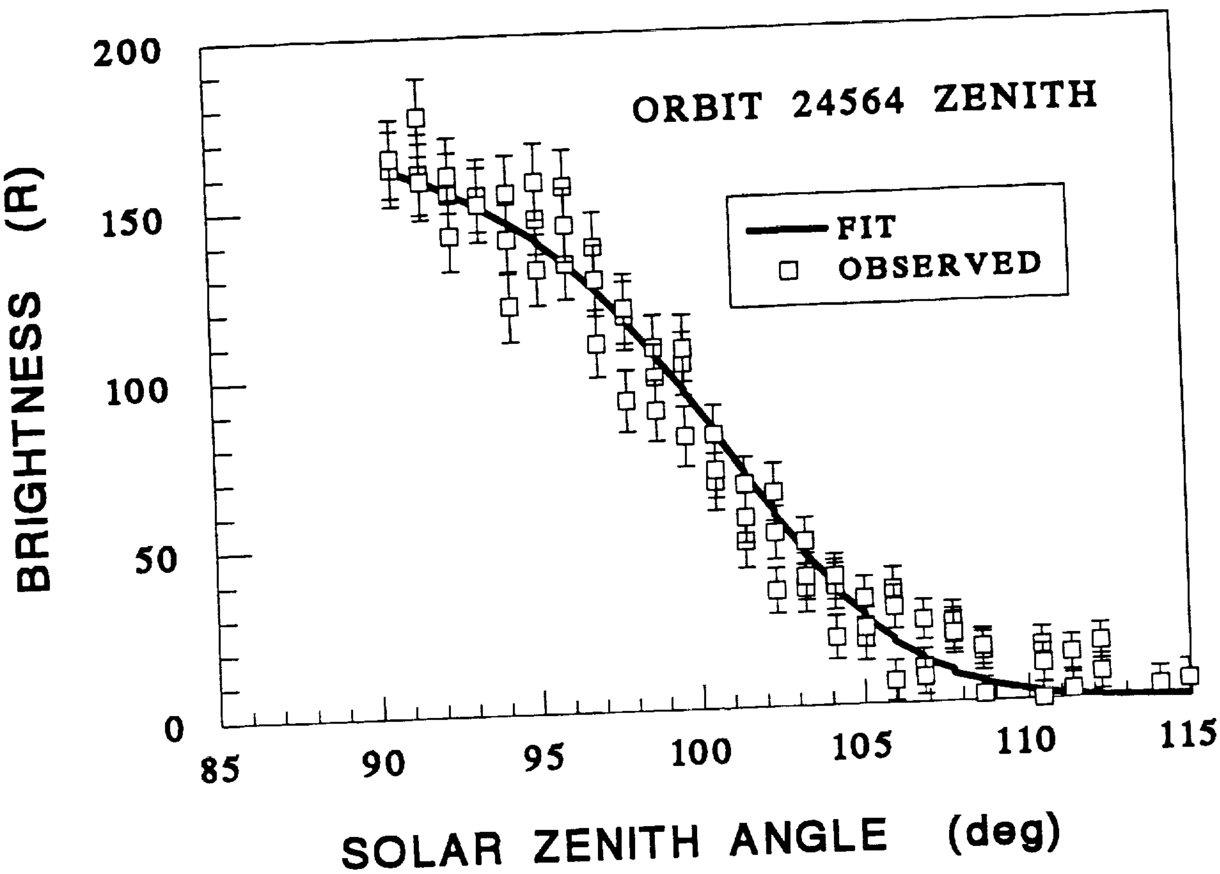

FIG. 14. The channel 2 VAE 7320 Å column emission rates measured within ±5 degrees of the zenith on AE-E orbit 24564 (data points) and the fit obtained using the parameters discussed in the text (solid line).

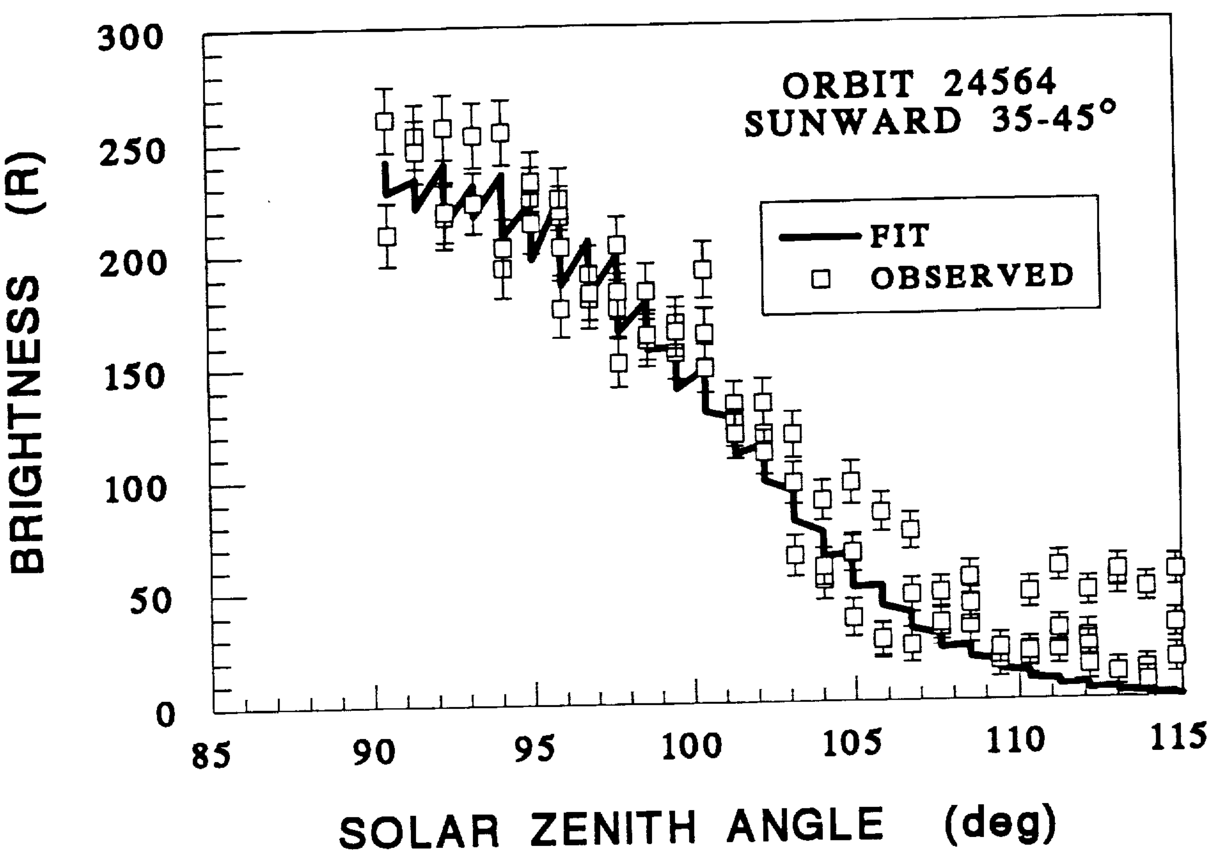

FIG. 15. The channel 2 VAE 7320 Å column emission rates measured in the sunward direction at elevation angles between 35 and 45 degrees on orbit 24564 (data points) and the fit obtained using the parameters discussed in the text (solid line).

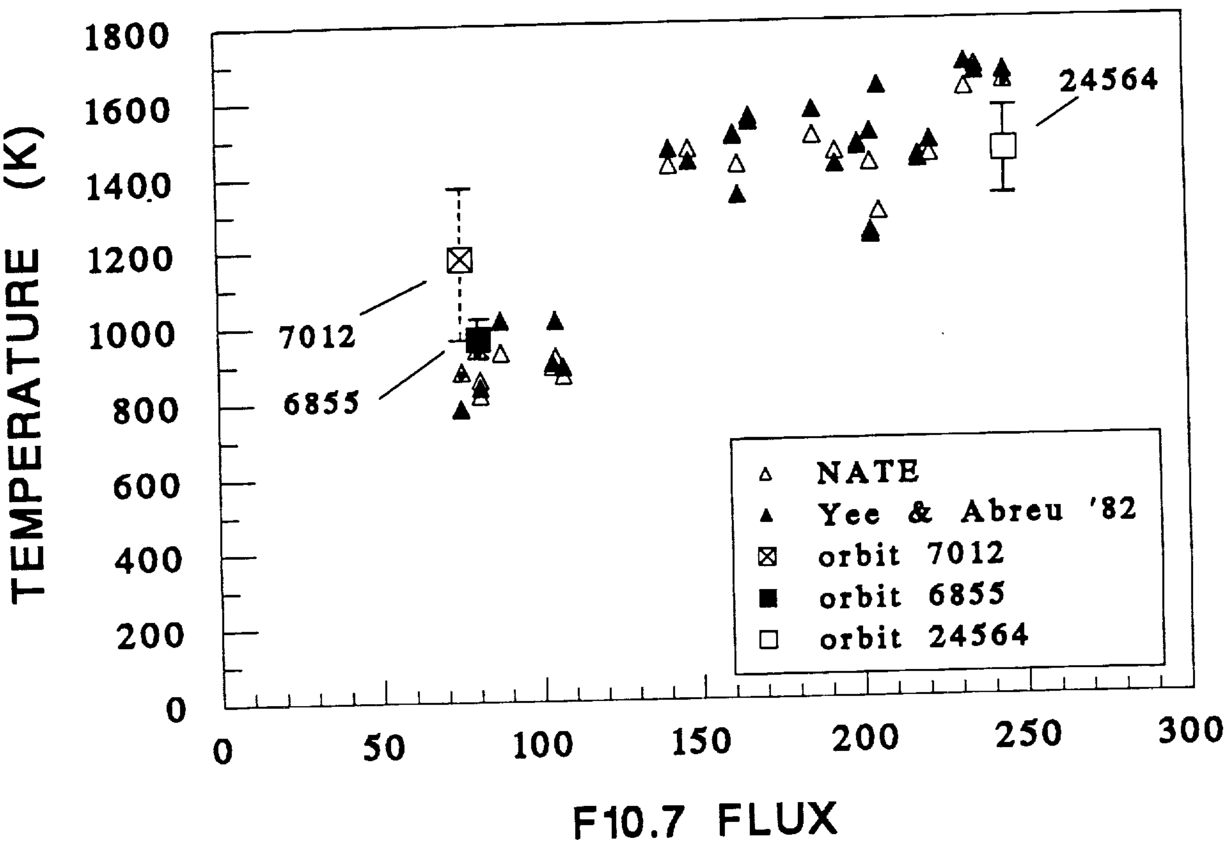

FIG. 16. The temperatures recovered in this work for AE-E orbits 6855, 7012 and 24564 (squares with error bars) compared with those deduced by *Yee and Abreu* (1982) from their analysis of zenith 7320 Å twilight observations (solid triangles). The temperatures measured by the *Neutral Atmosphere Temperature Experiment* are shown by the open triangles highlighted with central dots on orbits 6855, 7012 and 24564.

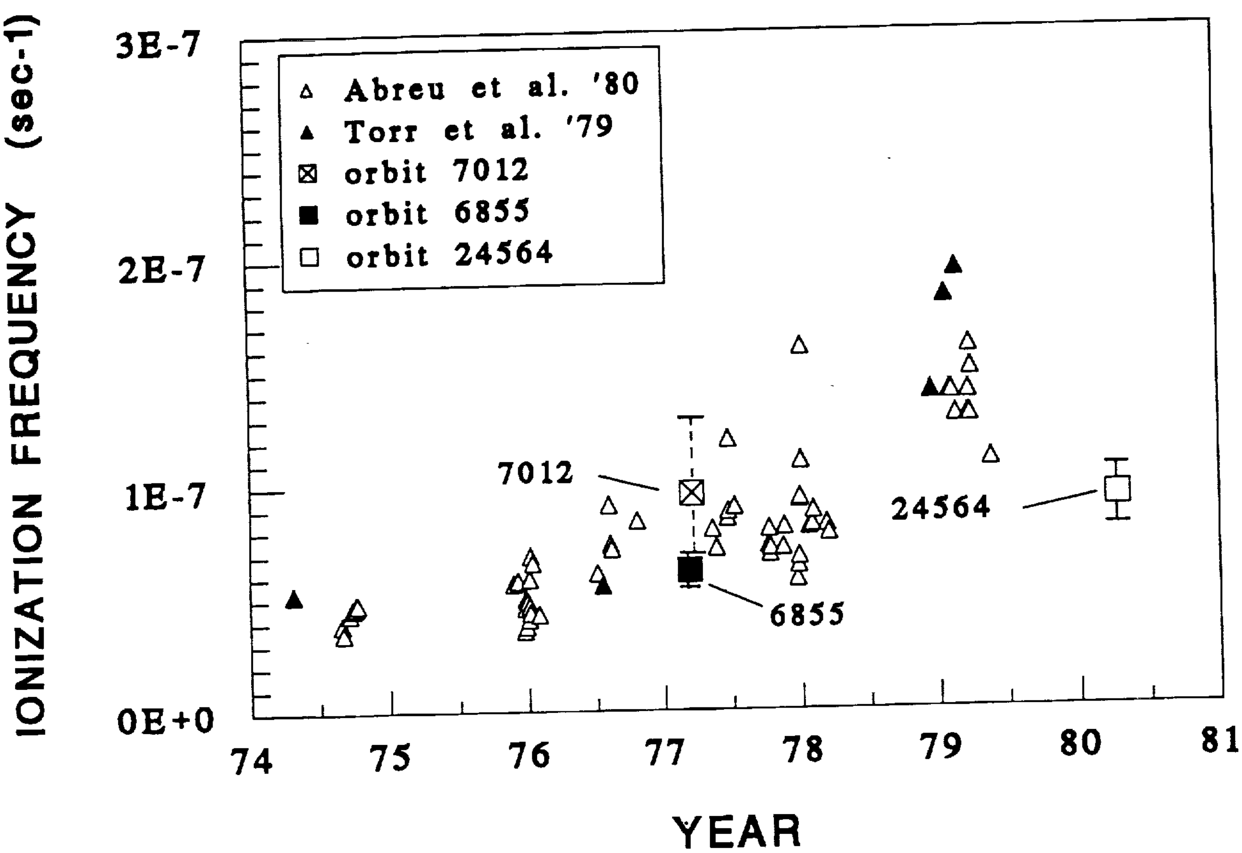

FIG. 17. The $O^+(^2P)$ ionization frequencies recovered in this work for AE-E orbits 6855, 7012 and 24564 (squares with error bars) compared with the frequencies deduced by *Abreu et al.* (1980) from dayglow 7320 Å observations (open triangles) and the frequencies calculated by *Torr et al.* (1979) from EUV flux measurements (solid triangles).

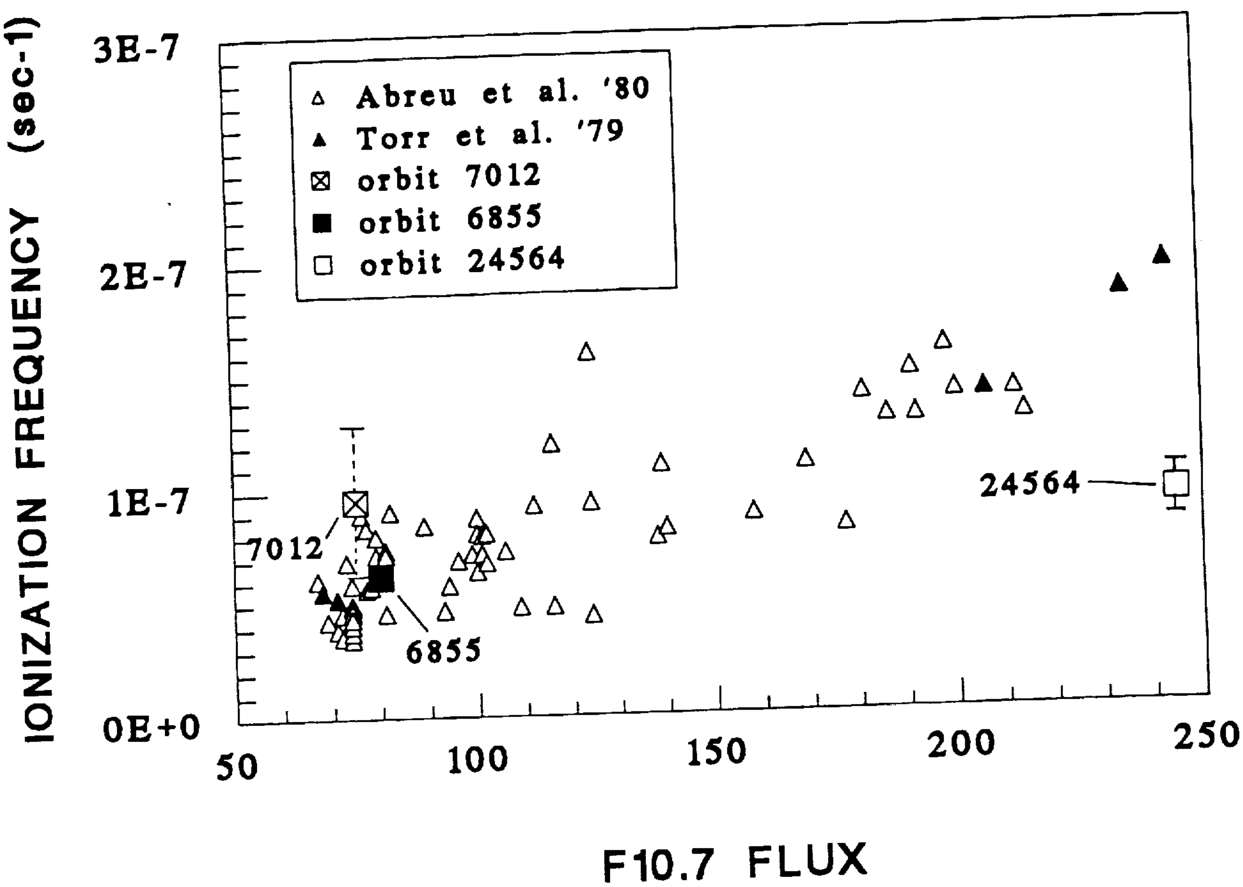

FIG. 18. The $O^+(^2P)$ ionization frequencies recovered in this work for AE-E orbits 6855, 7012 and 24564 (squares with error bars) compared with the frequencies deduced by *Abreu et al.* (1980) from dayglow 7320 Å observations (open triangles) and the frequencies calculated by *Torr et al.* (1979) from EUV flux measurements (solid triangles).

Table A1

AE-E orbits with spinning satellite and VAE observations at 7320 Å

Date yyddd	Orbit* #	Ch #	Spin type	Time (sec UT) on	off	Altitude (km) on	mid/ap	off	Local Solar Time (hr) on	mid	off
75352	353	2	N	57008	59367	952.1	140.9	1098.9	2.9	7.88	13.56
75354	372	1	N	16080	18447	1042.1	141.2	1001.1	2.85	8.21	13.53
75354	378	2	N	57712	60071	1053.8	140.9	987.2	2.89	8.34	13.56
75356	395	1	N	2816	5183	1023.8	140.8	1029.1	3.19	8.6	13.91
75356	397	2	N	16672	19039	1022.6	141	1029.8	3.22	8.64	13.94
75356	402	1	N	51304	53663	1027.3	140.8	1023.3	3.26	8.78	13.98
75356	406	1	N	78992	81359	1042.9	140.8	1006.2	3.27	8.86	13.99
75358	420	1	N	3112	5479	1051.8	145.1	997	3.44	9.06	14.13
75358	422	2	N	16944	19311	1066.9	145.1	981.6	3.42	9.1	14.11
75358	427	1	N	51512	53871	1097.1	145.1	932.9	3.4	9.21	14.02
75358	431	1	N	79216	81495	1059	145	898.4	3.58	9.28	13.97
75360	447	2	N	17080	19439	1032.5	145	1009.7	3.91	9.48	14.55
75360	452	1	N	51640	53999	1019.6	144.9	1003	4.03	9.6	14.6
75360	456	1	N	79656	81294	587.3	144.7	641.8	5.76	9.64	13.4
75362	470	1	N	3167	5534	972.3	145	1045.4	4.49	9.81	15.03
75364	496	1	N	9735	12102	894.4	145.5	1136	5.23	10.17	15.78
76022	798	1	N	84205	84836	386.5	145	1001.6	17.6	19	20.35
76024	818	1	N	45492	47851	956	144.4	985.8	10.01	15.09	20.66
76032	925	1	N	78820	81099	686.5	144.1	1150.6	12.48	17.02	22.8
76036	973	1	N	56588	58955	843.2	144.1	1054.2	12.7	17.78	23.29
76038	1001	2	N	72171	74530	769.2	144.4	1106.8	13.53	18.21	0.01
76040	1026	2	N	67331	69698	693.8	145.1	1195.6	14.29	18.53	0.83
76042	1048	2	N	41835	44202	875.5	140.8	974.5	13.93	18.85	0.5
76042	1054	2	N	82043	84410	851.4	141.1	1012.9	14.12	18.9	0.75
76048	1125	2	N	37843	40210	926.9	143.3	908.6	14.87	20.21	1.61
76052	1174	2	N	18387	20746	891.9	142.7	913.1	15.71	21.16	2.36
76054	1202	2	N	31466	33825	830.8	141.3	962.1	16.43	21.7	3.01
76093	1721	2	N	39296	41303	532.2	141.9	776.7	2.85	6.9	11.95
76096	1764	2	N	50136	52135	380.2	141	1871.3	10.66	14	18.04
76099	1801	2	N	25008	27015	543.1	139.6	723.4	4.15	8.17	13.46
76099	1810	2	N	82240	84239	519.9	139.4	731.6	4.4	8.33	13.68
76108	1931	2	I	69063	71062	667.7	137.1	530.5	5.66	10.77	14.83
76111	1967	2	I	36143	38150	317.7	137.9	927.7	8.63	11.39	17.63
76114	2008	2	I	32511	34510	738	139.6	438.3	6.83	12.07	15.86
76117	2049	2	I	28815	30814	517.7	141.4	369.1	8.67	12.79	16.29
76120	2091	2	I	29974	31981	720.9	141.9	433.4	8.26	13.75	17.62
76123	2133	2	I	30958	32957	477.8	140.5	644.4	10.37	14.69	19.57
76126	2174	2	N	24230	26237	727.6	138.2	399.8	9.7	15.47	18.88
76126	2183	2	N	79582	81581	744.5	137.6	373.9	9.79	15.57	18.86
76132	2269	2	I	84238	85405	380.8	152.1	236.9	13.76	17.03	19.18
76135	2302	2	I	27158	29157	1146.5	151.8	166.6	10.11	17.74	18.66

* when an observing sequence spans more than one orbit only the first orbit number is listed

Table A1. continued

Date yyddd	Orbit #	Ch #	Spin type	Time (sec UT) on	off	Altitude (km) on	mid/ap	off	Local Solar Time (hr) on	mid	off
76135	2311	2	I	82309	84316	991.5	151	758.7	11.04	11.6	12.2
76138	2344	2	I	26853	28852	654.2	151.7	450.6	13.28	18.65	22.57
76141	2387	1	I	32325	34324	395.7	151.5	725.4	15.9	19.49	0.89
76144	2426	1	I	12365	14364	553.2	152	543.5	15.61	20.17	0.62
76153	2557	1	I	39036	41035	458.3	156.6	639.5	18.57	22.77	3.84
76153	2563	2	I	75812	77811	460.3	156.9	636.9	18.67	22.89	3.92
76156	2594	1	I	6532	8235	923.1	155.9	175.3	16.67	23.5	0.49
76156	2600	2	I	43276	44979	1042.2	155.5	155.7	16.16	23.67	23.75
76159	2638	1	I	18500	20507	474.3	153.4	644.8	20.21	0.31	5.28
76159	2644	2	I	55372	57371	467.9	153	639.8	20.38	0.38	5.38
76162	2680	1	I	10716	12715	1107.1	152.1	180.9	17.44	0.9	2.08
76162	2689	2	I	65916	67923	1259.7	151.9	152.3	16.74	1.06	1.2
76165	2721	1	I	4684	6691	532.8	151.7	583.3	21.37	1.62	6.66
76168	2768	1	I	27892	29899	738.4	151.6	387.7	20.95	2.62	6.25
76168	2774	2	I	64819	66714	672.4	151.6	369.7	21.39	2.75	6.23
76171	2809	1	I	21076	23075	538.7	151.6	570.3	22.81	3.52	8.06
76171	2815	2	I	57835	59842	667.1	151.4	457.3	22.16	3.63	7.48
76177	2896	1	I	44043	46050	472.7	153	653.7	1.12	5.01	10.22
76177	2902	2	I	80947	82946	484.3	153.3	629	1.16	5.09	10.21
76180	2937	1	I	36699	38698	657.8	155.1	453.8	0.74	5.7	9.83
76180	2943	2	I	73539	75546	678	155.2	444.6	0.73	5.82	9.9
76186	3020	1	I	28450	30449	798.7	157.1	345.8	1.4	7.51	10.63
76186	3026	2	I	65178	67185	936.4	156.5	262.1	0.8	7.68	9.97
76189	3062	1	I	27898	29905	542.4	154.9	562.8	3.66	8.39	12.79
76189	3068	2	I	64570	66577	690.5	154.4	433.3	2.87	8.49	12.08
76192	3104	1	I	26818	28817	698.8	153.3	433.2	3.62	9.06	12.7
76192	3110	2	I	63658	65665	751.5	152.9	388.9	3.44	9.16	12.49
76210	3358	1	I	27049	29048	638.4	153.4	464	8.82	13.79	17.83
76210	3364	2	I	63825	65832	657.1	153.8	446.7	8.83	13.9	17.83
76213	3400	1	I	25625	27624	442.9	155.6	653.4	10.8	14.55	20.02
76213	3406	2	I	62377	64384	445.7	156	660	10.88	14.65	20.18
76216	3442	1	I	23288	24711	632.4	156.9	195.1	10.33	15.44	16.95
76216	3448	2	I	60001	62007	625.1	157.2	461.7	10.47	15.62	19.76
76219	3485	1	I	27296	29295	343.7	145.8	758.8	13.04	16.45	22.19
76219	3491	2	I	63952	65959	316.7	145.7	795	13.42	16.61	22.5
76222	3529	1	I	35936	37895	557.7	143.5	467.4	12.39	17.34	21.31
76222	3535	2	I	72520	74519	527.7	143.2	524.2	12.73	17.44	21.8
76225	3571	1	I	26320	28319	405.6	141.3	644.6	14.35	17.99	23.38
76225	3577	2	I	62872	64879	338.2	141.3	736.7	15	18.09	0.1
76228	3613	1	I	21464	23471	658.9	140.6	389	13.46	18.74	22.59
76228	3619	2	I	57720	59727	698.7	140.8	346.8	13.33	18.85	22.36
76231	3656	1	I	22632	24639	417.8	140.3	604.4	15.67	19.64	1.06
76231	3662	2	I	58888	60887	393.6	140.6	630.1	15.95	19.76	1.33
76234	3699	1	I	22280	24279	610.8	140.4	389.8	15.12	20.68	0.43

Table A1. continued

Date yyddd	Orbit #	Ch #	Spin type	Time (sec UT) on	off	Altitude (km) on	mid/ap	off	Local Solar Time (hr) on	mid	off
76234	3705	2	I	58767	60390	378.9	140.6	400.8	16.87	20.77	0.62
76237	3739	1	I	3823	5830	372.8	139.7	627.8	17.66	21.5	2.78
76243	3832	1	N	41103	43102	268.3	141.4	707.6	20.5	23.13	5.67
76243	3838	2	N	76839	78846	245.1	142	750.1	20.87	23.32	6.09
76246	3875	1	N	38311	38622	244.3	142	375.1	2.79	3.5	4.19
76249	3926	1	N	79423	81430	386.4	142.7	528.4	21.12	1.36	6.41
76255	4006	1	N	26038	28045	442.2	137.8	438.1	22.38	2.91	7.48
76255	4012	2	N	61150	63157	488.2	137.3	390.7	22.12	3.02	7.21
76264	4138	1	I	17510	19517	433.4	135.3	363.4	0.68	5.83	10.05
76264	4144	2	I	52246	54253	389.9	134.7	394.5	1.19	5.97	10.47
76271	4248	1	I	42701	44700	447.4	136	273.7	2.61	8.01	11.69
76274	4290	1	I	27157	29164	393.1	142.3	297.4	3.95	9.02	13.24
76274	4299	2	I	77893	79900	428.3	141.9	262.8	3.69	9.25	12.97
76277	4338	1	I	32757	34508	414.6	141.7	192.3	4.42	10.3	12.65
76277	4347	2	I	83101	85108	481.4	140.6	197.1	3.76	10.55	12.99
76283	4433	1	N	39501	41508	349.8	139.8	251.6	7.02	12.31	16.09
76283	4439	2	N	72788	74723	351.2	139.2	228.7	7.1	12.43	15.81
76286	4478	1	N	29604	31603	275.7	137.9	281.2	8.9	13.21	18.12
76286	4486	2	N	73452	75451	342.2	137.5	219.7	7.9	13.45	17.1
76292	4573	1	N	32460	34467	233.2	142.8	266.7	11.34	15.72	20.45
76292	4579	2	N	65068	67075	250.1	141.8	246.9	10.97	15.83	20.16
76295	4625	1	N	55756	57763	273.4	148.4	207.7	11.29	16.7	20.27
76298	4675	1	N	67691	69690	246.1	161.5	229.1	13.16	17.83	22.35
76301	4721	1	N	57939	59090	168.3	161.4	211.3	17.71	19.17	23.16
76304	4773	1	N	78403	80402	258.7	169.8	204.1	14.62	20.63	23.82
76319	5008	1	N	37514	39521	241.8	184.1	190.3	18.65	1.84	3.73
76319	5014	2	N	69466	71473	246	184.1	187.2	18.3	1.95	3.31
76322	5057	1	N	41202	43201	243.3	238.8	247.5	23.18	2.32	8.25
76322	5063	2	N	73154	75161	247.2	239.1	244.2	22.11	2.54	7.1
76340	5340	1	N	6849	12152	250	247.2	250.2	0.38	9.02	0.14
76346	5440	2	N	24041	29344	244.4	241.6	244.6	20.81	6.77	20.6
77003	5810	2	N	22542	27901	249.6	253.5	249.6	9.36	21.3	9.3
77007	5874	1	N	19054	19917	247.8	246.2	245.8	3.32	5.09	6.96
77007	5878	2	N	40502	41341	247.2	245.7	245.5	3.26	4.97	6.78
77007	5884	1	N	72630	73493	247.2	245.4	244.8	3	4.77	6.65
77009	5912	2	N	50094	55461	244.5	247.3	244.4	3.21	15.23	3.23
77016	6019	2	N	18533	19396	258.6	256.9	255.9	20.58	22.38	0.22
77016	6025	1	N	50614	51477	259.4	257.3	255.8	19.81	21.64	23.47
77016	6029	2	N	72006	72869	259.8	257.7	256.1	19.3	21.14	22.97
77034	6307	2	N	7516	8379	263.7	262.1	260.4	7.91	9.79	11.58
77034	6313	1	N	39636	40499	263.8	262.4	260.6	7.15	9.06	10.93
77034	6317	2	N	61044	61907	263.4	262.1	260.4	6.62	8.55	10.44
77036	6352	1	N	76996	82355	259	257.9	259.2	8.86	20.78	8.7
77040	6415	2	N	68508	72347	259.5	254	255.5	1.62	10.04	18.78

Table A1. continued

Date yyddd	Orbit #	Ch #	Spin type	Time (sec UT) on	Time (sec UT) off	Altitude (km) on	Altitude (km) mid/ap	Altitude (km) off	Local Solar Time (hr) on	Local Solar Time (hr) mid	Local Solar Time (hr) off
77043	6455	1	N	20716	21435	252	252.5	252.9	9.81	11.48	13.18
77043	6459	2	N	41916	42779	251.5	252.2	252.9	8.5	10.4	12.45
77047	6524	2	N	49619	54978	247.8	250.6	247.7	3.73	15.74	3.74
77052	6598	1	N	8483	9346	244.7	243.1	242.5	0.55	2.4	4.32
77052	6602	2	N	29907	30770	244	242.5	242.2	0.44	2.29	4.21
77052	6612	2	N	83467	84330	243.7	242.1	241.5	0.24	2.03	3.96
77063	6776	1	I	19554	24921	261.7	261.8	261.6	17.54	5.46	17.43
77068	6855	2	I	11962	17329	258.3	259	258.3	14.65	2.63	14.61
77077	7011	1	N	73225	76944	251.5	253.9	250.4	17.22	1.27	9.65
77081	7074	2	N	63705	69073	245.4	249.6	245.3	7.95	19.9	7.85
77087	7168	1	N	48009	53376	240	241.6	240	2.52	14.49	2.51
77108	7297	1	I	2224	5767	258.8	258.8	261	14.3	22.24	5.95
77100	7372	2	I	21824	27183	264.8	263.2	264.9	19.3	7.21	19.17
77108	7497	1	I	2224	7591	258.8	258.4	258.7	14.3	2.29	14.26
77132	7895	1	I	60470	65837	277.4	273.3	277.4	19.16	7.03	18.97
77138	7980	2	I	990	6349	270.2	271	270.2	20.62	8.51	20.39
77142	8055	1	I	59013	64381	269	267.6	269.1	17.23	5.2	17.14
77146	8122	2	I	73821	79180	267.9	264.7	267.9	14.29	2.2	14.15
77155	8257	1	I	22204	27571	261.5	261.8	261.5	9.71	21.62	9.59
77169	8492	2	I	74108	79475	252.8	251.1	252.9	0.66	12.61	0.59
77176	8600	1	I	50307	55674	281.6	282.1	281.8	20.34	8.2	20.12
77181	8672	2	I	7003	12370	279.3	280.9	279.4	17.95	5.82	17.74
77187	8770	1	I	17282	22498	278.3	276.4	279.1	14.28	1.85	13.45
77194	8882	2	I	16242	19793	275.8	274.6	276.9	9.67	17.58	1.33
77214	9211	1	I	59721	65088	266.7	263.2	266.8	21.47	9.38	21.34
77218	9279	2	I	79641	80768	264.6	263.6	263.2	18.56	20.91	23.45
77224	9366	1	I	28704	34071	288.6	282.7	288.7	11.35	23.2	11.1
77228	9436	2	I	61616	66975	284.8	281	284.9	11.05	22.91	10.83
77275	10191	1	N	65941	68260	251.4	252.2	253.3	8.34	13.4	18.74
77275	10191	1	N	68269	68908	253.3	253.5	254.1	18.81	20.15	21.48
77279	10249	2	N	31181	36452	278.8	254.8	280.6	3.63	15.42	3.14
77285	10345	1	N	31332	32299	279.6	278.2	278.3	2.29	4.3	6.39
77314	10816	1	N	60643	66002	269.6	268.1	270.3	7.97	19.9	7.82
77318	10880	2	N	58186	62881	281.3	278.6	279.1	20.76	7.22	17.77
77324	10979	1	N	75834	76769	274.7	273.6	273.6	2.77	4.73	6.78
77328	11041	2	N	64298	68153	272.7	271.3	278.3	0.27	8.9	17.33
77350	11396	1	N	73536	74127	281	280.4	280.3	10.89	12.08	13.37
77354	11456	2	N	48472	53839	279	280.8	279.1	18.34	6.19	18.12
77360	11550	1	N	43752	45543	279.9	280.1	275.7	20.32	0.44	4.41
77364	11617	2	N	55663	61030	273.9	273.7	274.1	1.82	13.71	1.64
78005	11705	1	N	11190	13109	270.3	268	267.5	22.69	2.55	6.82
78054	12026	2	N	31466	33825	830.8	141.3	962.1	16.43	21.7	3.01
78028	12085	1	N	78389	83748	320.6	324.8	321	8.53	20.35	8.16
78032	12144	2	N	54260	56899	320.3	319.3	322.4	6.61	12.41	18.25

Table A1. continued

Date yyddd	Orbit #	Ch #	Spin type	Time (sec UT) on	off	Altitude (km) on	mid/ap	off	Local Solar Time (hr) on	mid	off
79096	18868	1	I	74599	78094	453.6	457.7	457.6	4.62	11.95	19.64
79100	18929	1	I	71815	75350	452.6	459.8	454.9	4.94	12.29	19.95
79102	18960	1	I	73247	76598	452.3	459.9	454.9	5.19	12.15	19.29
79104	18992	1	I	74535	76886	452.1	457.8	458.7	4.81	9.64	14.85
79106	19023	1	I	75959	79702	452.6	458.4	454.1	4.93	13.05	20.86
79108	19054	1	I	77391	79542	453.8	458	456	5.21	9.85	14.51
79110	19085	1	I	78478	82109	453.7	456.4	454.6	4.04	11.86	19.38
79112	19115	1	I	74214	77837	454.7	454.7	454.7	4.06	12	19.69
79114	19146	1	I	75550	79173	455.8	453.4	454.4	4.04	11.92	19.73
79116	19177	1	I	76878	80493	456.6	452.2	454.1	4.09	11.81	19.71
79132	19424	1	I	76013	79636	452.2	449.5	457.1	3.66	11.62	19.2
79134	19455	1	I	77261	80884	452.1	449.7	456.8	3.47	11.43	19.1
79136	19486	1	I	78501	82124	451.8	454.7	456.1	13.68	16.24	18.95
79138	19517	1	I	79741	83364	452.3	450.7	455	3.24	11.02	18.88
79142	19578	1	I	76620	80307	452.1	453	452	3.21	10.9	18.98
79146	19640	1	I	79180	82923	451.4	455.2	449.5	3.48	11.31	19.33
79148	19670	1	I	74860	78603	451.2	455.5	449.2	3.66	11.59	19.49
79150	19701	1	I	76164	79907	451.4	455	449.1	3.85	11.93	19.75
79152	19731	1	I	71860	75483	452.3	454.2	449	4.07	11.99	19.56
79154	19762	1	I	73124	76755	453.3	453	449	4.13	12.08	19.81
79156	19793	1	I	74371	77994	454.3	451.9	448.8	4.25	12.09	19.87
79158	19824	1	I	75595	79218	454.9	451.1	448.5	4.24	12.05	19.94
79160	19855	1	I	76819	80442	454.9	450.6	448.4	4.35	11.97	19.93
79162	19886	1	I	78019	81642	454.5	450.2	448.6	4.35	11.88	19.84
79164	19917	1	I	79211	82834	453.4	450.2	449.1	4.29	11.85	19.75
79176	20103	1	I	80578	84201	447.1	448.8	455.2	3.25	11.22	18.83
79178	20133	1	I	76106	78977	447	447.8	453.7	3.05	9.44	15.37
79178	20133	1	I	78986	79729	453.7	455.2	455.4	15.37	17.01	18.7
79181	20180	1	I	80673	84297	447.3	448.9	454.5	3.08	10.86	18.72
79184	20222	1	I	57154	60785	447.1	450	453.2	3.04	10.73	18.68
79187	20267	1	I	50513	54136	447.1	451.5	451.1	3.23	10.8	18.72
79190	20318	1	I	77601	81224	447.3	451.9	449.5	3.67	11.24	18.95
79193	20364	1	I	76633	80256	448.1	451.1	449.2	4	11.86	19.42
79196	20410	1	I	75633	79256	450.1	448.8	449.2	4.31	12.21	19.85
79199	20457	1	I	80168	83791	452.2	446.9	448.5	4.37	12.25	20.08
79202	20503	1	I	79024	82647	453.4	445.9	447.8	4.27	11.94	19.89
79205	20549	1	I	77872	81503	453.5	445.5	447.5	4.16	11.76	19.72
79220	20781	1	I	77711	81334	447.2	446.8	450.8	3.53	11.49	19.2
79223	20827	1	I	76511	80134	446.9	447.7	450	3.38	11.23	19.09
79226	20871	1	I	64055	68038	446.3	449.8	447	3.17	11.57	20.27
79232	20966	1	I	78639	82261	445.3	452.3	445.4	3.8	11.41	19.15
79235	21012	1	I	77510	81133	445.4	451.8	445.3	4.03	11.76	19.34
79238	21059	1	I	81950	85573	446.3	450.2	445.5	4.1	11.98	19.57
79253	21290	1	N	81405	85028	447.6	448.6	449.8	16.31	17.78	19.3
79256	21335	1	N	74565	78188	443.7	447	451.5	12.2	15.79	19.27
79259	21381	1	N	78933	82555	443.5	442.4	452.8	3.91	11.78	19.34

Appendix 2

The following is a listing of the Fortran program used to extract 7320 Å emission rates and related orbital quantities from the AE-E Visible Airglow Experiment data files.

```
C                          Program  TWIVAEREAD
C
C
C       a version of the AE data base program VAEREAD.FOR
C                    created for the project
C
C     "An Assessment of Twilight Airglow Inversion Procedures
C          Using Atmosphere Explorer Observations"
C
C                          by I.C.McDade
C
C                    under NASA Grant NAG 5-1502
C
C This program extracts selected data and vectors from VAE data files
C The output files are used for graphical examination of the data and
C for input to the twilight inversion program TWIFITTER.PAS
C
C Logical unit assignments, all done internally:
      LOGICAL*1 ID
      CHARACTER*80 FSTR,F2STR, VSTR
      INTEGER*4 MODEX(7,3), LAM(7,3)
      REAL*4 OADATA(22),OADATL(22),RAY1(4),RAY2,STV(2),DC(2),
     >sun(3),v1(3),v2(3),v11(3),v21(3),r(3),sgeo(3),sgei(3),
     >sth,sph,Tmat(3,3),gst

C sun is the sun position vector in GEI coordinates
C v1 & v2 are the channel 1 & 2 line-of-sight vectors in GEI coords.
C r is the satellite spin axis vector in GEI coordinates
C sgeo & sgei are the satellite position vectors in GEO & GEI coords
C sth & sph are the satellite sherical coords in degrees
C Tmat is the 3x3 GEO to GEI transformation matrix

      COMMON/CVEC/V1,V2,V1L,V2L,R,sun,gst
      COMMON /CRAYL/ ICH,NSAT,IGZC,STV,DC,RAY1,RAY2,ICE,ISKIP
      COMMON /CVAERD/ ITIME,THET,ICH11,ICH12,ISQ11,ISQ12,ITIMEL,THETL,
     >IFW,IE,ICH11L,ICH12L,ISQ11L,ISQ12L,IATN1,
     >ICH2,ISQ2,IATN2,TBAF1,TBAF2,TBAF11,TBAF22,TAEL,TBEL,TPMT1,
     >TPMT2,TFW,
     >IEND4,IX,ISVIF,OADATA,OADATL
      DATA MODEX/'55F6','73FD','52F7','63F4','33F5','CLF2','42F3',
     >'73F4','52FD','42F5','48F6','55F7','CLF4','63F5',
     >'73F6','52FD','28F5','65F6','55F7','CLF2','63F5'/
      DATA LAM/5577, 7320, 5200, 6300, 3371, 0, 4278,
     >7320, 5200, 4278, 4861, 5577, 0, 6300,
     >7320, 5200, 2800, 6563, 5577, 0, 6300/

C Open input and output files

      TYPE 5
5     FORMAT (' Enter name of input VAE data file:')
      ACCEPT 10, VSTR
10    FORMAT (A80)
      OPEN (UNIT=4, FILE=VSTR, TYPE='OLD', READONLY,
```

```
     + FORM='UNFORMATTED')
      PRINT*, 'Enter NREADMAX ?'
      READ*, NREADMAX
      PRINT*, 'Do you want G&Z cor (1=Y, 0=N)?'
      READ*, IGZC
      PRINT*, 'Enter channel # (1 or 2) '
      READ*, ICH
      IF(ICH.eq.1) GOTO 11
      PRINT*,'Enter ch1 to ch2 zenith angle correction (if any) ?'
      READ*, zacor
11    PRINT*, 'MIN channel 1 zenith angle ?'
      READ*, ZMIN
      PRINT*, 'MAX channel 1 zenith angle ?'
      READ*, ZMAX
      TYPE 15
15    FORMAT (' Enter name of output file containing observations :')
      ACCEPT 10, FSTR
      OPEN (UNIT=20, NAME=FSTR, TYPE='NEW')
      TYPE 16
16    FORMAT (' Enter name of output file containing the vectors :')
      ACCEPT 10, F2STR
      OPEN (UNIT=21, NAME=F2STR, TYPE='NEW')

C Assign initial values:

      NS=0
      NERR=0
      NSQ=0
      NATN=0
      NAVG=0
      STO=0.
      ISVIF=1
      ISKIP=0

C Get start, stop times, and averaging parameter:

35    TYPE 40
40    FORMAT (' Enter start, stop times in seconds (default=0,86400):')
      ACCEPT *, JSTART, JSTOP
      ISTART = JSTART*1000
      IF (JSTOP .EQ. 0) JSTOP = 86400
      ISTOP = JSTOP*1000
      TYPE 45
45    FORMAT (' Enter Filter Wheel Position (10=all):')
      ACCEPT *, JFW

C Position Vae Data File to start time, obtain header information and
C check mode

      CALL SETUP(1)
      CALL INITV(4,ISTART,IDATE,IORB,ID,ISPINF,INF,MODE1,ITON,
     > ITOFF,IDMF,MODE2,ITON2,ITOFF2)
      MODE = MODE1
      IF (IDMF.EQ.1.AND.ISTART.GE.ITON2) MODE=MODE2
      NSAT = 1
      IF (ID .EQ. 'D') NSAT=2
      IF (ID .EQ. 'E') NSAT=3

C Read the Vae Data File, bin error-free channel one data,
C convert to Rayleighs, and store in arrays:

      DO 290 NREAD=1,NREADMAX
      CALL VAERD
      IF (IE .EQ. 'E    ') GOTO 260
```

```
      IF (JFW .NE. 10 .AND. JFW .NE. IFW) GOTO 290
      IF (OADATA(9).LT.ZMIN)GOTO 290
      IF (OADATA(9).GT.ZMAX)GOTO 290
      IF (IEND4.EQ.1.OR.ITIME.GT.ISTOP) STOP
      IF (ICH.EQ.2)GOTO 241
      IF (ISQ11.EQ.1.OR.ISQ12.EQ.1)GOTO 270
      IF (ISQ11L.EQ.1.OR.ISQ12L.EQ.1) GOTO 270
      IF (IATN1.EQ.1) GOTO 280
      GOTO 242
241   CONTINUE
      IF (ISQ2.EQ.1)GOTO 270
      IF (IATN2.EQ.1)GOTO 280
242   CONTINUE
      CALL RAYL
      ISKIP=1
      IF (ICE.NE.1) GOTO 290

      CALL SUNVEC(IDATE,ITIME,SUN,GST)
      sth=oadata(3)
      sph=oadata(4)
      if (oadata(4).lt.0.0)sph=360.0+oadata(4)
      gstr=gst/57.29578
      Tmat(1,1)=COS(gstr)
      Tmat(1,2)=-1.0*SIN(gstr)
      Tmat(1,3)=0.0
      Tmat(2,1)=SIN(gstr)
      Tmat(2,2)=COS(gstr)
      Tmat(2,3)=0.0
      Tmat(3,1)=0.0
      Tmat(3,2)=0.0
      Tmat(3,3)=1.0
      CALL CART(sth,sph,sgeo)
      CALL MAXMUL1(Tmat,sgeo,sgei)
      sgei(1)=sgei(1)*(oadata(1)+6370.0)
      sgei(2)=sgei(2)*(oadata(1)+6370.0)
      sgei(3)=sgei(3)*(oadata(1)+6370.0)

      IF(ICH.EQ.2) GOTO 245
      Av=(Ray1(1)+Ray1(2)+Ray1(3)+Ray1(4))/4.0
      Bright=Av
      Sig=SQRT(1.0*(ICH11+ICH12+ICH11L+ICH12L))*STV(1)/4.0
      za=ABS(OADATA(9))
      GOTO 246
245   Bright=RAY2
      Sig=SQRT(ABS(1.0*ICH2))*STV(2)
      za=ABS(OADATA(9)+zacor)
246   WRITE (20,251)ITIME,Bright,Sig,OADATA(1),za,OADATA(6)
      IF(ICH.EQ.1) WRITE (21,250)ITIME,sgei(1),sgei(2),sgei(3),
     >sun(1),sun(2),sun(3), v1L(1),v1L(2),v1L(3)
      IF(ICH.EQ.2) WRITE (21,250)ITIME,sgei(1),sgei(2),sgei(3),
     >sun(1),sun(2),sun(3), v2L(1),v2L(2),v2L(3)
      PRINT*,ITIME,Bright,Sig,OADATA(1),za,OADATA(6)
      250 FORMAT (1X,I8,9E13.5)
      251 FORMAT (1X,I8,'      ',1E13.5,'   ',1E13.5,'   ',
     > 1E13.5,'    ',1E13.5,'   ',1E13.5)

      GOTO 290
260   NERR = NERR + 1
      GOTO 290
270   NSQ = NSQ + 1
      GOTO 290
280   NATN = NATN + 1
      GOTO 290
290   CONTINUE
```

```
      STOP
      END

      SUBROUTINE VAERD

C This version reads VAX formatted VAE data.

C CALLING PROGRAM MUST PROVIDE COMMON /CVAERD/ AND PRESET IEND4
C TO ZERO.IEND4 IS RESET TO 1 UPON EOF ON VDF.IF CALLING ROUTINE
C DOES NOT CHECK THIS IT MAY GO INTO AN INFINITE LOOP UPON EOF.

      DIMENSION REC(295),IREC(295),IBUFF(295),BUFF(295),OADATA(22),
     >        OADATL(22),
     >        A1(3),A2(3),B1(3),B2(3),E(3),F(3),P(3),DF1(3),DF2(3),
     >        R(3),V1(3),V2(3),V1L(3),V2L(3),RMOON(3),SUN(3)
      LOGICAL*1 SATID(4),ID,SATID1,SATID2,SD1,SD2,NI1,NI2
      LOGICAL*4 MODE1,MODE2
      CHARACTER*40 INDNAME
      CHARACTER*4 IE
      INTEGER*4 SHFTR
      INTEGER*2 LEN
      EQUIVALENCE (REC,IREC),(IBUFF,BUFF),(SATID,IREC(3))

      COMMON /CVAERD/ITIME,THET,ICH11,ICH12,ISQ11,ISQ12,ITIMEL,THETL,
     >        IFW,IE,ICH11L,ICH12L,ISQ11L,ISQ12L,IATN1,ICH2,ISQ2,IATN2,
     >        TBAF1,TBAF2,TBAF11,TBAF22,TAEL,TBEL,TPMT1,TPMT2,TFW,IEND4,
     >        IX,ISVIF,OADATA,OADATL

      COMMON /CVEC/ V1,V2,V1L,V2L,R,sun,gst

      DATA P/0.,-.398,.917/,LORBIT/0/
      DATA SAVE1/2.0/, PI/3.14159/, FAC/57.29578/
      DATA ISW,IIREAD/2*0/, INUNIT/4/, IANGSW/0/, PI2/6.28318/

C READ HEADER AND FIRST RECORD UNLESS FILE IS PRE-POSITIONED USING
C ENTRY INITV

      IF ( ISW .NE. 0) GO TO 100

      READ(INUNIT,END=250,ERR=250) (IREC(I),I=1,12)

      IDATE=IREC(1)
      IORBIT=IREC(2)
      ISF=1

      READ(INUNIT,END=250,ERR=250) (IBUFF(K),K=1,295)

      ISW=1
100   IIREAD=IIREAD+1
      IF (IIREAD.NE.1) GO TO 400
      DO 120 K=1,295
120   IREC(K)=IBUFF(K)
      IF(REC(275).GT.23.0.AND.BUFF(275).LT.1.0)REC(275)=REC(275)-24.0
      IF(REC(277).GT.179.0.AND.BUFF(277).LT.-179.0)REC(277)=REC(277)-
     >360.0
      IF(REC(277).LT.-
     >179.0.AND.BUFF(277).GT.179.0)REC(277)=REC(277)+360.0
      IF(REC(281).GT.179.0.AND.BUFF(281).LT.-179.0)REC(281)=REC(281)-
     >230.0

      READ(INUNIT,END=250,ERR=250) (IBUFF(K),K=1,295)
```

```
C IF ORBIT IS SPINNING, FIND OA VECTORS NEEDED FOR INTERPOLATIONS

      IAFLAG=1
      IF(ISF.NE.1.OR.ISVIF.EQ.0)GOTO 260
      DO 190 K=284,295
190   IF(REC(K).LT.-1000.OR.REC(K).GT.1000)IAFLAG=0
      IF(IAFLAG.EQ.0)GOTO 260
      IF(LORBIT.EQ.IORBIT)GOTO 200
      LORBIT=IORBIT
      CALL SUNVEC(IDATE,ITIME,SUN,gst)
      CALL CROSS(P,SUN,E)
200   CALL CART(REC(287),REC(286),A1)
      CALL CART(REC(293),REC(292),A2)
      CALL CART(BUFF(287),BUFF(286),B1)
      CALL CART(BUFF(293),BUFF(292),B2)
      DO 210 NN=1,3
      DF1(NN)=A1(NN)-B1(NN)
210   DF2(NN)=A2(NN)-B2(NN)
      CALL CROSS(DF2,DF1,R)
      CALL DETER(A1,B1,R,DET1)
      CALL DETER(A2,B2,R,DET2)
      GAMMA=PI2-ANGLE(A1,B1)
      CMCH1=COS(REC(285)/FAC)
      CMCH2=COS(REC(291)/FAC)
      CALL LUNVEC(A1,A2,CMCH1,CMCH2,RMOON)
      GO TO 260

C IF EOF, SET FLAG AND RETURN

250   IEND4=1
      GO TO 4

C UNPACK THE DATA RECORD

260   IF( REC(15) .LE. 1.0 ) GO TO 280
      IF ( SAVE1 .NE. 2 ) GO TO 270
      REC(16) = 1.570681
      REC(17) = 0.0
      REC(15) = 1.0
      GO TO 290
270   REC(15)= SAVE1
      GO TO 300
280   SAVE1 = REC(15)
290   DELTH = .125 * REC(17)
      THET1 = REC(16) - DELTH
      THET2 = REC(16) + .0626 * REC(17) -DELTH
300   ITIME = IREC(1) - 125
      ITIMEL = IREC(1) - 63
      TBAF1 = REC(3)
      TBAF2 = REC(4)
      TBAF11 = REC(5)
      TBAF22 = REC(6)
      TAEL = REC(7)
      TBEL = REC(8)
      TPMT1 = REC(9)
      TPMT2 = REC(10)
      TFW = REC(11)

C JJ = INDEX TO STATUS BITS

400   JJ = IIREAD * 4 + 14
      ITIME = ITIME + 125
      ITIMEL = ITIMEL + 125
      IF ( IREC(JJ+1) .NE. -1 ) GO TO 410
```

```
      ICH11 = -1
      ICH12 = -1
      GO TO 420
410   ICH11 = JIBITS(IREC(JJ+1),16,16)
      ICH12 = JIBITS(IREC(JJ+1),0,16)
420   IF ( IREC(JJ+2) .NE. -1 ) GO TO 430
      ICH11 = -1
      ICH12 = -1
      GO TO 440
430   ICH11L = JIBITS(IREC(JJ+2),16,16)
      ICH12L = JIBITS(IREC(JJ+2),0,16)
440   IF(IIREAD.NE.1) ICH2 = IREC(JJ+3)
      ITEMP = IREC(JJ)

C ZENITH ANGLE CALCULATIONS (OLD METHOD)

      THET = 0.0
      THETL = 0.0
      IF(THET1.GT.PI2 .OR. THET2.GT.PI2 .OR. REC(15).GT.1.0)GO TO 450
      IF(IANGSW .EQ. 1) GO TO 450
      THET1 = THET1 + DELTH
      THET = ACOS(COS(THET1) * REC(15)) * 57.29583
      IF(THET1 .LT. 0.0 ) THET = 360.0 - THET
      IF(THET1 .GE. 6.28318) THET1 = THET1 - 6.28318
      IF(THET1 .GT.3.14159) THET = 360.0 - THET
      THET2 = THET2 + DELTH
      THETL = ACOS(COS(THET2) * REC(15)) * 57.29583
      IF(THET2 .LT. 0.0) THETL = 360.0 - THETL
      IF(THET2 .GE. 6.28318) THET2 = THET2 - 6.28318
      IF(THET2 .GT. 3.14159) THETL = 360.0 - THETL
450   CONTINUE

C UNPACK STATUS WORD

      IWORD=JIBITS(ITEMP,31,1)
      IF ( IWORD .EQ. 0 ) GO TO 500
      IE='E '
      GO TO 501
500   IE='  '
501   ISQ2=JIBITS(ITEMP,24,1)
      ISQ11=JIBITS(ITEMP,19,1)
      ISQ12=JIBITS(ITEMP,18,1)
      ISQ11L=JIBITS(ITEMP,17,1)
      ISQ12L=JIBITS(ITEMP,16,1)
      IATN1=JIBITS(ITEMP,9,1)
      IATN2=JIBITS(ITEMP,8,1)
      IFW=JIBITS(ITEMP,0,3)

C PERFORM OA INTERPOLATIONS

      RAT=(IIREAD-1)/64.
      RATL=(IIREAD-.5)/64.

      DO 700 N=1,8
      OADATA(N)=REC(273+N)+(BUFF(273+N)-REC(273+N))*RAT
700   OADATL(N)=REC(273+N)+(BUFF(273+N)-REC(273+N))*RATL
      IF(OADATA(2).LT.0.0)OADATA(2)=OADATA(2)+24.0
      IF(OADATA(2).EQ.0.0)OADATA(2)=24.0
      IF(OADATL(2).LT.0.0)OADATL(2)=OADATL(2)+24.0
      IF(OADATA(8).LT.-180.0)OADATA(8)=OADATA(8)+360.0
      IF(OADATL(8).LT.-180.0)OADATL(8)=OADATL(8)+360.0

      IF(ISF.EQ.1)GOTO 720
      DO 710 N=9,22
```

```
      OADATA(N)=REC(273+N)+(BUFF(273+N)-REC(273+N))*RAT
710   OADATL(N)=REC(273+N)+(BUFF(273+N)-REC(273+N))*RATL
      GOTO 800

720   OADATA(9)=REC(282)+RAT*8.*REC(283)
      IF(OADATA(9).GE.180.)OADATA(9)=OADATA(9)-360.
      IF(OADATA(9).LE.-180.)OADATA(9)=OADATA(9)+360.
      OADATA(10)=REC(283)
      OADATL(9)=REC(282)+RATL*8.*REC(283)
      IF(OADATL(9).GE.180.)OADATL(9)=OADATL(9)-360.
      IF(OADATL(9).LE.-180.)OADATL(9)=OADATL(9)+360.
      OADATL(10)=REC(283)
      IF(ISVIF.EQ.0)GOTO 800
      IF(IAFLAG.EQ.0)GOTO 750
      DELTA=RAT*GAMMA
      CD=COS(DELTA)
      CE=COS(GAMMA-DELTA)
      CALL SOLVE(A1,B1,R,CD,CE,0,DET1,V1)
      CALL SPHERE(V1,OADATA(14),OADATA(13))
      OADATA(11)=ANGLE(V1,SUN)*FAC
      OADATA(12)=ANGLE(V1,RMOON)*FAC
      CALL MULT(SUN,E,P,V1,F)
      CALL SPHERE(F,OADATA(15),OADATA(16))
      CALL SOLVE(A2,B2,R,CD,CE,0,DET2,V2)
      CALL SPHERE(V2,OADATA(20),OADATA(19))
      OADATA(17)=ANGLE(V2,SUN)*FAC
      OADATA(18)=ANGLE(V2,RMOON)*FAC
      CALL MULT(SUN,E,P,V2,F)
      CALL SPHERE(F,OADATA(21),OADATA(22))

      DELTAL=RATL*GAMMA
      CDL=COS(DELTAL)
      CEL=COS(GAMMA-DELTAL)
      CALL SOLVE(A1,B1,R,CDL,CEL,0,DET1,V1L)
      CALL SPHERE(V1L,OADATL(14),OADATL(13))
      OADATL(11)=ANGLE(V1L,SUN)*FAC
      OADATL(12)=ANGLE(V1L,RMOON)*FAC
      CALL MULT(SUN,E,P,V1L,F)
      CALL SPHERE(F,OADATL(15),OADATL(16))
      CALL SOLVE(A2,B2,R,CDL,CEL,0,DET2,V2L)
      CALL SPHERE(V2L,OADATL(20),OADATL(19))
      OADATL(17)=ANGLE(V2L,SUN)*FAC
      OADATL(18)=ANGLE(V2L,RMOON)*FAC
      CALL MULT(SUN,E,P,V2L,F)
      CALL SPHERE(F,OADATL(21),OADATL(22))
      GOTO 800

750   DO 755 N=11,22
      OADATA(N)=-99999.
755   OADATL(N)=-99999.

C APPLY DEAD TIME CORRECTION

800   IF(ICH11 .LT. 0) GO TO 810
      ICH11=ICH11/(1-ICH11/1.11E5)
      ICH12=ICH12/(1-ICH12/1.11E5)
810   IF(ICH11L .LT. 0) GO TO 820
      ICH11L=ICH11L/(1-ICH11L/1.11E5)
      ICH12L=ICH12L/(1-ICH12L/1.11E5)
820   IF(ICH2 .LT. 0) GO TO 830
      ICH2=ICH2/(1-ICH2/4.44E5)
830   IF (IIREAD.EQ.64) IIREAD=0
      IX=IIREAD
      4 RETURN
```

```
      ENTRY INITV(IUNTP,JTIMEP,IDDATE,IORB,ID,ISPINF,INF,
     >MODE1,ITON,ITOFF,IDMF,MODE2,ITON2,ITOFF2)
      INUNIT= IUNTP
      IIREAD = 0
      ISW = 0
      SAVE1 = 2.0
      JTIME= JTIMEP - 8000
      READ(INUNIT,END=4,ERR=4) (IREC(I),I=1,12)
      ID = SATID(1)
      IDDATE = IREC(1)
      IDATE=IDDATE
      IORB = IREC(2)
      IORBIT=IORB
      IF(ID.EQ.'C'.OR.ID.EQ.'c') INDNAME=
     +'SPRLC$DISK1:[VAECOMMON.IND]VDFC.DAT'
      IF(ID.EQ.'D'.OR.ID.EQ.'d') INDNAME=
     +'SPRLC$DISK1:[VAECOMMON.IND]VDFD.DAT'
      IF(ID.EQ.'E'.OR.ID.EQ.'e') INDNAME=
     +'SPRLC$DISK1:[VAECOMMON.IND]VDFE.DAT'
      OPEN(UNIT=9,NAME=INDNAME,STATUS='OLD',READONLY,ERR=179)
      GOTO 900
179   TYPE *, 'ERROR OPEN'
900   READ(9,910,END=940)SATID1,IORB1,MODE1,SD1,NI1,IDATE1,
     +ITON1,ITOFF1,MT1
910   FORMAT(A1,1X,I5,1X,A4,1X,2A1,1X,3(I5,1X),I3)
      IF (IORB1.NE.IORB) GOTO 900
      IORB2=0
      READ(9,910,END=920)SATID2,IORB2,MODE2,SD2,NI2,IDATE2,
     +ITON2,ITOFF2,MT2

      ISF=0
      IF (SD1.EQ.'S') ISF=1
      ISPINF=ISF
      INF=0
      IF (NI1.EQ.'N') INF=1
      ITON=ITON1
      ITOFF=ITOFF1

920   IDMF=0
      IF(IORB1.EQ.IORB2) THEN
      IDMF=1
      ELSE
      MODE2='    '
      ITON2=0
      ITOFF2=0
      ENDIF
      CLOSE(UNIT=9)
      GOTO 950
940   TYPE *,'ORBIT NOT FOUND IN INDEX'
      CLOSE(UNIT=9)
      STOP

950   CONTINUE

      READ(INUNIT,END=4,ERR=4) (IBUFF(K),K=1,295)
      ISW= ISW+1
      IF(IBUFF(1) .LT. JTIME) GO TO 950
      RETURN

      ENTRY SETUP(IANGZ)
      IANGSW= IANGZ
      GO TO 4
```

```
      END

      FUNCTION ANGLE(V1,V2)
      DIMENSION V1(1),V2(1)
      ANGLE=ACOS((V1(1)*V2(1)+V1(2)*V2(2)+V1(3)*V2(3)) /
     >SQRT((V1(1)**2+V1(2)**2+V1(3)**2)*(V2(1)**2+V2(2)**2+V2(3)**2)))
      RETURN
      END

      SUBROUTINE CROSS(A,B,C)
      DIMENSION A(1),B(1),C(1)
      C(1)=A(2)*B(3)-A(3)*B(2)
      C(2)=A(3)*B(1)-A(1)*B(3)
      C(3)=A(1)*B(2)-A(2)*B(1)
      CL=SQRT(C(1)**2+C(2)**2+C(3)**2)
      C(1)=C(1)/CL
      C(2)=C(2)/CL
      C(3)=C(3)/CL
      RETURN
      END

      SUBROUTINE MULT(SUN,E,P,V,F)
      DIMENSION SUN(1),E(1),P(1),V(1),F(1)
      F(1)=SUN(1)*V(1)+SUN(2)*V(2)+SUN(3)*V(3)
      F(2)=E(1)*V(1)+E(2)*V(2)+E(3)*V(3)
      F(3)=P(1)*V(1)+P(2)*V(2)+P(3)*V(3)
      RETURN
      END

      SUBROUTINE CART(THETA,PHI,W)
      DIMENSION W(1)
      T=THETA*.01745329
      P=PHI*.01745329
      W(1)=COS(T)*COS(P)
      W(2)=COS(T)*SIN(P)
      W(3)=SIN(T)
      RETURN
      END

      SUBROUTINE SPHERE(V,TH,PH)
      DIMENSION V(1)
      AV=SQRT(V(1)**2+V(2)**2+V(3)**2)
      V(1)=V(1)/AV
      V(2)=V(2)/AV
      V(3)=V(3)/AV
      PH=ATAN2(V(2),V(1))*57.29578
      TH=ASIN(V(3))*57.29578
      RETURN
      END

      SUBROUTINE SOLVE(X,Y,Z,CAX,CAY,CAZ,DET,V)
      DIMENSION X(1),Y(1),Z(1),V(1)
      IF(DET.EQ.0.0)GOTO 100
      V(1)= (CAX*(Y(2)*Z(3)-Y(3)*Z(2)) + X(2)*(Y(3)*CAZ-CAY*Z(3))
     >+ X(3)*(CAY*Z(2)-Y(2)*CAZ)) / DET
      V(2)= (X(1)*(CAY*Z(3)-Y(3)*CAZ) + CAX*(Y(3)*Z(1)-Y(1)*Z(3))
     >+ X(3)*(Y(1)*CAZ-CAY*Z(1))) / DET
      V(3)= (X(1)*(Y(2)*CAZ-CAY*Z(2)) + X(2)*(CAY*Z(1)-Y(1)*CAZ)
     >+ CAX*(Y(1)*Z(2)-Y(2)*Z(1))) / DET
      RETURN
100   V(1)=0.
      V(2)=0.
      V(3)=0.
      RETURN
```

```
      END

      SUBROUTINE DETER(X,Y,Z,DET)
      DIMENSION X(1),Y(1),Z(1)
      DET= X(1)*(Y(2)*Z(3)-Y(3)*Z(2)) + X(2)*(Y(3)*Z(1)-Y(1)*Z(3))
     > + X(3)*(Y(1)*Z(2)-Y(2)*Z(1))
      RETURN
      END

      SUBROUTINE LUNVEC(A1,A2,G,H,RMOON)
      DIMENSION A1(1),A2(1),RMOON(1)
      A=A1(1)
      B=A1(2)
      C=A1(3)
      D=A2(1)
      E=A2(2)
      F=A2(3)
      S = (E*C-B*F)**2 + (A*F-D*C)**2 + (E*A-D*B)**2
      Q = (A*H-D*G)*(F*A-D*C) + (E*G-B*H)*(E*C-B*F)
      T = (E*G-B*H)**2 + (A*H-D*G)**2 - (E*A-D*B)**2
      R = (2*Q)**2 - 4*S*T
      IF(R.LT.0.)GOTO 100
      RMOON(3) = (2*Q+SQRT(R)) / (2*S)
      V = H-F*RMOON(3)
      W = G-C*RMOON(3)
      RMOON(1) = (W*E-V*B) / (E*A-D*B)
      RMOON(2) = (V*A-D*W) / (E*A-D*B)
      RETURN

      100 RMOON(1)=0.
      RMOON(2)=0.
      RMOON(3)=0.
      RETURN
      END

      SUBROUTINE SUNVEC(IDATE,ITIME,SUN,gst)
      DIMENSION SUN(1)
      DATA RAD/57.29578/
      REAL*8 DJ,FDAY
      FDAY=FLOAT(ITIME)/86400000.
      IYR=IDATE/1000
      IDAY=IDATE-IYR*1000
      DJ=365*IYR+(IYR-1)/4+IDAY+FDAY-0.5D0
      T=DJ/36525.
      VL=DMOD(279.696678+.9856473354*DJ,360.D0)
      gst=dmod(279.690983+.9856473354*DJ+360.*FDAY+180.,360.D0)
      G=DMOD(358.475845+.985600267*DJ,360.D0)/RAD
      SLONG=VL+(1.91946-.004789*T)*SIN(G)+.020094*SIN(2.*G)
      OBLIQ=(23.45229-0.0130125*T)/RAD
      SLP=(SLONG-.005686)/RAD
      SIND=SIN(OBLIQ)*SIN(SLP)
      COSD=SQRT(1.-SIND**2)
      SDEC=ATAN(SIND/COSD)
      SRASN=3.14159-ATAN2(1/TAN(OBLIQ)*SIND/COSD,-COS(SLP)/COSD)
      SUN(1)=COS(SRASN)*COS(SDEC)
      SUN(2)=SIN(SRASN)*COS(SDEC)
      SUN(3)=SIN(SDEC)
      RETURN
      END

      SUBROUTINE RAYL

C SUBROUTINE RAYL CONVERTS RAW VAE COUNTS TO RAYLEIGHS, AND STORES
C THE VALUES IN RAY1(1:4) AND RAY2. THE CHANNEL NUMBER REQUESTED
```

```
C MUST BE IN ICH AND THE SATELLITE NUMBER (C=1,D=2,E=3) MUST BE
C IN NSAT.  FIRST, DARK COUNT IS ESTIMATED FROM THE
C PHOTOMULTIPLIER TUBE TEMPERATURE, THEN THE SENSITIVITY IS
C INTERPOLATED FOR THE SPECIFIED FILTER WHEEL TEMPERATURE, FILTER
C WHEEL POSITION, CHANNEL, AND SATELLITE.
C SUBROUTINE ALSO SUBTRACTS OUT THE GALACTIC AND ZODIACAL BACKGROUND
C IF IGZC=1.

C CALLING PROGRAM MUST SUPPLY /CVAERD/ AND /CRAYL/ IN COMMON

C Modification 6/15/88 to work with galactic and zodiacal background
C subtraction on SPRLC.
C * errors detected in VAEREAD on 1/7/91 fixed here *
C Calling program must initialize ISKIP to 0 and then set it to 1
C immediately after RAYL is called for the first time.

      INTEGER*2 LEN
      INTEGER*4 RA(4),DEC(4),ELAT(4),ELON(4)
      CHARACTER*4 IE
      DIMENSION GAL(5,120,60),ZOD(5,60,30),
     >      OA(22),OAL(22),RAY1(4),IFM(7,2,3),FBW(7,2,3)
      DIMENSION C1(2,3),C2(2,3),TPM(2),OLDTPM(2),DC(2),S(7,7,2,3),
     >      C(98),D(98),E(98),STV(2),OLDTFW(2),IOLDFW(2)

      EQUIVALENCE (C,S(1)),(D,S(99)),(E,S(197))

      COMMON /CVAERD/ITIME,THET,ICH11,ICH12,ISQ11,ISQ12,ITIMEL,THETL,
     >      IFW,IE,ICH11L,ICH12L,ISQ11L,ISQ12L,IATN1,ICH2,ISQ2,IATN2,
     >      TBAF1,TBAF2,TBAF11,TBAF22,TAEL,TBEL,TPM,TFW
     >      ,IEND4,IX,ISVIF,OA,OAL

      COMMON /CRAYL/ICH,NSAT,IGZC,STV,DC,RAY1,RAY2,ICE,ISKIP

      DATA OLDTPM/0.,0./,OLDTFW/0.,0./,IOLDFW/0,0/
      DATA C1/.1544,.175,.1658,.1677,.1757,.1759/
      DATA C2/4.5,4.6,19.02,11.85,11.57,-1.827/

      DATA C/ 20.0, 19.6, 19.4, 19.4, 19.9, 21.8, 24.4,
     2      101.5, 79.3, 66.8, 57.3, 51.1, 45.9, 44.2,
     3      12.2, 11.5, 11.1, 11.0, 11.1, 12.0, 13.5,
     4      23.6, 20.7, 19.2, 18.6, 18.4, 18.6, 19.6,
     5      35.2, 35.3, 35.8, 36.7, 37.9, 39.4, 41.4,
     6      0.0,  0.0,  0.0,  0.0,  0.0,  0.0,  0.0,
     7      10.7, 10.4, 10.6, 10.9, 11.4, 12.1, 12.8,
     1      0.30, 0.27, 0.25, 0.24, 0.24, 0.24, 0.25,
     2      0.00, 0.00, 0.00, 0.00, 0.00, 0.00, 0.00,
     3      1.45, 1.13, 0.95, 0.82, 0.73, 0.65, 0.63,
     4      0.15, 0.15, 0.15, 0.16, 0.17, 0.17, 0.19,
     5      0.24, 0.24, 0.23, 0.23, 0.24, 0.26, 0.29,
     6      0.15, 0.14, 0.14, 0.14, 0.14, 0.15, 0.17,
     7      0.61, 0.61, 0.62, 0.64, 0.66, 0.68, 0.72 /
      DATA D/ 80.0, 72.1, 68.5, 72.1, 77.8, 87.3,106.6,
     2      7.6,  7.6,  7.9,  8.4,  9.6, 12.2, 16.3,
     3      26.0, 24.2, 23.3, 23.5, 24.4, 26.2, 29.2,
     4      9.7,  8.5,  8.2,  8.1,  8.1,  8.1,  8.3,
     5      12.2, 11.3, 11.1, 11.1, 11.1, 11.2, 11.6,
     6      0.0,  0.0,  0.0,  0.0,  0.0,  0.0,  0.0,
     7      22.2, 17.6, 16.7, 16.3, 16.4, 19.7, 20.4,
     1      0.13, 0.12, 0.11, 0.11, 0.11, 0.11, 0.11,
     2      0.00, 0.00, 0.00, 0.00, 0.00, 0.00, 0.00,
     3      0.10, 0.10, 0.10, 0.11, 0.12, 0.16, 0.21,
     4      0.24, 0.19, 0.18, 0.18, 0.18, 0.21, 0.22,
     5      0.76, 0.69, 0.65, 0.69, 0.74, 0.83, 1.02,
     6      0.37, 0.34, 0.33, 0.33, 0.34, 0.37, 0.41,
```

```
     7       0.14, 0.13, 0.13, 0.13, 0.13, 0.13, 0.13 /
      DATA E/124.4, 88.8, 73.7, 61.7, 53.9, 47.2, 44.2,
     2       11.0, 10.3, 10.1, 10.1, 10.4, 11.7, 14.1,
     3       42.9, 42.9, 42.8, 42.9, 42.9, 42.9, 42.9,
     4       22.8, 21.2, 20.4, 20.7, 21.3, 22.8, 29.3,
     5       12.7, 12.7, 13.2, 15.8, 21.8, 29.3, 42.4,
     6       0.0,  0.0,  0.0,  0.0,  0.0,  0.0,  0.0,
     7       19.8, 19.6, 20.4, 22.5, 24.2, 46.2, 72.8,
     1       0.26, 0.24, 0.23, 0.23, 0.24, 0.26, 0.33,
     2       0.00, 0.00, 0.00, 0.00, 0.00, 0.00, 0.00,
     3       0.15, 0.14, 0.14, 0.14, 0.14, 0.16, 0.19,
     4       0.23, 0.23, 0.24, 0.26, 0.29, 0.54, 0.86,
     5       1.27, 0.91, 0.76, 0.63, 0.55, 0.48, 0.28,
     6       0.60, 0.60, 0.60, 0.60, 0.60, 0.60, 0.60,
     7       0.16, 0.16, 0.16, 0.19, 0.27, 0.36, 0.52 /

      DATA IFM/ 55, 73, 52, 63, 33, 0, 42,
     >       63,    0, 73, 42, 55, 52, 33,
     >       73, 52, 42, 48, 55,     0, 63,
     >       48,    0, 52, 63, 73, 42, 55,
     >       73, 52, 28, 65, 55,     0, 63,
     >       65,    0, 52, 63, 73, 28, 55 /

      DATA FBW/ 29.8, 20.0, 22.5, 22.7,   0.0,  0.0, 23.0,
     >       22.7, 0.0, 20.0, 23.0, 29.8, 22.5,  0.0,
     >       29.0, 21.0, 19.0, 0.0, 25.0,  0.0, 20.5,
     >       0.0,  0.0, 21.0, 20.5, 29.0, 19.0, 25.0,
     >       15.8, 20.1, 0.0,  0.0, 19.5,  0.0, 21.0,
     >       0.0,  0.0, 20.1, 21.0, 15.8,  0.0, 19.5 /

      ICE=0

      IF(IFW.LT.1.OR.IFW.GT.7)GOTO 300
      IF(TPM(ICH).EQ.OLDTPM(ICH))GOTO 100
      IF(TPM(ICH).GT.40.0.OR.TPM(ICH).LT.-20.0)TPM(ICH)=OLDTPM(ICH)
      OLDTPM(ICH)=TPM(ICH)
      DC(ICH)=EXP(C1(ICH,NSAT)*(TPM(ICH)-C2(ICH,NSAT)))

100   IF(TFW.EQ.OLDTFW(ICH).AND.IFW.EQ.IOLDFW(ICH))GOTO 200
      IF(TFW.GT.40.0.OR.TFW.LT.-20.0)TFW=OLDTFW(ICH)
      OLDTFW(ICH)=TFW
      IOLDFW(ICH)=IFW
      S1=S(IFIX(TFW+30.)/10,IFW,ICH,NSAT)
      S2=S(IFIX(TFW+40.)/10,IFW,ICH,NSAT)
      STV(ICH)=S1+(TFW/10.-IFIX(TFW)/10)*(S2-S1)

200   IF(ICH.EQ.2)GOTO 250
      RAY1(1)=(ICH11-DC(1))*STV(1)
      RAY1(2)=(ICH12-DC(1))*STV(1)
      RAY1(3)=(ICH11L-DC(1))*STV(1)
      RAY1(4)=(ICH12L-DC(1))*STV(1)
      GOTO 500

250   RAY2=(ICH2-DC(2))*STV(2)
      GOTO 500

300   RAY2=0
      DO 400 I=1,4
400   RAY1(I)=0.
      RETURN

500   IF(IGZC.EQ.0)RETURN

C Only open and read the data file the first time RAYL is called.
```

```
      IF(ISKIP.EQ.0) CALL GZREAD(GAL,ZOD)
      IF(ICH.EQ.2)GOTO 600
      LAM=IFM(IFW,ICH,NSAT)
      IF(LAM.NE.0)GOTO 530
      ICE=4
      RETURN

530   CONTINUE

      ICE=1
      IF(OA(13).LT.-180..OR.OA(13).GT.180.)ICE=2
      IF(OA(14).LT.-90..OR.OA(14).GT.90.)ICE=2
      IF(OA(15).LT.-90..OR.OA(15).GT.90.)ICE=2
      IF(OA(16).LT.-180..OR.OA(16).GT.180.)ICE=2
      IF(ICE.EQ.2)RETURN
      IF(OA(13).LT.0.)OA(13)=OA(13)+360.
      IF(OAL(13).LT.0.)OAL(13)=OAL(13)+360.
      IF(OAL(13).GT.350..AND.OA(13).LT.10.)OA(13)=OA(13)+360.
      IF(OAL(13).LT.10..AND.OA(13).GT.350.)OAL(13)=OAL(13)+360.
      DRA=OAL(13)-OA(13)
      DDEC=OAL(14)-OA(14)
      DELAT=OAL(15)-OA(15)
      OAL(16)=ABS(OAL(16))
      OA(16)=ABS(OA(16))
      DELON=OAL(16)-OA(16)

C * the following is changed in this program      1/7/91
      RA(1)=IFIX(OA(13)+0.25*DRA)/3 +1
      RA(2)=IFIX(OA(13)+0.25*DRA*3.)/3 +1
      RA(3)=IFIX(OAL(13)+0.25*DRA)/3 +1
      RA(4)=IFIX(OAL(13)+0.25*DRA*3.)/3 +1
      DEC(1)=IFIX(OA(14)+0.25*Ddec+90.)/3 +1
      DEC(2)=IFIX(OA(14)+0.25*Ddec*3 +90.)/3 +1
      DEC(3)=IFIX(OAL(14)+0.25*Ddec+90.)/3 +1
      DEC(4)=IFIX(OAL(14)+0.25*Ddec*3. + 90.)/3 +1
      ELAT(1)=IFIX(ABS(OA(15)+0.25*DELAT))/3 + 1
      ELAT(2)=IFIX(ABS(OA(15)+0.25*DELAT*3))/3 +1
      ELAT(3)=IFIX(ABS(OAL(15)+0.25*DELAT))/3 +1
      ELAT(4)=IFIX(ABS(OAL(15)+0.25*DELAT*3))/3 +1
      ELON(1)=IFIX(OA(16)+0.25*DELON)/3 +1
      ELON(2)=IFIX(OA(16)+0.25*DELON*3.)/3 +1
      ELON(3)=IFIX(OAL(16)+0.25*DELON)/3 +1
      ELON(4)=IFIX(OAL(16)+0.25*DELON*3.)/3 +1

      IF(LAM.EQ.42.OR.LAM.EQ.33.OR.LAM.EQ.28)   LI = 1
      IF(LAM.EQ.52.OR.LAM.EQ.48)    LI = 2
      IF(LAM.EQ.55)      LI = 3
      IF(LAM.EQ.63.OR.LAM.EQ.65)    LI = 4
      IF(LAM.EQ.73)      LI = 5

      DO 550 I=1,4
      IF(RA(I).GT.120.OR.RA(I).LT.1)RA(I)=1
      IF(ELON(I).GT.60)ELON(I)=60
      IF(ELON(I).LT.1)ELON(I)=1
      IF(ELAT(I).GT.30)ELAT(I)=30
      IF(DEC(I).GT.60)DEC(I)=60

C * following elon(I) & elat(I) replace faulty RA(I) & DEC(I)
      IF(GAL(LI,RA(I),DEC(I)).GT.0.OR.
     >ZOD(LI,elon(I),elat(I)).GT.0.) THEN
      GOTO 545
      ENDIF
```

```
      GAL(LI,RA(I),DEC(I))=0.
      ZOD(LI,RA(I),DEC(I))=0.
      ICE=-1
C * original "DEC(I))*16." in 545 changed
C * original "IL" in cont 545 changed to "li"
545   RAY1(I) = RAY1(I) - ( (GAL(LI,RA(I),DEC(I))) +
     & ZOD(li,ELON(I),ELAT(I)))*FBW(IFW,ICH,NSAT)

550   CONTINUE

      RETURN

600   ICE=1
      IF(OAL(19).LT.-180..OR.OAL(19).GT.180.)ICE=2
      IF(OAL(20).LT.-90..OR.OAL(20).GT.90.)ICE=2
      IF(OAL(21).LT.-90..OR.OAL(21).GT.90.)ICE=2
      IF(OAL(22).LT.-180..OR.OAL(22).GT.180.)ICE=2
      IF(ICE.EQ.2)RETURN
      IF(OAL(19).LT.0.)OAL(19)=OAL(19)+360.
      IRA2=IFIX(OAL(19))/3 +1
      IF(IRA2.GT.120)IRA2=120
      IDEC2=IFIX(OAL(20)+90.)/3 +1
      IF(IDEC2.GT.60)IDEC2=60
      IELAT2=IFIX(ABS(OAL(21)))/3+1
      IF(IELAT2.GT.30)IELAT2=30
      IELON2=IFIX(ABS(OAL(22)))/3 +1
      IF(IELON2.GT.60)IELON2=60
      LAM=IFM(IFW,ICH,NSAT)
      IF(LAM.EQ.42.OR.LAM.EQ.33.OR.LAM.EQ.28)    LI = 1
      IF(LAM.EQ.52.OR.LAM.EQ.48)     LI = 2
      IF(LAM.EQ.55)      LI = 3
      IF(LAM.EQ.63.OR.LAM.EQ.65)     LI = 4
      IF(LAM.EQ.73)      LI = 5
      IF(LAM.NE.0)GOTO 640
      ICE=4
      RETURN
640   IF(GAL(LI,IRA2,IDEC2).GT.0.)GOTO 650
      GAL(LI,IRA2,IDEC2)=0.
      ICE=-1
C * following "li" replaces original faulty IL
650   RAY2 = RAY2 - (GAL(LI,IRA2,IDEC2) +
     &        ZOD(li,IELON2,IELAT2))*FBW(IFW,ICH,NSAT)
      RETURN
900   ICE=3
      RETURN
      END

      SUBROUTINE GZREAD(GAL,ZOD)

C Subroutine GZREAD returns a 120x60 array of galaxy data and a 60x30
C array of zodiacal light data for each of 5 wavelengths.

      DIMENSION   GZDAT(45000), GAL(5,120,60), ZOD(5,60,30)
      OPEN(12,FILE='SPRLC$DISK1:[VAECOMMON.IND]GALZOD.DAT',TYPE='OLD',
     &        READONLY)
      READ(12,1000,END=5) GZDAT
1000  FORMAT(1X,15F5.2)
5     IC = 0
C     There are 5 pairs of galaxy and zodiacal light data (one for each
C     wavelength).
      DO 10 I = 1, 5
C     Read galaxy data for one wavelength
      DO 20 K = 1, 60
      DO 30 J = 1, 120
```

```
      IC = IC + 1
      GAL(I,J,K) = GZDAT(IC)
30    CONTINUE
20    CONTINUE
C     Read zodiacal light data for one wavelength
      DO 40 N = 1, 30
      DO 50 M = 1, 60
      IC = IC + 1
      ZOD(I,M,N) = GZDAT(IC)
50    CONTINUE
40    CONTINUE
10    CONTINUE
      RETURN
      END

      SUBROUTINE MAXMUL1(A,B,C)
C     IMPLICIT DOUBLE PRECISION (A-H,O-Z)
      DIMENSION A(3,3),B(3),C(3)
      C(1)=A(1,1)*B(1)+A(1,2)*B(2)+A(1,3)*B(3)
      C(2)=A(2,1)*B(1)+A(2,2)*B(2)+A(2,3)*B(3)
      C(3)=A(3,1)*B(1)+A(3,2)*B(2)+A(3,3)*B(3)
      RETURN
      END
```

Appendix 3

The following is a listing of the Pascal (VAX-11) program used to invert the AE-E Visible Airglow Experiment measurements of the $O^+(^2D-^2P)$ twilight airglow emission at 7320 Å.

```
program TWIFITTER (input,output);
{     program for inverting multi-directional twilight          }
{   AE VAE 7320 Å observations developed for the project:       }
{                                                               }
{  An Assessment of Twilight Airglow Inversion Procedures       }
{         Using Atmosphere Explorer Observations                }
{                                                               }
{                    by I.C.McDade                              }
{                                                               }
{              under NASA Grant NAG 5-1502                      }
{                                                               }
{                                                               }
{  this self-contained VAX-11 PASCAL program will return:       }
{                                                               }
{        the atomic oxygen scale height,  H (km)                }
{        the O+(2P) ionization frequency, Iinf (sec-1)          }
{    and the O-atom density @ 250 km,     O250 (cm-3)           }
{                                                               }
{  that best fit the input 7320-30 Å column emission rates      }
{                                                               }
{                                                               }
{   many of the functions and procedures are taken from:        }
{                                                               }
{    Numerical Recipes: The Art of Scientific Computing         }
{ by W.H.Press, B.P.Flannery, A.Teukolsky and W.T.Vetterling    }
{       Cambridge University Press, New York, 1986              }
{                                                               }
{   other aspects are based on the formulation described by     }
{   McDade et al. J.Geophys.Res., Vol 96, pp. 259-266, 1991     }
{

function   gammln (xx: real): real;
 const
  stp = 2.50662827465;
  half = 0.5;
  one = 1.0;
  fpf = 5.5;
 var
  x,tmp,ser: double;
  j: integer;
  cof: array[1..6] of double;
begin
 cof[1]:= 76.18009173;
 cof[2]:= -86.50532033;
 cof[3]:= 24.01409822;
 cof[4]:= -1.231739516;
 cof[5]:= 0.120858003e-2;
 cof[6]:= -0.536382e-5;
 x:= XX-one;
 tmp:= x+fpf;
```

```
 tmp:= (x+half)*ln(tmp)-tmp;
 ser:= one;
 for j:= 1 to 6 do
  begin
   x:= x+one;
   ser:= ser+cof[j]/x
  end;
 gammln:= sngl(tmp+ln(stp*ser))
end;


procedure  gser (a,x: real; var gamser,gln: real);
 label 1;
 const
  itmax = 100;
  eps = 3.0e-7;
 var
  n: integer;
  sum,del,ap: real;
begin
 gln:= gammln(a);
 if  (x <= 0.0) then
  begin
   if  (x < 0.0) then
    begin
     writeln('pause in GSER - x less than 0');
     readln
    end;
   gamser:= 0.0
  end
 else
  begin
   ap:= a;
   sum:= 1.0/a;
   del:= sum;
   for n:= 1 to itmax do
    begin
     ap:= ap+1.0;
     del:= del*x/ap;
     sum:= sum+del;
     if  (abs(del) < abs(sum)*eps) then
      goto 1
    end;
   writeln('pause in GSER-a too large,itmax too small');
   readln;
1:
   gamser:= sum*exp(-x+a*ln(x)-gln)
  end
 end;


 procedure  gcf (a,X: real; var gammcf,gln: real);
  label
   1;
  const
   itmax = 100;
   eps = 3.0e-7;
  var
   n: integer;
   gold,g,fac,b1,b0,anf,ana,an,a1,a0: real;
 begin
  gln:= gammln(a);
  gold:= 0.0;
```

```
 a0:= 1.0;
 a1:= x;
 b0:= 0.0;
 b1:= 1.0;
 fac:= 1.0;
 for n:= 1 to itmax do
  begin
   an:= 1.0*n;
   ana:= an-a;
   a0:= (a1+a0*ana)*fac;
   b0:= (b1+b0*ana)*fac;
   anf:= an*fac;
   a1:= x*a0+anf*a1;
   b1:= x*b0+anf*b1;
   if  (a1 <> 0.0) then
    begin
     fac:= 1.0/a1;
     g:= b1*fac;
     if  (abs((g-gold)/g) < eps) then
      goto 1;
     gold:= g
    end
  end;
 writeln('pause in GCF-a too large,itmax too small');
 readln;
1:
 gammcf:= exp(-x+a*ln(x)-gln)*g
end;


function  gammp (a,x: real): real;
 var
  gammcf,gln: real;
begin
 if  ((x < 0.0) or (a <= 0.0)) then
  begin
   writeln('pause in GAMMP-invalid arguments');
   readln
  end;
 if  (x < (a+1.0)) then
  begin
   gser(a,x,gammcf,gln);
   gammp:= gammcf
  end
 else
  begin
   gcf(a,x,gammcf,gln);
   gammp:= 1.0-gammcf
  end
end;


function  erf (x: real): real;
begin
 if  (x < 0.0) then
  begin
   erf:= -gammp(0.5,sqr(x))
  end
 else
  begin
   erf:= gammp(0.5,sqr(x))
  end
end;
```

```
const
 TWO_PI = 6.283185307179586476925287; {value of Two pi}
 PI = 3.141592653589793238462643;{Value of PI}
 R = 6370.0;  {Approximate Earth Radius}


[GLOBAL]
function   INRANGE (VALUE,MIN,MAX: REAL): REAL;
 var
  NRANGES: REAL;
  N: INTEGER;
begin
 if  (VALUE < MIN) or (VALUE >= MAX) then {value outside range}
  begin                          {get how many times}
   VALUE:= VALUE-MIN;            {convert from min to max to}
   MAX:= MAX-MIN;                {0 to (max-min) }
   NRANGES:= VALUE/MAX;          {by dividing by range}
   N:= TRUNC(NRANGES);           {get no of complete intervals}
   if  NRANGES < 0.0 then
    N:= N-1;                     {make trunc work correctly}
   VALUE:= MAX*(NRANGES-N);      {get the in range value}
   INRANGE:= VALUE+MIN;          {add on the minimum offset}
  end
 else
  begin                          {otherwise the value}
   INRANGE:= VALUE;              {is already in range}
  end;                           {so do nothing}
end;                             {back to caller}

[EXTERNAL]
function   MTH$ASIN(X: REAL): REAL;
EXTERNAL;

[EXTERNAL]
function   MTH$ACOS(X: REAL): REAL;
EXTERNAL;

[GLOBAL]
function   ASIND(X: REAL): REAL;
begin
 ASIND:= 360.0*INRANGE ( MTH$ASIN(X),0,TWO_PI )/TWO_PI;
end;

[GLOBAL]
function   SIND(X: real): real;
begin
 SIND:= SIN(X*TWO_PI/360.0);
end;

[GLOBAL]
function   COSD(X: real): real;
begin
 COSD:= COS(X*TWO_PI/360.0);
end;

function   angle (v11,v12,v13,v21,v22,v23: real): real;
{returns angle in degrees between two Cartesian vectors}
 var
  a,b,c: real;
begin
 a:= v11*v21+v12*v22+v13*v23;
 b:= v11*v11+v12*v12+v13*v13;
```

```
  c:= v21*v21+v22*v22+v23*v23;
  angle:= MTH$ACOS(a/sqrt(b*c))*360.0/TWO_PI;
 end;

{----------------------------START OF MAIN---------------------------}

 type
  glndata = array[1..1000] of real;
  glmma = array[1..3] of real;
  glncabynca = array[1..3,1..3] of real;
  gllista = array[1..3] of integer;
  glnalbynal = array[1..3,1..3] of real; {for MRQCOF,with nalp=3}
  glcovar = array[1..3,1..3] of real;    {for COVSRT,with ncvm=3}
  glnpbynp = array[1..3,1..3] of real;   {for GAUSSJ,with np=3}
  glnpbymp = array[1..3,1..3] of real;   {for GAUSSJ,with np=3 & mp=3}
  glnp = array[1..3] of integer;         {for GAUSSJ,with np=1}
  vect = array[1..3,1..1000] of real;    {for direction vectors}

 var
  pv,vv,sv: vect; {satellite position,line-of-sight & sun GEI vectors}
  X,Y,SIG,alt,za,fit,time,sza: glndata; {time & X should be same}
  A,DYDA: glmma;
  LISTA: gllista;
  covar,ALFA,dummy: glncabynca;
  CHISQ,ALAMDA,chisqo,deltachisq,lnO250,O500: real;
  Xs,XsN2,Flux,WXs: array[1..23] of real;
  N2250,KO,KN2: real;
  I,J,ndata,mfit,maxhindx,deltah: integer;
  infile,vecfile,outfile: text;
  infilename,vecfilename,outfilename: varying[80]of char;
  glochisq: real;
  glbeta: glmma; {for MRQMIN}

{------------------------BRIGHT-----------------------------------}

 procedure  BRIGHT (I: integer; H,Iinf,lnO250: real; var INT: real);
  var
   W,V,O250,Vtemp,Ohm,N2hm: real;
   h1,h2,za1,za2,hm,chim: real;             {NB chi is SZA not SDA}
   a,X,Y,F,TAU,XN2,YN2,HN2,FN2,TAUN2: real;
   k,j: integer;
   IFxWXs: real;
   pos1,posm,sun: array[1..3] of real;
   B: real;
 begin
  O250:= exp(lnO250);
  HN2:= H*16.0/28.0;
  IFxWXs:= 6.7857e-18; {Integrated flux shape x xsection}
  Int:= 0.0;
  h1:= alt[I];
  za1:= za[I];
  pos1[1]:= pv[1,I];
  pos1[2]:= pv[2,I];
  pos1[3]:= pv[3,I];
  sun[1]:= sv[1,I];
  sun[2]:= sv[2,I];
  sun[3]:= sv[3,I];
  for K:= 1 to maxhindx do
   begin {integration along line of sight I}
    h2:= h1+deltah;
    za2:= ASIND((R+h1)*SIND(180.0-za1)/(R+h2));
    B:= za1-za2;
```

```
W:= SIND(B)*(R+h1)/SIND(za2);
if  (B = 0.0) then
 W:= h2-h1;
posm[1]:= pos1[1]+0.5*W*vv[1,I]; {GEI vectors for mid element}
posm[2]:= pos1[2]+0.5*W*vv[2,I];
posm[3]:= pos1[3]+0.5*W*vv[3,I];
chim:= ANGLE(sun[1],sun[2],sun[3],posm[1],posm[2],posm[3]);
hm:= (h1+h2)/2;                    {mean altitude of  element}
if  (chim >= 90.0) then  {Chapman Funcs from eq17.21 of}
                          {Banks&Kockarts}
 begin
  a:= (R+hm)*COSD(chim-90.0)-R;  {minimum ray height}
  if  (a > 100.0) then
   begin
    Y:= (R+a)/H;                 {Y for O}
    YN2:= (R+a)/HN2;             {Y for N2}
F:= sqrt(pi*Y/2.0)*(1+erf(sqrt(Y/2.0)*COSD(chim)/SIND(chim)));
FN2:=sqrt(pi*YN2/2.0)*(1+erf(sqrt(YN2/2.0)*COSD(chim)/SIND(chim)));
    Ohm:= O250*exp(-(hm-250)/H);        {[O] at hm}
    N2hm:= N2250*exp(-(hm-250)/HN2);    {[N2] at hm}
    V:= 0.0;
    for j:= 1 to 23 do {start of wavelength loop}
     begin
      TAU:= O250*exp(-(a-250)/H)*H*1e5*Xs[j]*F;
      TAUN2:= N2250*exp(-(a-250)/HN2)*HN2*1e5*XsN2[j]*FN2;
      Vtemp:= Ohm*exp(-TAU)*exp(-TAUN2)*Flux[j]*WXs[j];
      Vtemp:= Vtemp*Iinf/IFxWXs;      {normalize to parameter Iinf}
      Vtemp:= Vtemp*0.781*0.219/(0.219+KO*Ohm+KN2*N2hm);
      V:= V+Vtemp;
     end; {end of wavelength loop}
    INT:= INT+0.1*W*V;
   end; {end of if  a>100.0}
 end; {end of if  chim >=90}
if  (chim < 90.0) then {Chapman Funcs from eq17.17 of }
                       {Banks & Kockarts}
 begin
  X:= (R+hm)/H;
  XN2:= (R+hm)/HN2;
  F:=sqrt(pi*X/2.0)*exp((X/2)*sqr(COSD(chim)));
  F:=F*(1-erf(sqrt(X/2.0)*COSD(chim)));
  FN2:= sqrt(pi*XN2/2.0)*exp((XN2/2)*sqr(COSD(chim)));
  FN2:= FN2*(1-erf(sqrt(XN2/2.0)*COSD(chim)));
  Ohm:= O250*exp(-(hm-250)/H);        {[O] at hm}
  N2hm:= N2250*exp(-(hm-250)/HN2);    {[N2] at hm}
  V:= 0.0;
  for j:= 1 to 23 do { start of wavelength loop}
   begin
    TAU:= Ohm*H*1e5*Xs[j]*F;     {attenuation due to O}
    TAUN2:= N2hm*HN2*1e5*XsN2[j]*FN2; {"" due to N2}
    Vtemp:= Ohm*exp(-TAU)*exp(-TAUN2)*Flux[j]*WXs[j]; {prod at hm}
    Vtemp:= Vtemp*Iinf/IFxWXs;     {normalize to parameter Iinf}
    Vtemp:= Vtemp*0.781*0.219/(0.219+KO*Ohm+KN2*N2hm);
    V:= V+Vtemp;
   end; {end of wavelength loop}
  INT:= INT+0.1*W*V; {add contribution from chim,hm and }
                     {convert to Rayleighs}
 end; {end of if  chim <90}
fit[I]:= INT; {keep fit to obs I for output}
h1:= h2;
za1:= za2;
pos1[1]:= pos1[1]+W*vv[1,I]; {GEI vectors next element}
pos1[2]:= pos1[2]+W*vv[2,I];
pos1[3]:= pos1[3]+W*vv[3,I];
```

```
   end; {end of integration along line of sight I}
 end; {of procedure BRIGHT}

{----------------------FUNCS----------------------------}

 procedure  FUNCS (i: integer; a: glmma; var y: real; var dyda: glmma);
  var
   ai,af,yi,yf: real;
 begin
  BRIGHT(I,A[1],A[2],A[3],y);
  ai:= 0.999*A[1];
  af:= 1.001*A[1];
  BRIGHT(I,ai,A[2],A[3],yi);
  BRIGHT(I,af,A[2],A[3],yf);
  DYDA[1]:= (yi-yf)/(ai-af);
  ai:= 0.999*A[2];
  af:= 1.001*A[2];
  BRIGHT(I,A[1],ai,A[3],yi);
  BRIGHT(I,A[1],af,A[3],yf);
  DYDA[2]:= (yi-yf)/(ai-af);
  ai:= 0.999*A[3];
  af:= 1.001*A[3];
  BRIGHT(I,A[1],A[2],ai,yi);
  BRIGHT(I,A[1],A[2],af,yf);
  DYDA[3]:= (yi-yf)/(ai-af);
 end; {end of procedure  FUNCS}

{---------------------GAUSSJ-----------------------------}

 procedure  gaussj (var a: glnpbynp; n,np: integer; var b: glnpbymp;
m,mp: integer);
  var
   big,dum,pivinv: real;
   i,icol,irow,j,k,l,ll: integer;
   indxc,indxr,ipiv: glnp;
 begin
  for j:= 1 to n do
   begin
    ipiv[j]:= 0
   end;
  for i:= 1 to n do
   begin
    big:= 0.0;
    for j:= 1 to n do
     begin
      if  (ipiv[j] <> 1) then
       begin
        for k:= 1 to n do
         begin
          if  (ipiv[k] = 0) then
           begin
            if  (abs(a[j,k]) >= big) then
             begin
              big:= abs(a[j,k]);
              irow:= j;
              icol:= k
             end
           end
          else if  (ipiv[k] > 1) then
           begin
            writeln('pause 1 in gaussj-singular matrix');
            readln
           end
```

```
        end
      end
    end;
  ipiv[icol]:= ipiv[icol]+1;
  if  (irow <> icol) then
   begin
    for l:= 1 to n do
     begin
      dum:= a[irow,l];
      a[irow,l]:= a[icol,l];
      a[icol,l]:= dum
     end;
    for l:= 1 to m do
     begin
      dum:= b[irow,l];
      b[irow,l]:= b[icol,l];
      b[icol,l]:= dum
     end
   end;
  indxr[i]:= irow;
  indxc[i]:= icol;
  if  (a[icol,icol] = 0.0) then
   begin
    writeln('pause 2 in gaussj-singular matrix');
    readln
   end;
  pivinv:= 1.0/a[icol,icol];
  a[icol,icol]:= 1.0;
  for l:= 1 to n do
   begin
    a[icol,l]:= a[icol,l]*pivinv
   end;
  for l:= 1 to m do
   begin
    b[icol,l]:= b[icol,l]*pivinv
   end;
  for ll:= 1 to n do
   begin
    if  (ll <> icol) then
     begin
      dum:= a[ll,icol];
      a[ll,icol]:= 0.0;
      for l:= 1 to n do
       begin
        a[ll,l]:= a[ll,l]-a[icol,l]*dum
       end;
      for l:= 1 to m do
       begin
        b[ll,l]:= b[ll,l]-b[icol,l]*dum
       end
     end
   end
 end;
for l:= n downto 1 do
 begin
  if  (indxr[l] <> indxc[l]) then
   begin
    for k:= 1 to n do
     begin
      dum:= a[k,indxr[l]];
      a[k,indxr[l]]:= a[k,indxc[l]];
      a[k,indxc[l]]:= dum
```

```
        end
      end
    end

 end; {end of procedure  gaussj}

{------------------------COVSRT-------------------------------}

 procedure  covsrt (var covar: glcovar; ncvm: integer; ma: integer;
lista: gllista; mfit: integer);
   var
    j,i: integer;
    swap: real;
  begin
   for j:= 1 to ma-1 do
    begin
     for i:= j+1 to ma do
      begin
       covar[i,j]:= 0.0
      end
    end;
   for i:= 1 to mfit-1 do
    begin
     for j:= i+1 to mfit do
      begin
       if  (lista[j] > lista[i]) then
        begin
         covar[lista[j],lista[i]]:= covar[i,j]
        end
       else
        begin
         covar[lista[i],lista[j]]:= covar[i,j]
        end
      end
    end;
   swap:= covar[1,1];
   for j:= 1 to ma do
    begin
     covar[1,j]:= covar[j,j];
     covar[j,j]:= 0.0
    end;
   covar[lista[1],lista[1]]:= swap;
   for j:= 2 to mfit do
    begin
     covar[lista[j],lista[j]]:= covar[1,j]
    end;
   for j:= 2 to ma do
    begin
     for i:= 1 to j-1 do
      begin
       covar[i,j]:= covar[j,i]
      end
    end
  end; {end of procedure  covstr}

 {--------------------------MRQCOF---------------------------}

  procedure  mrqcof (x,y,sig: glndata; ndata: integer; var a: glmma;
 mma: integer; lista: gllista; mfit: integer; var alpha: glnalbynal; var
 beta: glmma; nalp: integer; var chisq: real);
    var
     k,j,i: integer;
```

```
    ymod,wt,sig2i,dy: real;
    dyda: glmma;
begin
 for j:= 1 to mfit do
  begin
   for k:= 1 to j do
    begin
     alpha[j,k]:= 0.0
    end;
   beta[j]:= 0.0
  end;
 chisq:= 0.0;
 for i:= 1 to ndata do
  begin
   FUNCS(i,a,ymod,dyda);
   sig2i:= 1/(sig[i]*sig[i]);
   dy:= y[i]-ymod;
   for j:= 1 to mfit do
    begin
     wt:= dyda[lista[j]]*sig2i;
     for k:= 1 to j do
      begin
       alpha[j,k]:= alpha[j,k]+wt*dyda[lista[k]]
      end;
     beta[j]:= beta[j]+dy*wt
    end;
   chisq:= chisq+dy*dy*sig2i
  end;
 for j:= 2 to mfit do
  begin
   for k:= 1 to j-1 do
    begin
     alpha[k,j]:= alpha[j,k]
    end
  end
end; {end of procedure  MRQCOF}
{----------------------MRQMIN------------------------------}

 procedure  mrqmin (x,y,sig: glndata; ndata: integer; var a: glmma;
mma: integer; lista: gllista; mfit: integer; var covar,alpha:
glncabynca; nca: integer; var chisq,alamda: real);
 label 99;
  var
   k,kk,j,ihit: integer;
   atry,da: glmma;
   oneda: glncabynca;
 begin
  if  (alamda < 0.0) then
   begin
    kk:= mfit+1;
    for j:= 1 to mma do
     begin
      ihit:= 0;
      for k:= 1 to mfit do
       begin
        if  (lista[k] = j) then
         ihit:= ihit+1
       end;
      if  (ihit = 0) then
       begin
        lista[kk]:= j;
```

```
        kk:= kk+1
       end
      else if  (ihit > 1) then
       begin
        writeln('pause 1 in routine MRQMIN');
        writeln('Improper permtuation in LISTA');
        readln;
       end
     end;
    if  (kk <> (mma+1)) then
     begin
      writeln('pause 2 in routine MRQMIN');
      writeln('Improper permtuation in LISTA');
      readln;
     end;
    alamda:= 0.001;
    MRQCOF(x,y,sig,ndata,a,mma,lista,mfit,alpha,glbeta,nca,chisq);
    glochisq:= chisq;
    for j:= 1 to mma do
     begin
      atry[j]:= a[j]
     end
  end;
 for j:= 1 to mfit do
  begin
   for k:= 1 to mfit do
    begin
     covar[j,k]:= alpha[j,k]
    end;
   covar[j,j]:= alpha[j,j]*(1.0+alamda);
   oneda[j,1]:= glbeta[j]
  end;
 GAUSSJ(covar,mfit,nca,oneda,1,1);
 for j:= 1 to mfit do
  da[j]:= oneda[j,1];
 if  (alamda = 0.0) then
  begin
   COVSRT(covar,nca,mma,lista,mfit);
   goto 99
  end;
 for j:= 1 to mfit do
  begin
   atry[lista[j]]:= a[lista[j]]+da[j]
  end;

 for J:= (MFIT+1) to MMA do
  begin
   ATRY[LISTA[J]]:= A[LISTA[J]]
  end;

 MRQCOF(x,y,sig,ndata,atry,mma,lista,mfit,covar,da,nca,chisq);
 if  (chisq < glochisq) then
  begin
   alamda:= 0.1*alamda;
   glochisq:= chisq;
   for j:= 1 to mfit do
    begin
     for k:= 1 to mfit do
      begin
       alpha[j,k]:= covar[j,k]
      end;
     glbeta[j]:= da[j];
```

```
      a[lista[j]]:= atry[lista[j]]
     end
   end
  else
   begin
    alamda:= 10.0*alamda;
    chisq:= glochisq
   end;
99:
 end; {end of procedure  MRQMIN}

{-------------------------GETDATA-----------------------------}

 procedure  GETDATA;
  var
   j,k,nfiles,nobs: integer;
 begin
  i:= 0;
  ndata:= 0;
  writeln('Enter number of input file pairs to be read     :');
  readln(nfiles);
  for j:= 1 to nfiles do
   begin
    writeln('Enter name of brightness input data file: ');
    readln(infilename);
    writeln('Enter name of GEI vectors input file                  : ');
    readln(vecfilename);
    writeln('Enter # of data points  : ');
    readln(nobs);
    open(infile,infilename,old);
    reset(infile);
    open(vecfile,vecfilename,old);
    reset(vecfile);
    for k:= 1 to nobs do
     begin
      ndata:= ndata+1;
      i:= i+1;
      readln(infile,X[i],Y[i],sig[i],alt[i],za[i],sza[i]);
      read(vecfile,time[i],pv[1,i],pv[2,i],pv[3,i],
           sv[1,i],sv[2,i],sv[3,i],vv[1,i],vv[2,i],vv[3,i]);
      ZA[i]:= ANGLE(pv[1,i],pv[2,i],pv[3,i],vv[1,i],vv[2,i],vv[3,i]);
     end; {end of one file nobs read loop}
    close(infile);
    close(vecfile);
   end; {end of nfiles loop}
  writeln;
  writeln('Enter name of fitted brightness output file      : ');
  readln(outfilename);
 end; {end of procedure GETDATA}

{-------------------------------------------------------------}

begin { main body of program}

  for I:= 1 to 3 do
   for j:= 1 to 3 do
    dummy[i,j]:= 0; {set dummy to zeros}

  Xs[1]:=  0.18e-18; {total O XSections Richards & Torr JGR 1988}
  Xs[2]:=  1.3e-18;
  Xs[3]:=  3.0e-18;
  Xs[4]:=  4.8e-18;
```

```
Xs[5]:=  5.9e-18;
Xs[6]:=  6.8e-18;
Xs[7]:=  6.5e-18;
Xs[8]:=  7.3e-18;
Xs[9]:=  7.3e-18;
Xs[10]:= 8.0e-18;
Xs[11]:= 9.1e-18;
Xs[12]:= 9.3e-18;
Xs[13]:= 10.0e-18;
Xs[14]:= 11.0e-18;
Xs[15]:= 11.0e-18;
Xs[16]:= 12.0e-18;
Xs[17]:= 12.0e-18;
Xs[18]:= 12.0e-18;
Xs[19]:= 12.0e-18;
Xs[20]:= 12.0e-18;
Xs[21]:= 12.0e-18;
Xs[22]:= 12.0e-18;
Xs[23]:= 10.0e-18;

WXs[1]:=  0.0373e-18;{O+(2P) R&T '88 + Torr,Photchem.of Atmos.1985}
WXs[2]:=  0.276e-18;
WXs[3]:=  0.654e-18;
WXs[4]:=  1.08e-18;
WXs[5]:=  1.35e-18;
WXs[6]:=  1.59e-18;
WXs[7]:=  1.50e-18;
WXs[8]:=  1.74e-18;
WXs[9]:=  1.74e-18;
WXs[10]:= 2.01e-18;
WXs[11]:= 2.30e-18;
WXs[12]:= 2.35e-18;
WXs[13]:= 2.61e-18;
WXs[14]:= 2.99e-18;
WXs[15]:= 2.96e-18;
WXs[16]:= 3.18e-18;
WXs[17]:= 3.13e-18;
WXs[18]:= 3.06e-18;
WXs[19]:= 3.08e-18;
WXs[20]:= 2.99e-18;
WXs[21]:= 2.93e-18;
WXs[22]:= 2.92e-18;
WXs[23]:= 0.469e-18;

XsN2[1]:=  0.60e-18;{total N2 XSections Torr Photchem. of Atmos. 1985}
XsN2[2]:=  2.32e-18;
XsN2[3]:=  5.40e-18;
XsN2[4]:=  8.15e-18;
XsN2[5]:=  9.65e-18;
XsN2[6]:=  10.60e-18;
XsN2[7]:=  10.08e-18;
XsN2[8]:=  11.58e-18;
XsN2[9]:=  11.60e-18;
XsN2[10]:= 14.60e-18;
XsN2[11]:= 18.00e-18;
XsN2[12]:= 17.51e-18;
XsN2[13]:= 21.07e-18;
XsN2[14]:= 21.80e-18;
XsN2[15]:= 21.85e-18;
XsN2[16]:= 24.53e-18;
XsN2[17]:= 24.69e-18;
XsN2[18]:= 23.20e-18;
XsN2[19]:= 22.38e-18;
XsN2[20]:= 23.10e-18;
```

```
XsN2[21]:= 23.20e-18;
XsN2[22]:= 23.22e-18;
XsN2[23]:= 29.75e-18;

flux[1]:=  0.117; {Shape of modified F74113 reference spectrum}
flux[2]:=  0.044;
flux[3]:=  0.700;
flux[4]:=  0.457;
flux[5]:=  0.067;
flux[6]:=  0.037;
flux[7]:=  0.257;
flux[8]:=  0.117;
flux[9]:=  1.000;
flux[10]:= 0.143;
flux[11]:= 0.094;
flux[12]:= 0.047;
flux[13]:= 0.056;
flux[14]:= 0.041;
flux[15]:= 0.043;
flux[16]:= 0.066;
flux[17]:= 0.104;
flux[18]:= 0.186;
flux[19]:= 0.051;
flux[20]:= 0.078;
flux[21]:= 0.228;
flux[22]:= 0.050;
flux[23]:= 0.033;

GETDATA;
writeln(' First variable in list to be 1)H 2)Iinf or 3)[O]@250 ');
readln(lista[1]);
writeln('Second variable "  "   "   " 1)H 2)Iinf or 3)[O]@250 ');
readln(lista[2]);
writeln(' Third variable "  "   "   " 1)H 2)Iinf or 3)[O]@250 ');
readln(lista[3]);
writeln('Enter the # of parameters to be adjusted: ');
readln(mfit);
writeln('Enter initial H       : ');
readln(A[1]);
writeln('      initial Iinf    : ');
readln(A[2]);
writeln('      initial [O]@250: ');
readln(A[3]);
A[3]:= ln(A[3]);
writeln('      assumed [N2]@250: ');
readln(N2250);
writeln('N2 quenching coef kN2: ');
readln(KN2);
writeln(' O quenching coef kO : ');
readln(KO);
writeln('number of altitude intervals for BRIGHT: ');
readln(maxhindx);
writeln('altitude interval in kilometers: ');
readln(deltah);
chisqo:= 1e20;
deltachisq:= 1e20;
alamda:= -1.0; {initialization with negative alamda}
I:= 0;
while (deltachisq > 0.1) do
 begin
  I:= I+1;
  MRQMIN(x,y,sig,ndata,a,3,lista,mfit,covar,alfa,3,chisq,alamda);
  writeln('          H = ',A[1]);
  writeln('       Iinf = ',A[2]);
```

```
    writeln('    [O]@250 = ',exp(A[3]));
    writeln('chi sqred  = ',chisq);
    writeln('end of ',I,'th iteration');
    writeln('alamda= ',alamda);
    writeln;
    if  (chisq < chisqo) then
     begin
      deltachisq:= chisqo-chisq;
      chisqo:= chisq;
     end; {end of if }
   end; {end of while}
  alamda:= 0.0; {set alamda to zero for final call}
  MRQMIN(x,y,sig,ndata,a,3,lista,mfit,covar,alfa,3,chisq,alamda);
  writeln('alpha matrix:-');
  writeln(alfa[1,1],alfa[1,2],alfa[1,3]);
  writeln(alfa[2,1],alfa[2,2],alfa[2,3]);
  writeln(alfa[3,1],alfa[3,2],alfa[3,3]);
  writeln;
  writeln('covariance matrix:-');
  writeln(covar[1,1],covar[1,2],covar[1,3]);
  writeln(covar[2,1],covar[2,2],covar[2,3]);
  writeln(covar[3,1],covar[3,2],covar[3,3]);
  writeln;
  writeln('       H = ',A[1]: 7,'+/-',sqrt(covar[1,1]): 7);
  writeln('      I* = ',A[2]: 7,'+/-',qrt(covar[2,2]): 7);
  writeln('[O]@250 = ',exp(A[3]): 7,'+/-',100*(exp(sqrt(covar[3,3]))-
      1.0): 7,'%');
  O500:= exp(A[3])*exp((250.0-500.0)/A[1]);
  writeln('    [O]@500 = ',O500: 7);
  O500:= exp(A[3])*exp((250.0-500.0)/(A[1]+sqrt(covar[1,1])));
  writeln('    [O]@500+= ',O500: 7);
  O500:= exp(A[3])*exp((250.0-500.0)/(A[1]-sqrt(covar[1,1])));
  writeln('    [O]@500-= ',O500: 7);writeln;
  writeln('chi sqred  = ',chisq);writeln;
  writeln;
  open(outfile,outfilename,new);
  rewrite(outfile);
  for i:= 1 to ndata do
   begin
    write(outfile,X[i],' ',fit[i],' ',y[i],' ');
    writeln(outfile,sig[i],' ',za[i],' ',SZA[i]);
   end; {end of read loop}
  close(outfile);

end. {end of program TWIFITTER}
```